DOT/FAA/AR-00/37

Office of Aviation Research
Washington, D.C. 20591

Report of the 12A Working Group on Determination of Critical Ice Shapes for the Certification of Aircraft

September 2000

Final Report

This document is available to the U.S. public through the National Technical Information Service (NTIS), Springfield, Virginia 22161.

U.S. Department of Transportation
Federal Aviation Administration

NOTICE

This report is available at the Federal Aviation Administration William J. Hughes Technical Center's Full-Text Technical Reports page: actlibrary.tc.faa.gov in Adobe Acrobat portable document format (PDF).

Technical Report Documentation Page

1. Report No. DOT/FAA/AR-00/37	2. Government Accession No.	3. Recipient's Catalog No.
4. Title and Subtitle REPORT OF THE 12A WORKING GROUP ON DETERMINATION OF CRITICAL ICE SHAPES FOR THE CERTIFICATION OF AIRCRAFT		5. Report Date September 2000 6. Performing Organization Code
7. Author(s)		8. Performing Organization Report No.
9. Performing Organization Name and Address Federal Aviation Administration William J. Hughes Technical Center Atlantic City International Airport, NJ 08405		10. Work Unit No. (TRAIS) 11. Contract or Grant No.
12. Sponsoring Agency Name and Address U.S. Department of Transportation Federal Aviation Administration Office of Aviation Research Washington, DC 20591		13. Type of Report and Period Covered Final Report 14. Sponsoring Agency Code AIR-100
15. Supplementary Notes The Federal Aviation Administration Technical Monitor was James Riley		

16. Abstract

Task 12A of the Federal Aviation Administration (FAA) Aircraft In-Flight Icing Plan states that the "FAA, along with industry and research organizations, shall form a working group to explore categories of ice accretions that represent potential safety problems on aircraft" with the goal of developing guidance material on the determination of critical ice accretion shapes and roughness in aircraft certification. Accordingly, the 12A Working Group, on critical ice shapes used in icing certification, was formed under the joint leadership of the FAA and the National Aeronautics and Space Administration (NASA) in November 1997. This report describes the activities and findings of the 12A Working Group and its recommended actions for progress to meet the goals stated in the FAA Aircraft In-Flight Icing Plan.

The working group reviewed existing guidance material pertaining to the determination of critical ice shapes; prepared and distributed a survey to manufacturers to gather information as to current practices followed by manufacturers in the determination of critical ice shapes in certification; and surveyed publicly available data on aerodynamic effects of ice accretions (primarily glaze ice accretions). It was found that nearly all publicly available data is two-dimensional, with aerodynamic measurements mainly at low Reynolds numbers. Based on this finding, the working group recommended that the research community acquire more three-dimensional data, and also obtain additional measurements at Reynolds numbers more representative of actual flight conditions.

The working group formulated a more formal definition of critical ice shape and described two approaches, an "airfoil sensitivity approach" and a "comprehensive aerodynamic approach," that could result in improved practices and guidance material. These approaches should be viewed as complementary, not mutually exclusive. The first has the potential to provide benefits in the relatively short run, while the other would have to await major progress in development and validation of computer programs.

The working group reached a consensus that progress requires experimental work, although it is hoped that computational tools, because of their versatility and relative affordability, will also be developed and utilized as fully as possible. These tools could be computational fluid dynamics (CFD) tools, but could also use simpler methods allowing the estimation of 3D wing results working from experimental 2D section data. Data of a high quality, from wind tunnels capable of achieving high Reynolds numbers, is needed to adequately assess questions concerning the influence of ice shape features on the aerodynamic effects of ice shapes. Fundamental work is needed in the measurement and quantification of ice roughness.

The consensus of the working group was that the next most important area of research was scaling, including both aerodynamic scaling and ice shape scaling. The working group hopes that its findings and recommendations will be useful to research organizations in formulating investment strategies for icing research.

17. Key Words Ice accretion, Critical ice shape, Icing certification, Airfoil	18. Distribution Statement This document is available to the public through the National Technical Information Service (NTIS) Springfield, Virginia 22161.		
19. Security Classif. (of this report) Unclassified	20. Security Classif. (of this page) Unclassified	21. No. of Pages 213	22. Price

Form DOT F1700.7 (8-72) Reproduction of completed page authorized

TABLE OF CONTENTS

LIST OF FIGURES

EXECUTIVE SUMMARY

Task 12A of the Federal Aviation Administration (FAA) Aircraft In-Flight Icing Plan states that the "FAA, along with industry and research organizations, shall form a working group to explore categories of ice accretions that represent potential safety problems on aircraft" with the goal of developing guidance material on the determination of critical ice accretion shapes and roughness in aircraft certification. Accordingly, the 12A Working Group was formed under the joint leadership of the FAA and National Aeronautics and Space Administration (NASA) in November 1997. The working group adopted the following charter: "Develop guidance material, working methods, and recommendations for establishing the criticality of ice accretion characteristics on aircraft aerodynamic performance and handling qualities." However, the working group determined that sufficient information and methods were not yet available to provide guidance material concerning the determination of critical ice shapes in certification. Steps were taken toward the development of such information and methods, and steps deemed necessary for further progress were described. This report describes the activities and findings of the 12A Working Group and its recommended actions for progress to meet the goals stated in the FAA Aircraft In-Flight Icing Plan and the charter of the working group.

The working group reviewed existing guidance material pertaining to the determination of critical ice shapes. This guidance material was determined to be very general and not to provide a working definition of "critical ice shape" or a description of engineering practices to be followed in the determination of such shapes.

The working group prepared and distributed a survey to manufacturers to gather information as to current practices followed by manufacturers in the determination of critical ice shapes in certification. The responses showed these practices to be extremely varied, relying heavily on engineering judgment. The simulations tools used are predominantly two-dimensional (2D).

The working group surveyed publicly available data on aerodynamic effects of ice accretions. Only glaze ice was evaluated in detail. Information concerning other types of ice accretions may be found in the bibliography in appendix E. This report includes in its appendices a database constructed as part of this effort. (The database is also available from the FAA William J. Hughes Technical Center on electronic media.) This database can be useful to both industry and FAA Aircraft Certification Offices, providing a kind of reality check in the evaluation of candidate critical ice shapes. However, it was found that nearly all publicly available data is two-dimensional with aerodynamic measurements mainly at low Reynolds numbers. Based on this finding, the working group recommended that the research community acquire more three-dimensional data and also obtain additional measurements at Reynolds numbers more representative of actual flight conditions.

A more formal definition of critical ice shape was formulated and discussed that could be employed in the development of improved guidance material. The discussion emphasized use of measurable quantities related to aircraft performance and handling qualities.

The working group described two approaches that it believed could result in improved practices and guidance material. These approaches should be viewed as complementary, not mutually

exclusive. One has the potential to provide benefits in the relatively short run, while the other would have to await major progress in development and validation of computational methods.

The first approach, which will be termed the "airfoil sensitivity approach," places greater emphasis on the airfoil and its sensitivity to contamination represented by various geometries (representative of ice accretions) at a range of locations of the airfoil. Less emphasis is placed on the attempted prediction of particular ice shapes presumed to actually accrete at atmospheric conditions believed to be critical. It is suggested that such an approach could shift attention to earlier stages in the design phase and could potentially provide both safety and economic benefits. Emphasis on this approach is partly based on the assumption that the capability of available tools to determine ice shapes with sufficient accuracy in conditions most likely to be critical ("high" static temperatures, large liquid water content (LWC), large droplets) has still not been fully evaluated (although it is a very active area of research at this time). It is also a matter of not knowing the icing condition that will produce the most critical ice accretion even if the tools were available. In order that this approach be effective, more experimental data are needed on the effects of ice shape geometries and locations on the various types of airfoils in current use. Without such experimental data to guide the applicant in selection of types and locations of ice to assess for the many configurations to be accounted for, the process would be difficult to implement in a way that provides benefits in terms of both efficiency and safety.

The second approach, which will be termed the "comprehensive aerodynamic approach," involves the development of powerful computational tools and is quite fully outlined in this report. The computational tools would have to be validated using an experimental database much expanded over that currently available as a prerequisite for acceptance of such tools in certification.

As noted, both the airfoil sensitivity approach and the comprehensive aerodynamic approach require substantially more experimental data to be used with confidence. Experimental data are needed for both 2D and three-dimensional (3D) configurations, straight and swept wing, various flight configurations (cruise, hold, landing), and higher Reynolds numbers.

The consensus of the 12A Working Group was that research was most needed now in the characterization of ice roughness for different types of ice ("sandpaper," residual/intercycle ice, glaze, etc.); the investigation of the aerodynamic effects resulting from parametric variation of characteristic ice accretion features (such as upper horn height and location), and the investigation of aerodynamic effects resulting from variation of airfoil characteristics.

The working group reached a consensus that these items require experimental work, although it is hoped that computational tools, because of their versatility and relative affordability, will also be developed and utilized as fully as possible. These tools could be computational fluid dynamics (CFD) tools, but could also use simpler methods allowing the estimation of 3D wing results working from experimental 2D section data. Data of a high quality, from wind tunnels capable of achieving high Reynolds numbers, is needed to adequately assess questions concerning the influence of ice shape features on the aerodynamic effects of ice shapes. Fundamental work is needed in the measurement and quantification of ice roughness.

The consensus of the working group was that the next most important area of research was scaling, including aerodynamic scaling (How should an ice shape accreted on a model of one size be scaled so that it will give the same aerodynamic effects on a model of another size?) and ice shape scaling (How can tunnel parameters be adjusted so that different combinations of parameters give comparable ice shapes?).

The working group anticipates that its findings and recommendations will be useful to research organizations in formulating investment strategies for icing research.

1. INTRODUCTION.

Task 12A of the Federal Aviation Administration (FAA) Aircraft In-Flight Icing Plan [1] (see appendix A) states that the "FAA, along with industry and research organizations, shall form a working group to explore categories of ice accretions that represent potential safety problems on aircraft" with the goal of developing guidance material on ice accretion shapes and roughness and resultant effects on performance/stability and control. The working group was to address several categories of ice accretion, including (but not limited to) glaze ice, rime ice, "large-droplet ice," "beak ice," "sandpaper" ice, residual ice, and intercycle ice. These categories were to be considered during various phases of flight (such as takeoff, landing, climb, and hold) for operational ice protection systems, failed ice protections systems, and unprotected surfaces. Accordingly, the 12A Working Group was formed under the joint leadership of the FAA and National Aeronautics and Space Administration (NASA) in November 1997. The working group adopted the following charter: "Develop guidance material, working methods, and recommendations for establishing the criticality of ice accretion characteristics on aircraft aerodynamic performance and handling qualities."

However, the 12A Working Group found that the data and methods required for developing the general guidance material require further research. Although it was unable to accomplish its main goal, the working group accomplished necessary "subtasks" toward that goal and sketched approaches and research necessary to the eventual development of general guidance material pertaining to the determination of critical ice shapes for aircraft certification.

The discussions within the working group helped to clarify the difficulties in developing guidance material. Manufacturers and certification officials shared information which underlined the fact that the determination of critical ice shape for an aircraft type is very specific to the aerodynamic performance (as well as the systems design) for that aircraft type. Thus it should not be anticipated that guidance material can formulate a universal approach to the problem of critical ice shape determination for all aircraft types. However, guidance material can be provided on definitions, procedures, and methods that will be common to all aircraft icing certifications.

The working group included representatives from the following organizations who attended meetings and participated in the preparation of this report: AARDC Tower C; Airline Pilots Association; Beech Aircraft; BFGoodrich Aerospace—Ice Protection Systems; Boeing; De Havilland, Inc.; Federal Aviation Administration; Galaxy Scientific Corporation; JAA/DGAC-F; McDonnell Douglas; NASA Glenn Research Center; Ohio Aerospace Institute; Sikorsky Aircraft; University of Illinois at Urbana-Champaign; and Wichita State University. (See appendix B for a list of all working group members.)

The working group met twice in 1997 and 1998, and subgroups worked between meetings to develop material useful in defining critical ice shapes and procedures for certification. Other than meetings, its work was accomplished through email and telephone conferences.

There was much discussion at both meetings of the definition of "critical" ice shape/ice shape features. The following definition achieved general acceptance.

"Critical ice shapes are those with ice accretion geometries and features representative of that which can be produced within the icing certification envelope that result in the largest adverse effects on performance and handling qualities over the applicable phases of flight of the aircraft."

This definition is discussed in section 3.1, "Definition of Critical Ice Shape and Discussion of Definition."

2. CURRENT GUIDANCE, METHODS, AND DATA.

2.1 CURRENT ADVISORY MATERIAL.

In this section, FAA advisory material, which involves critical ice shapes, is briefly reviewed.

The word "critical" is used in FAA advisory material in various contexts. It generally indicates a condition or set of conditions most likely to be conducive to the largest adverse effects on a component or system. A more specific definition, or methods to be followed in determining criticality, may not be provided. In such cases, the applicant either relies on accepted engineering practice or proposes and justifies practices applicable for particular certification.

In the case of critical ice shapes, the advisory material does not provide a specific definition or method, but does indicate factors that can or should be taken into consideration in the determination of critical ice shapes. It is implicitly assumed that such definitions and methods are available in accepted engineering practices, or else will be proposed and justified by the applicant. The following passages from two Advisory Circulars (ACs) indicate factors that should be accounted for in the determination of critical ice shapes.

AC 20-73, § 17e, states:

"Wind tunnel and/or dry air flight tests with ice shapes should be utilized. If an ice shape that is most critical for both handling characteristics and performance can be determined, then it is only necessary to flight test the most critical shape; otherwise, various shapes should be flight tested to investigate the aircraft's controllability, maneuverability, stability, performance, trim and stall characteristics for all combinations of weight, c.g., flap and landing gear configurations. Where practicable, the most critical ice shapes should be tested in combination with all other expected ice accretions to determine the full impact on aircraft performance."

This passage explicitly refers to "an ice shape that is most critical for both handling and performance," thus identifying two factors in determining criticality. It also states that wind tunnel and/or dry air flight tests should be utilized. It does not describe how handling and performance are to be taken into account. However, the Flight Test Harmonization Working Group is addressing the question of handling and performance requirements with ice shapes.

AC 23.1419-2A, § 9b, states:

> "The 45-minute hold criterion should be used in developing critical ice shapes for which the operational characteristics of the overall airplane are to be analyzed.... The critical ice shapes derived from this analysis should be compared to critical shapes derived from other analyses (climb, cruise, and descent) to establish the most critical artificial [simulated] ice shapes to be used during dry air flight tests."

This passage indicates that flight regime (45-minute-hold, climb, cruise, and descent) is another factor that should be considered in the analysis done by the applicant to determine critical ice shapes. The effects of these critical ice shapes from various regimes are to be compared to determine the most critical ice shape(s) for the flight testing in dry air with simulated ice shape. It should be noted that § 9 of the AC states, "All analyses should be validated either by tests or by previously FAA-approved methods."

In summary, the ACs state that critical ice shapes are to be critical with respect to aircraft performance and handling, and that the various flight regimes are all to be considered. The use of tunnels in generating ice shapes is recognized, but an explicit definition of critical ice shape is not given, nor are methods for determination of ice shape criticality described.

2.2 CURRENT METHODOLOGY.

At its first meeting, the working group determined that it would be helpful in completing its tasks to have available a compendium of information on ways in which airframe manufacturers currently determine critical ice shapes in certification. Accordingly, a subgroup was formed to obtain such information directly from the manufacturers.

A survey was prepared by a subgroup of the 12A Working Group. The survey covered other aspects of certification, and only the sections directly relevant to the 12A task are included in appendix C. It was recognized that some of the responses by manufacturers might touch on proprietary matters, and thus assurances of confidentiality were made to the respondents. The results were compiled by the subgroup, and distributed and discussed within the working group.

A narrative (see appendix D) has been prepared based on the results of the survey. In order to comply with the assurances of confidentiality, this narrative is necessarily quite general. Nonetheless, it does provide an overview of methods which are currently in use.

2.3 AERODYNAMIC EFFECTS OF GLAZE ICE.

This section presents the results of a subgroup's survey of published data regarding ice accretions and the resultant effects on aerodynamic performance. The applicability of these data to defining simulated ice shapes for certification was evaluated by correlating performance effects with ice shape characteristics.

The working group planned, in accordance with the FAA Icing Plan, to consider the effects of the following types of ice: sandpaper ice (a thin layer of ice composed of roughness elements), residual ice (ice remaining after a deicer cycle), rime ice, glaze ice, large-droplet ice (spanwise ridge accretions aft of the typical impingement zone for Appendix C of FAR 25 encounters),

beak ice (single horn ice shape on the upper surface), and intercycle ice (ice accumulated between deicer cycles). These categories of ice were to be considered during various phases of flight, such as takeoff, landing, climb, and hold, for operational ice protection systems, failed ice protection systems, and unprotected surfaces. However, because of the amount of data available and the limitations on the time and resources of the working group, such a comprehensive study was not possible for this report. Instead, a bibliography was prepared of the aerodynamic effects of weather-related contamination and tabulations of glaze ice effects were assembled. Finally, a preliminary attempt to correlate the drag penalties with accreted ice features (upper horn height, angle, and position) is shown. It is hoped that the information presented here will help in guiding the determination of critical ice shapes.

2.3.1 Comments on the Bibliography.

The bibliography appears in appendix E of this report. It includes 180 papers published to date which present experimental measurements or analytical predictions of the aerodynamic effects of glaze ice, rime ice, ice roughness, frost, rain, freezing rain and drizzle, ground anti/deicing fluids, and protuberances used to simulate different kinds of contamination. These papers are cited in this report, along with the applicable reference, in the following format: (E.1).

2.3.2 Summary of Published Studies.

It was not possible to review all the papers listed in the bibliography, but over 100 of them were summarized with regard to the type of information provided. Appendix F summarizes the studies reviewed and includes various types of weather-related surface contamination. Reported are the test facility, the models tested, the kind of contamination considered, and the type of aerodynamic data reported. The first column in appendix F gives the reference number from the bibliography (appendix E). This appendix was prepared to give an idea of the types of studies that have been reported in the literature to provide assistance in determining where there are research gaps. It should also help to identify literature of a particular type for future study.

2.3.3 Tabulations of Performance Data.

In addition to the summary table discussed above, a tabulation was prepared of drag and lift effects reported for studies relevant to glaze ice accretion at conditions within the FAA FAR 25 Appendix C envelope. Appendix G of this report presents the drag increase and lift loss due only to protuberances, glaze ice accretion, or simulated ice (i.e., castings of ice accretions or manufactured representations) as reported in the literature reviewed. To limit the scope of this review further, only results from tests using unswept airfoils are included in appendix G.

Table G-1 gives data for studies using various kinds of protuberances, while table G-2 reports studies that used accreted ice or simulated ice. In both parts of the table, each study is identified with the reference number from the bibliography (appendix E), the figure or table number from which performance data were obtained, and the airfoil identification along with its chord. Table G-1 includes a description of the protuberance used. Table G-2 contains additional information about the ice or ice simulation studied. The shape is identified based either on the authors' description or on the figure or table in the paper where the ice was described, the icing conditions for accreted ice are given, and a two-dimensional plot of the ice shape is shown.

The coordinates of the ice shapes on which the plots are based were obtained by methods discussed below. Some studies reported ice shapes without sufficient definition to permit coordinates to be determined; for example, two-dimensional coordinate data could not be obtained when only a photograph of the ice was given or when there was no way to scale the ice shape illustrated. Such studies were not included in table G-2. Although the emphasis is on glaze ice, when a study included both glaze and rime ice, the rime results are also reported for completeness.

The order of presentation of shapes and performance data is that used by the original publication on which it is based. In the paper of Olsen, et al. [2] (E.122),* icing tests were repeated at the same conditions as part of several test series to demonstrate effects of different parameters on ice shape and drag. Similar results were then also repeated in the reported figure s. To maintain consistency with that publication's order of presentation, these shapes and results are repeated in table G-2 as well. Note that in some cases ice shapes appear to have somewhat different characteristics for the same icing conditions. These differences are indicative of the repeatability of icing tests.

The description of the contamination in both tables G-1 and G-2 includes three characteristic dimensions. The choice of which dimensions of the ice most affect the aerodynamic penalties followed two National Advisory Committee on Aeronautics (NACA) studies from the 1950s. Bowden [3] (E.19) concluded from a study using spoilers that drag increases approximately linearly with the height of the spoiler and also increases with the distance of the spoiler from the leading edge. For ice accretions, Gray [4] (E.60) identified the upper horn height and angle as critical to the loss in aerodynamic performance. Since the upper horn size and location determine the size and location of the upper-surface separation bubble, these dimensions directly influence aerodynamic performance and are therefore logical choices as critical dimensions. For this study, then, the upper horn height-to-chord ratio, h/c, dimensionless chordwise location, x/c, and angle, θ, relative to the chord line will be reported for each ice shape. These characteristic dimensions are shown in figure 1. (These definitions, in particular the measurement convention for θ, are not identical to those used in some current studies, for example, recent LEWICE 2.0 validation studies. These definitions have not yet been standardized, but definitions are under consideration by the 11A Working Group.)

Figure 1(a) illustrates a glaze shape with well-defined features. If a straight reference line is drawn along the upper trailing edge of the most prominent feature of the main ice shape, the x-coordinate of the intersection of the line with the airfoil surface is the characteristic location of that ice shape. The height of the feature, h, is measured from the airfoil surface where the trailing edge of the feature would intersect the surface. The angle, θ, is the angle between the chord line and the upper horn trailing-edge line. The angle is positive if measured clockwise from the chord line, as in figure 1(a), and negative if measured counterclockwise. For studies with ice or simulated ice reported in table G-2, the characteristic dimensions were found by plotting the digitized ice shape and using image-analysis software to record locations, lengths, and angles of the prominent feature.

*Note: The bibliography number (listed in appendix E) is given in parentheses after the reference number, which is given in brackets.

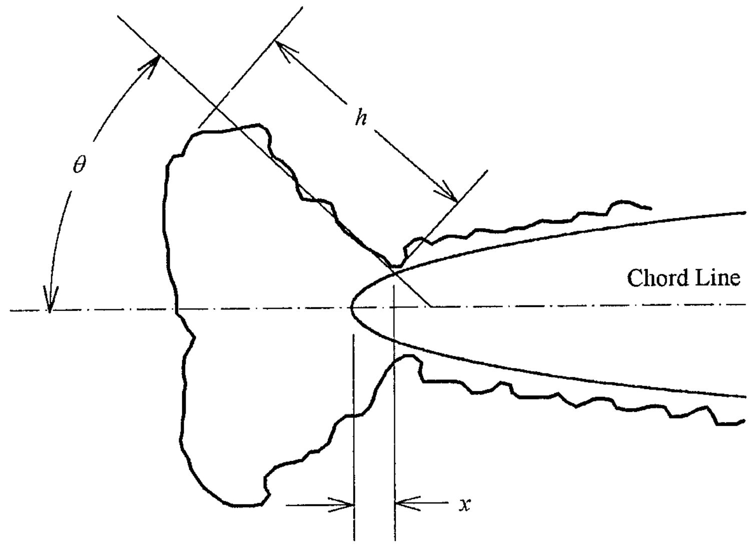

(a) Definition of Characteristic Dimensions.

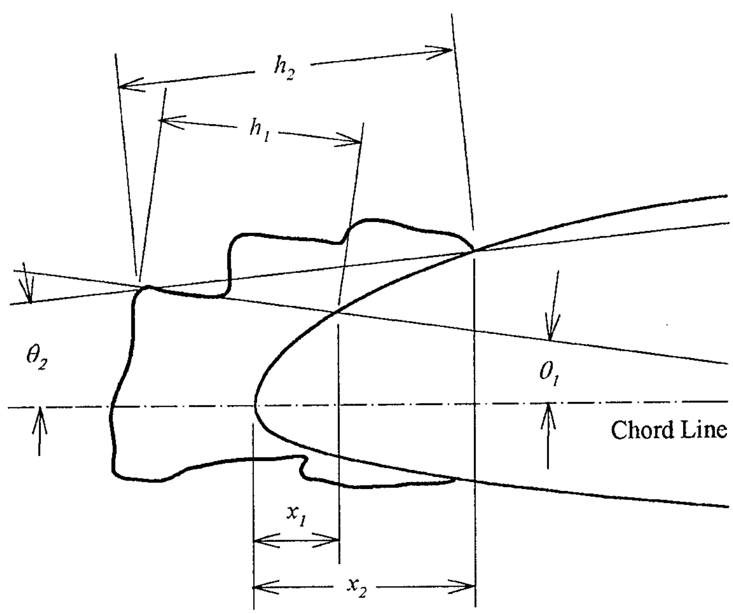

(b) Ambiguity of Characteristic Dimensions for Some Shapes

FIGURE 1. CHARACTERIZATION OF ICE SHAPE DIMENSIONS (Parameters *H* And θ From Gray [60])

Protuberances were assumed to simulate the upper horn of a glaze ice accretion, and the characteristic dimensions were defined accordingly. The *x/c* values were taken at the center of the protuberance at its base on the airfoil. Because some studies have used different conventions, for example, the position of the front of the protuberance, the locations reported in the source reference may differ somewhat from values in table G-1. For the Kim and Bragg study [5] (E.98) the values of *x/c* were calculated from the published θ and known airfoil coordinates. Papadakis, et al. [6] (E.126) reported a spoiler angle, θ, measured from a line normal to the chord line such that positive angles resulted if the protuberance leaned toward the trailing edge of the airfoil and negative if it leaned forward. Thus, the values of θ shown in table G-1 for the Papadakis data are 90° greater than the θs given in reference [6] (E.126).

For some ice shapes, definition of the characteristic dimensions was not as evident as that shown in figure 1(a). Figure 1(b) shows ice with a large central structure and only slightly smaller features aft. For this kind of shape, it is possible to define more than one set of characteristic dimensions. For example, one set can be based on a reference line drawn along the trailing edge of the main ice shape, while for a second set, it extends from the main peak to the apparent impingement limit of the ice growth. Note that θ_1 is positive while θ_2 is negative in this example. For this study, most accretions similar to that of figure 1(b) were characterized by the first set of dimensions. Clearly, however, the ambiguity involved could result in significant differences in the way two observers might characterize the same ice shape. Which set of dimensions best correlates the aerodynamic penalties would need to be established by further study. For very short accretion times, ice shapes were too poorly defined to estimate characteristic dimensions; for these situations, no characteristics have been reported in the table (see, for example, table G-2.1, runs 129 and 202.)

Gray [4] (E.60) reported his own measurements of horn height, h, and horn angle, θ. To gain some sense of the uncertainty in the characteristic dimensions in table G-2, Gray's published values were compared with results using the methods of the present study. Horn height was found to agree with Gray's values within ±10% and horn angle agreed within ±2.5°. The values given in table G-2 for the Gray study for h/c and θ are taken from reference [4] (E.60). For a few shapes, Gray gave no value for θ. For those cases, the angle given in appendix G was measured using present methods from Gray's published ice shapes.

Finally, both parts of appendix G give aerodynamic data along with the Reynolds number at which data were obtained. If the Reynolds number was not reported in the source publication, it was calculated from the published velocity, static temperature, and airfoil chord. The only work for which this was not possible was the Bowden study [3] (E.19), for which neither the velocity nor the Reynolds number for the spoiler experiments was specified.

For all studies, the increase in drag is given in the table along with the angle of attack for which it was found. ΔC_d values are not shown in the table for angles of attack greater than 8 or 9°, although data were sometimes published for higher angles. The last two columns give the change in angle of attack at which the maximum lift coefficient was observed, $\Delta\alpha_{Cl,max}$, and the change in maximum lift coefficient, $\Delta C_{l,max}$, due to the ice contamination. Data were not included from published curves if it was not evident that sufficiently high α's had been tested to show the maximum lift coefficient. Bowden's [3] (E.19) curves, for example, ended with C_l

continuing to increase with α. The lift curves reported by Addy, et al. [7] (E.5) also failed to peak out, but communication with the first author indicated the test airfoils demonstrated vibration characteristics typical of those at maximum lift; thus, the maximum lift coefficients reported by Addy, et al. were assumed to be $C_{l,max}$. When the tables of drag and lift were published, the data for appendix G were taken from these tabulations. In some cases, data were provided by the authors. If data were only available in graphical form, the values in appendix G were obtained by digitizing the published data plots.

Table G-1 lists studies alphabetically and includes all relevant studies reviewed. Table G-2 is also organized alphabetically, but requires more space for each study due to the ice shape images included. For this reason, it is divided into several subsections. First, each study is contained in a separate subsection; for example, table G-2.1 covers only the results of Addy, et al. [7] (E.5). Several of Bragg's studies [8, 9, 10, and 11] (E.24, E.25, E.28, and E.29) are grouped together in table G-2.2 because the same ice shapes were used for all. The Flemming and Lednicer [12] (E.56) work included extensive data on nine different airfoils; thus, table G-2.4 is further subdivided into subsubsections (i) through (ix), each devoted to one airfoil. Gray [4] (E.60) used only one airfoil but presented so many test conditions and ice shapes that table G-2.5 is also subdivided according to the page of the original report on which the shape and performance data were given. The Shin and Bond papers [13 and 14] (E.150 and E.151) presented data from the same study in different ways. Information from both references were combined for inclusion in the single subsection table G-2.7.

In general, data were not critically reviewed before including them in appendix G. However, based on an inspection of the original ice tracings supplied by Flemming, the identifying run labels for the ice shapes of runs 637 and 726 for Flemming and Lednicer are reversed in figure 30 of reference [12] (E.56). Thus, the run identifications in table G-2.4(ii) are based on the tracings rather than the report. Also, the Papadakis, et al. [6] (E.126) study involved tests with both a 12- and a 24-in-chord NACA 0011. While the 24-in.-chord clean-airfoil lift data reported were consistent with NACA 4-digit airfoil results given by Abbott and von Doenhoff [15] (E.3), the 12-in-chord data were not. Thus, pending a better understanding of the discrepancy, the latter were not included table G-1.

2.3.4 Correlations of Drag Increase.

Vernon Gray, working for NACA and later NASA, published correlations relating the drag increase to icing conditions [4, 16, 17, 18, 19] (E.60, E.61, E.62, E.63, E.64). These correlations were based on data obtained in what is now the NASA Glenn Icing Research Tunnel (IRT). Unfortunately, there appears to be little physical basis for these correlations, and the correlating parameter was simply a collection of terms developed into a form that worked for Gray's data. A fundamental problem with this approach is that it cannot be applied universally to results from all icing tunnels or to flight because different tunnels sometimes produce somewhat different ice shapes for the same icing conditions, and tunnel ice shapes may not agree with in-flight accretions. The methods and instruments used to calibrate the medium volume diameter (MVD) and liquid water content (LWC) in icing tunnels have not been standardized. Furthermore, even if instrumentation were standardized, differences in flow quality, in the uniformity of relevant parameters across the test section, and in tunnel physical features would probably still give variations in ice shapes from tunnel to tunnel. It has not even been possible to apply Gray's

1958 correlation to data taken later in the IRT [2] (E.122); this is almost certainly because of changes in the IRT calibration techniques and instruments through the years. Thorough documentation of the IRT calibration and methods has only been maintained in the last two decades, and calibration information from Gray's time appears to have been lost. Note also that Gray's correlation incorporates static rather than total temperature, with the consequence that the errors tend to be large at high speeds.

Subsequent work by Bragg [20] (E.21) and by Flemming and Lednicer [12] (E.56) provided drag correlations based on ice accretion terms that appear to overcome some of the shortcomings of the Gray correlation. However, to obtain a correlation that is universally applicable, it is best to correlate aerodynamic performance effects with the ice features that most affect the performance. As noted above, those features have been identified by Gray and by Bowden [3] (E.19) as upper-horn height, angle, and position, identified in figure 1.

For this report, limited work was done to look at the effectiveness of incorporating these three dimensions into a parameter which would correlate aerodynamic penalty data. One combination was the product, $(h/c)\sin(\theta + \alpha)$. This expression gives the nondimensional height of the ice or protuberance normal to an undisturbed streamline. In figure 2, the increase in drag due to the ice is plotted against $(h/c)\sin(\theta + \alpha)$ for all of the published studies listed in tables G-1 and G-2 for angles of attack, α, less than or equal to 3.2°. The legend on the figure indicates the source of the data (where the number refers to bibliography entries), the airfoil used in each study, and the type of contamination. A variety of airfoils is included with chords from 2.69 to 72 inches. Contamination includes ice produced in icing tunnels, simulated ice (including ice castings and fabricated representations), and various kinds of protuberances. Data for protuberances are only included when the contamination was located at or upstream of $x/c = 0.05$. Locations aft of this are not typical of glaze ice formed in appendix C conditions, which is the focus of this report. Aerodynamic penalties appearing in this correlation were obtained from icing tunnels as well as aerodynamic tunnels.

Although there is significant scatter in the data shown in figure 2, ΔC_d generally increases with $(h/c)\sin(\theta + \alpha)$ for low angles of attack. Note that the Olsen, et al. [2] (E.122) data are consistent with the Gray [4] (E.60) results when this correlating parameter is used, while Olsen reported little agreement between the Olsen and Gray data when the Gray correlation was used. The determination of the importance of dimensionless chordwise position of the downstream edge of the ice, x/c, and its inclusion in a correlating parameter will require further study. One possibility might be to include the airfoil thickness at x/c as an additional parameter in the h/c term. (See x in figure 1.)

Correlations for higher angles of attack have not been considered in this preliminary study. Furthermore, different definitions of the horn height and angle [21] might need to be considered; alternate definitions were not evaluated. The correlation of figure 2 suggests that it should be possible to obtain a good estimate of the drag increase due to ice by testing with very simple shapes attached to the upper surface of the airfoil. Studies using this approach have recently been reported by Kim and Bragg [5] (E.98) and Papadakis, et al. [6] (E.126). Additional work to develop meaningful correlating parameters for both drag increase and lift loss is recommended.

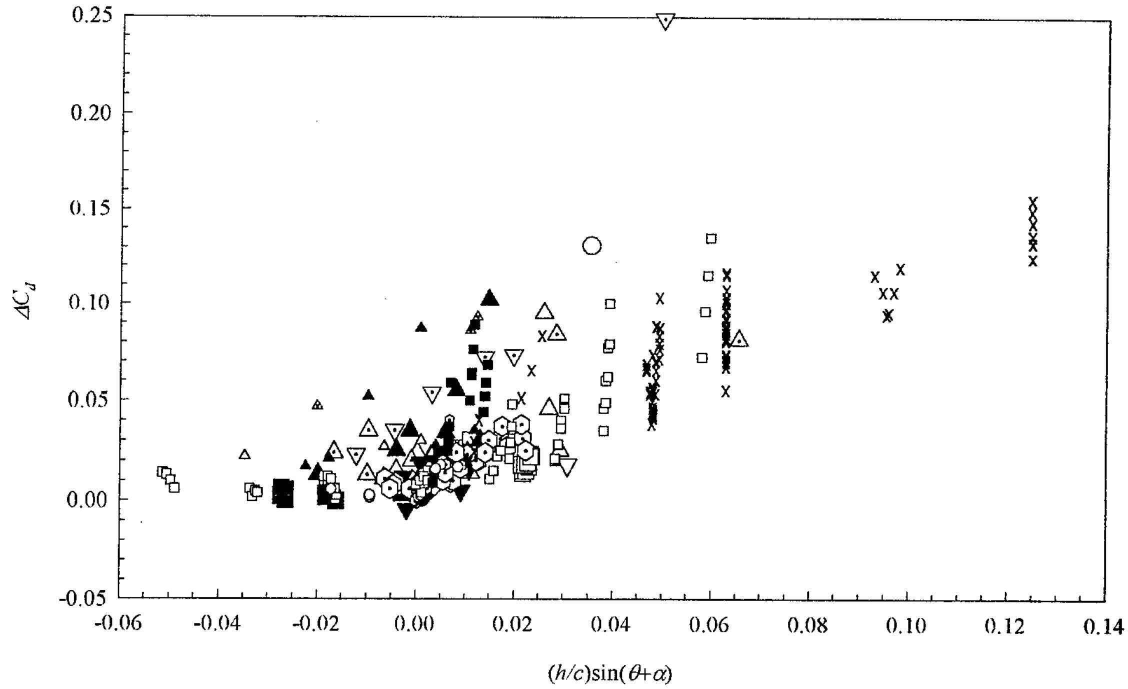

	No.	Reference	Airfoil	Ice Description
○	5	Addy, et al, AIAA-97-0174, 1997	comm. transp.	accreted ice
●	19	Bowden, NACA TN 3564, 1956	NACA 0011	spoilers
□	24,25 28,29	Bragg, *J. Aircraft*, vol 25, 1988 and CR 191007, 1993 Bragg and Coirier, AIAA-85-0409, and AIAA-86-0484	NACA 0012	simulated ice
■	34	Bragg, et al, AIAA-82-0582, 1982	NACA 63A415	simulated ice
◇	46	Calay, et al, *J. Aircraft*, vol 34, 1997	NACA 0012	wedges
△	56	Flemming and Lednicer, NASA CR 3910, 1985	NACA 0012	accreted ice
◬	56	Flemming and Lednicer, NASA CR 3910, 1985	SC1095	accreted ice
▲	56	Flemming and Lednicer, NASA CR 3910, 1985	SSC-A09	accreted ice
▵	56	Flemming and Lednicer, NASA CR 3910, 1985	VR-7	accreted ice
◬	56	Flemming and Lednicer, NASA CR 3910, 1985	SC1094	accreted ice
▴	56	Flemming and Lednicer, NASA CR 3910, 1985	SC1012	accreted ice
▽	56	Flemming and Lednicer, NASA CR 3910, 1985	OH-58	accreted ice
▽	56	Flemming and Lednicer, NASA CR 3910, 1985	NACA 0012	accreted ice
▼	56	Flemming and Lednicer, NASA CR 3910, 1985	CCA	accreted ice
⬡	60	Gray, NACA TN 4151, 1958	NACA 65A004	accreted ice
⊙	82	Jacobs, NACA TR 446, 1933	NACA 0012	protuberances
▫	98	Kim and Bragg, AIAA-99-03150, 1999	NLF(1)-0414F	upper horn simulation
▪	110	Lee, et al, AIAA-98-0490, 1998	NACA 23012	full-span step
◦	122	Olsen, et al, NASA TM 83556, 1984	NACA 0012	accreted ice
x	126	Papadakis, et al, AIAA-99-0096, 1999	NACA 0011	spoilers

FIGURE 2. DRAG INCREASE DUE TO ACCRETED ICE (Simulated Ice or Protuberances. Angle of Attach, 0 to 3°.)

2.3.5 Methods Used to Obtain Ice-Shape Coordinates.

The ice-shape coordinates used for the plots in table G-2 were generally obtained by digitizing ice-shape image published in the studies reviewed using image-analysis software (SigmaScan Pro). The software was operated in an automatic line-tracing mode with *x*, *y* coordinates recorded every 5th pixel. To obtain full-size coordinates, the image was first calibrated to a scale recorded with the image. The conventional origin of the coordinate system, at the leading-edge of the clean airfoil, was used. The scale for the shapes was determined either directly from dimensions on the published source or by inference by matching known airfoil coordinates with the published image of the airfoil shape. The digitizing method follows only the outside line of a shape, so some features may be lost from the original. For example, when two features, such as adjacent feathers, share a common boundary, this boundary line may not be included in the digitized coordinates.

When the source figure included several ice shapes drawn on the same airfoil for comparison, it was sometimes difficult to identify the line for each shape, especially in the feather regions behind the main airfoil. For most of these cases, original ice-shape tracings were available to assist in defining the correct shape. Gray's [4] (E.60) ice-shape images were published with a 1/4-in grid. However, due to the small size of the images, the magnification required for analysis resulted in thick grid lines and poor definition of scale; consequently, coordinates reported are probably accurate to only ± 0.05 in. For many of the ice shapes published by Olsen, et al. [2] (E.122), sources other than the published figure s were available with better definition of the scale, so these were used to establish ice-shape coordinates.

For some studies, coordinate information was available without digitizing the published ice-shape images. The coordinates given for the Addy, et al. [7] (E.5) ice shapes were provided by the first author. The coordinates for the shapes used in Bragg's studies for references 8, 9, 10, and 11 (E.24, E.25, E.28, and E.29) were published in reference 9 (E.25) and reproduced here. The coordinates for the Shin and Bond studies [13 and 14] (E.150 and E.151) were supplied from the NASA Glenn Icing Branch archives.

Nondimensional clean airfoil coordinates for the NACA airfoils were generally obtained from tables and methods described in Abbott and von Doenhoff [15] (E.3). However, for the Gray study [4] (E.60) the NACA 65A004 coordinates were taken from Brun, et al. [22]. Other airfoil coordinates were supplied by the authors of the various studies.

All parts of Appendices F and G were prepared in Excel 97 format and are available from the FAA. In addition, the ice-shape and clean-airfoil coordinates used for the plots in table G-2 are given in tables on a CD distributed as an addendum to this report. The addendum tables are also in Excel 97 format. They are organized to be consistent in numbering with table G-2. For example, the ice-shape coordinates for the data of table G-2.5(i) are in table A-5(i).

3. CONSIDERATIONS FOR IMPROVED METHODS AND GUIDANCE.

3.1 DEFINITION OF CRITICAL ICE SHAPE AND DISCUSSION OF DEFINITION.

The following definition was adopted by the working group after considerable discussion:

> "Critical ice shapes are those with ice accretion geometries and features representative of that which can be produced within the icing certification envelope that result in the largest adverse effects on performance and handling qualities over the applicable phases of flight of the aircraft."

This definition is similar to guidance in ACs (see above), but goes beyond, in that it focuses on ice accretion geometries and particular features which may contribute to criticality.

The following discussion addresses the identification of ice accretion geometries and features and the expression of performance and handling-qualities effects in terms of measurable quantities.

Ice accretion geometries and features include ice thickness, ice horn characteristics, and ice surface texture. The ice thickness refers to the height of the ice above the aircraft surface, as well as its location and its distribution on the aircraft surface. An ice horn is a distinctive protuberance of ice extending outward from the aircraft surface noticeably more than any surrounding ice. The horn's features include its length, its location on the aircraft surface, and its angle with respect to that surface, as well as its surface characteristics.

The "largest adverse effects on performance" refer to ice shapes and ice features which result in the largest loss in lift, the largest decrease in stall angle, the greatest increase in drag, and/or the largest change in pitching moment which may be realized under the certification conditions. The largest adverse effects on handling qualities refer to ice shapes and ice features that exhibit the greatest effects on the aerodynamics of aircraft control.

Occasionally, a stall strip is used to simulate ice accretion on an aircraft wing surface. A stall strip is a long piece of material having a rectangular or triangular cross section. It is attached to a wing surface to simulate an ice horn. The strip's location on the wing, as well as its angle with respect to the wing, can have a large effect on the aerodynamic performance of the wing. Maximum lift coefficient, stall angle, maximum drag, and maximum change in lift coefficient are often all strongly affected by the location and angle of the stall strip on the wing. The stall bar orientation that results in the maximum degradation of these parameters is the critical condition. This orientation must be consistent with ice accretions that are to be expected within the certification envelope over the applicable phases of flight.

In the case of a control surface, ice accretion on the leading edge of a horizontal stabilizer, for instance, may be tolerable from the standpoint of lift and drag on the component; however, the ice accretion may diminish the effectiveness of the elevator. The ice that diminishes the elevator effectiveness most is the critical ice shape. This ice shape must be produced within the certification envelope and during the applicable phases of flight.

3.2 AN "AIRFOIL SENSITIVITY APPROACH" TO CRITICAL ICE SHAPES.

This approach is based on current knowledge and methods concerning airfoil sensitivity to contamination.

The intent of the FAA's icing regulations is to ensure that the certificated aircraft type has no unsafe characteristics in the most adverse icing conditions. Contemporary certification

engineering practice for most aircraft typically consists of a progressive process involving determination of impingement limits, ice shape determination, and testing in a tunnel or on a full-scale flight test article, ultimately concluded by flight in natural icing conditions. Such an approach may be characterized as comprising an intensive "inductive" process. The process relies on current tools (for example, computer codes, tunnels, or tankers) for determining ice shapes. It is dependent on individual expertise and judgment in determining the most severe icing conditions and critical ice shapes, and does not take place until late in the design process or until after that process is completed. Thus, the design may have been optimized for the uncontaminated state before icing has been considered.

Icing incidents and accidents have raised the possibility that not all potential problem areas are being examined and addressed during certification. An approach that could be supplementary to (and perhaps an alternative to some parts of) the current approach would place greater emphasis earlier in the process on the determination of the sensitivity of airfoil performance characteristics to contamination and less emphasis on the determination of actual ice shapes. Such an approach might be called a "deductive process," emphasizing a shift in emphasis. As used here, the term "deductive" process involves the determination of sensitivity of airfoil characteristics to contamination. Specifically, analysis of airfoil response to contamination may yield critical information on how the airfoil reacts to the effects of shapes as a function of the size and chordwise position of the test shape on the airfoil. This analysis contrasts with predicting ice shapes that would accrete in specific icing cloud conditions. The effects in one or more critical aerodynamic characteristics may then be evaluated to determine limits of ice protection in both chord and span, and acceptable decrement of the aircraft performance and handling characteristics. Some of the analyses may need to consider configuration-dependent design features as well as airfoil characteristics.

Performance and handling characteristics may be evaluated as the ultimate effect of the shape on the lift curve, drag polar, pitching moment, hinge moment, and related characteristics. Thus, it may be practical to make design and certification decisions weighting airfoil sensitivity more heavily than shapes determined using currently available tools.

The deductive approach described here was first researched by Jacobs [23] and has more recently been studied by Bragg, et al. [5], Papadakis, et al. [6], and others. The data of Jacobs was probably first applied in a deductive way by Johnson [24] who used it to argue for extending the boot further aft. Jacobs studied the aerodynamic effects of protuberances of varying height placed at the leading edge and at various chordwise locations. In general, the results of Jacobs and of Johnson showed that aft of the leading edge, a maximum decrement in lift and stall angle occurred at a specific chordwise location and that the adverse effect diminished aft of that position.

One conclusion is that understanding the type and magnitude of the aerodynamic decrements could make possible early consideration in the design process of degraded operational characteristics and other design features of the airplane relating to performance or handling characteristics. While the studies of Jacobs [23], Johnson [24], and other early researchers were limited in the scope of the aerodynamic characteristics examined and the shapes employed, the method has been expanded by contemporary investigators, and there is no reason that the technique could not be applied to various aerodynamic characteristics. Such sensitivity studies

may include more than one test shape, such as roughness elements and three-dimensional shapes. Appendix H lists 14 Code of Federal Regulations (CFR) Part 23, Subpart B requirements and a preliminary matrix showing which aerodynamic characteristics(s) may be relevant to each requirement.

Some manufacturers already rely in part on techniques of this general nature to determine the most adverse or "critical" accretion features for certain aerodynamic characteristics. These techniques may be applied during the preliminary design stage of product development to evaluate the iced-aircraft response characteristics of the design, possibly with the intent of modifying the design to improve its ice contaminated characteristics, or they may be used during flight test and certification. One current manufacturer employs certain stylized protuberance shapes during flight testing. Location, shape, and dimension parameters of the protuberance are based upon pre-existing knowledge of a shape, representative of the most adverse conditions that may be expected in the natural icing environment. That knowledge is tempered by past experience of the airfoil response.

In summary, deductive processes placing more emphasis on airfoil sensitivity to contamination, as opposed to inductive analyses relying more upon determining ice accretion shapes, may provide a rational supplement to preliminary design of the aircraft, design of the airfoil ice protection system, and also contribute to an acceptable and efficient means to demonstrate compliance.

3.3 A "COMPREHENSIVE AERODYNAMIC APPROACH" TO CRITICAL ICE SHAPES.

In developing an approach for the assessment of critical ice shapes, it can be instructive to consider what amounts to a technology roadmap. This roadmap is motivated by a critical ice shape approach based on an aerodynamic point of view. Not all of the technology and tools are currently available to fully exploit the aerodynamic ice shape assessment approach described below. This discussion will first describe technical elements that would constitute such an assessment approach, then suggest a set of research activities that could lead to the development of the requisite capability. This roadmap could then serve as guidance for long-term technical investment by interested research and regulatory organizations.

3.3.1 Concept.

The need for a "critical ice shape" is based on the idea that by finding what could conservatively be called the worst ice shape from an aerodynamic point of view, (within the constraints of the icing envelope and proposed flight operations) a manufacturer could demonstrate that the proposed aircraft could continue to operate with degraded but still acceptable performance. Current information on performance degradation associated with ice deposition suggests that in some, perhaps many, cases there is not one ice shape that would degrade all performance characteristics equally. Thus it may be desirable to evaluate performance features with respect to the minimal amounts of ice deposition required to exceed some critical level of performance (including control) degradation. Therefore, in this approach "critical" would be based on the minimum amount of degradation or change in an aerodynamic parameter that would result in a degradation of aircraft performance that significantly impacts the safety of flight.

The concept would be outlined as follows:

a. Determine the performance characteristics that should be evaluated, such as C_l, C_d, C_m.

b. Evaluate the critical values for each of these parameters for each surface of interest with consideration of different phases of flight.

c. Examine the roughness/protuberance or its features (i.e., horn length, horn angle, roughness level, ice mass, etc.) that can cause the surface of interest to fall below the critical level for each performance characteristic at each phase of flight.

d. Determine the icing conditions that could produce an ice accretion with these features.

This process would have the potential of comprehensively identifying the various icing conditions that could lead to failure of the aircraft system. As a result, appropriate ice protection schemes could be identified to insure that the aircraft would operate safely under the icing conditions deemed critical for the aircraft of interest. This would also allow the ice protection system to be designed to provide the level of protection deemed necessary to remain above the critical performance levels.

The process outlined above shifts the evaluation towards the examination of aerodynamic effects and away from the identification of a critical ice shape. This seems a more natural and rational approach and has the added benefit of identifying those characteristics of an ice accretion which play a critical role for a given icing scenario. This allows for greater consideration of icing effects during the design process and could potentially lead to the development of a more comprehensive understanding of the capabilities of the aircraft during an icing encounter.

3.3.2 Example.

As an example of the method described above, consider the task of determining the critical ice shape for the horizontal tail of an aircraft. Following the steps in the approach outlined above

a. The first step is to determine what level of degradation in lift, drag, pitching moment, hinge moment, rolling moment, etc., will present a potential safety problem in the various phases of flight. If we consider first the landing phase, the primary function of the horizontal tail is to provide down force to provide longitudinal trim for the aircraft. Assume that in the most severe combination of factors, airspeed, ground effect, wing flap setting, power setting, etc., that a C_L of 0.7 down is required to trim the aircraft. This must be produced at the tail angle-of-attack seen by the actual aircraft and with elevator deflection.

b. Now the designer needs to analyze what protuberance/roughness can produce this loss in lift performance of the horizontal tail. At this stage, this need not be a predicted ice accretion or roughness level but merely a roughness or protuberance with characteristics similar to environmental contamination. Situations to consider include, but should not be limited to, leading-edge horns of various sizes, locations, and angles; spanwise ridges of various heights and chordwise locations; localized surface roughness at various locations and sizes; the entire upper surface covered with roughness; etc. As a result of this

analysis, candidate roughness/protuberances are identified. Assume that in this case no roughness considered produced the critical loss in lift. However, leading-edge horns of greater than $h/c = 0.04$ located aft of $x/c = 0.01$ and approximately normal to the surface produce maximum lifts < 0.7. In addition, spanwise ridges greater than $h/c = 0.01$ located aft of $x/c = 0.55$ also cause $C_L < 0.7$ to be attained due to loss in elevator effectiveness.

c. Finally, the designer needs to determine if the roughness/protuberance that produces the critical loss in performance can be accreted within the assumed ice accretion envelope. For this example, it might be that the horn shape is too large to be accreted within the parameters of appendix C. However, runback scenarios may not exclude that a ridge could form under some conditions similar to the shape identified in step b. Therefore, the runback shape would be a critical ice accretion.

The analysis would then consider other flight phases and surfaces to determine if other critical ice accretions exist.

3.3.3 A Long-Term Research Strategy to Develop Tools for a Comprehensive Aerodynamic Approach.

The process described above requires a significant amount of analysis. As such, there is a need for the development of robust computational tools in order that a manufacturer can implement such a strategy without prohibitive costs in terms of dollars and labor that might be entailed for an experimentally based (as opposed to computationally based) approach. Thus, the proposed research plan is centered on computational flow dynamics (CFD) development with experimental work focused on validation and short-term evaluation of trends and relationships.

The ultimate tool that might be envisioned for such an analysis would be a design code which determines the ice shape and location that produce the critical aerodynamic loss, coupled with an inverse ice accretion code that identifies the icing condition that might produce such a shape. This tool could be used to examine an aircraft design for susceptibility to icing during various stages of flight. Such a tool does not exist at this time. Perhaps research into this field could be undertaken to determine what ice shape geometries produce the worst aerodynamic characteristics subject to constraints related to icing parameters such as ice accretion exposure time, cloud liquid water content, and droplet size. For now, this appears to be a more long-term objective but something that may be considered for a feasibility study.

In the more immediate future, there appear to be three elements of an overall research strategy that should be undertaken in a coordinated effort. These elements are depicted in figure 3 which shows a timeline and degree of complexity associated with each of the elements. The idea is that useful data, information, or tools can be developed at the end of each phase and thus provide return on investment throughout the life of the research effort. This would also allow for revision and refinement of the tasks constituting each of the elements as they progress.

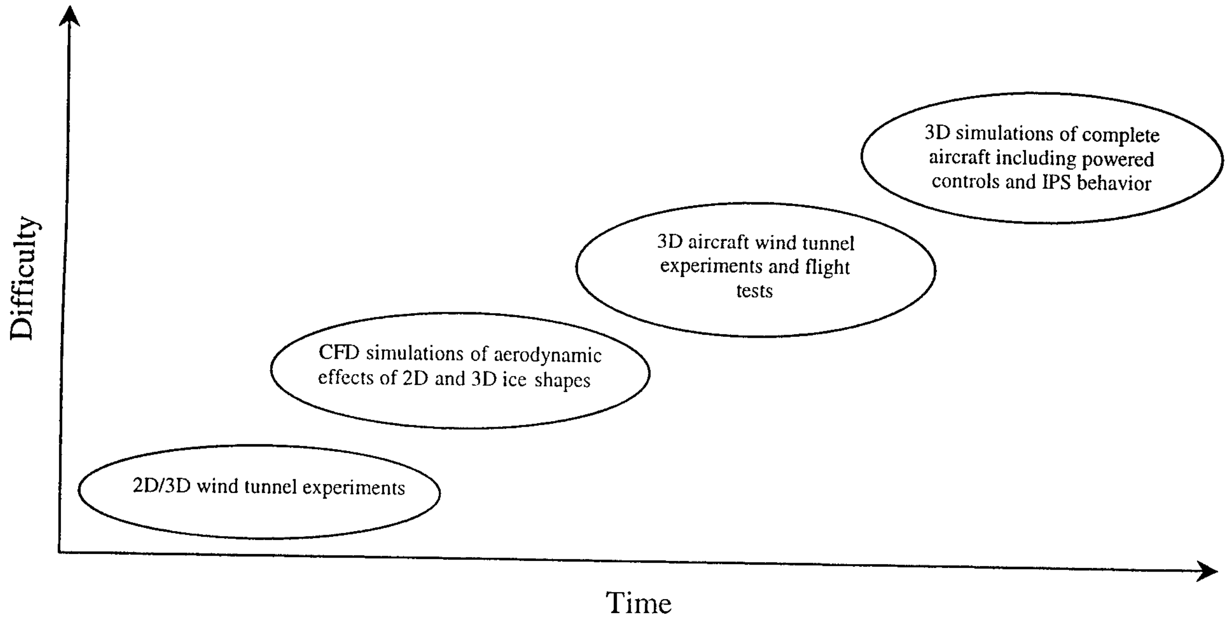

FIGURE 3. CRITICAL ICE SHAPE ANALYSIS DEVELOPMENT SPACE

The earliest phase would consist mainly of experimental efforts. These would be directed at providing early insight into trends in performance parameters with respect to ice shape features as well as into the relationships between the ice shape characteristics that might play a role in the critical limits associated with each performance parameter. Additionally these experimental activities would provide validation data for the evaluation of the computational tools.

Initially, the experimental work would focus on 2D airfoils and would augment research currently underway. (The literature study done for the survey of glaze ice accretion data showed that the great preponderance of the data is for 2D, single-element airfoils. The study indicates that more high quality aerodynamic data is needed even for the 2D, single-element case. This research would explore experimentally the relationship between roughness/protuberance characteristics (size, location, shape, horn angle, etc.) and degradation in C_l, C_d, C_m, and C_h. This research would also relate the performance degradation to airfoil geometry including flaps, slats, etc. The experimental research would be focused on understanding the relationship between roughness/protuberance geometry, airfoil geometry, and performance degradation, and would include a sensitivity analysis of these relationships.

The next part of the experimental research should explore the 3D effects. Initially this should include an extension of the 2D work. The research would focus on wings and add parameters such as sweep, twist, and taper to the model geometry variables. The protuberances tested would include geometry characteristics that are 3D such as swept-wing ice shape scallops and other spanwise variations. The final step in the experimental work suggested here would be to examine the complex 3D interactions that can occur on actual aircraft and affect the sensitivity of a design to ice accretion aerodynamic effects. These would include things like power effects, engine nacelle/wing interactions, wing/fuselage/nacelle interactions, etc. Aircraft manufacturers suggest that these interactions are very important and currently this knowledge appears to be

company proprietary, specific to classes of aircraft, and held by a relatively few practitioners. The magnitude and importance of these effects need to be identified and the most important ones studied in more detail. The goal should be to systematically study these effects experimentally so that this information is available for use by all participants in research, design, certification, and operation of aircraft. Understanding the 3D effects is important to full implementation of the critical ice shape assessment method outlined here.

The second phase of the effort would be centered on development of CFD analysis tools that can evaluate the effects of ice shapes on aerodynamic performance. The main thrust of this work would be on examination of the ability to predict aerodynamic performance degradation associated with unsteady, separated flow over rough surfaces. This will require associated efforts on grid generation and turbulence modeling in order to allow accurate simulation of such behavior. In addition to these development efforts sensitivity studies will be required to determine the accuracy required to provide acceptable determination of the critical ice shape feature associated with each performance characteristic.

Since CFD tools are currently still in development for clean airfoils, it may be beneficial to develop cooperative activities with mainstream CFD research organizations in order to maximize return on investment through utilization of existing experience in this field. This would suggest seeking out those research organizations that might be developing CFD tools to examine problems that contain one or more of the characteristics mentioned in the previous paragraph.

The final phase of the research plan would be directed at application of CFD tools to the simulation of actual flight maneuvers that may be undertaken during and/or subsequent to an icing encounter. For example, how might an unpowered aileron respond during a bank with various ice shape configurations on the leading edge? The creation of robust computational tools to provide this type of analysis would allow examination of dynamic behaviors associated with ice shape features and assist in the identification of potential or real accident scenarios.

Detailed plans for each of these phases would require a thorough examination of current capabilities and a feasibility analysis for determination of just how to extend current methods to meet the desired goals. A separate effort may be needed to address such issues and to provide a guide for investment in future research.

4. CONCLUSION.

The 12A Working Group identified approaches that can serve as the basis for improved methods and guidance in the determination of critical ice shapes. These approaches require research investment in both experimental data and improved analytical tools. The working group devoted most of one of its two meetings to discussion and prioritization of research investment. (See appendix I for a more complete presentation of the discussion topics and prioritization voting.) The consensus was that research was most needed now in the following areas:

- Characterization of ice roughness for different types of ice (sandpaper, residual/intercycle ice, glaze, etc.)

- Investigation of the aerodynamic effects resulting from parametric variation of characteristic ice accretion features (such as upper horn height and location)

- Investigation of aerodynamic effects resulting from variation of airfoil characteristics

The working group reached a consensus that all these items require experimental work, although it is hoped that computational tools, because of their versatility and relative affordability, will also be developed and utilized as fully as possible. These tools could be CFD tools, but could also be simpler methods allowing the estimation of 3D wing and airfoil results working from experimental 2D section data. High quality data, including those from wind tunnels capable of achieving high Reynolds numbers, are needed to adequately assess questions as to the influence of ice shape features on the aerodynamic effects of ice shapes. Fundamental work is needed in the measurement and quantification of ice roughness.

The consensus of the working group was that the next most important area of research was scaling, in particular, aerodynamic scaling (How should an ice shape accreted on a model of one size be scaled so that it will give the same aerodynamic effects on a model of another size?) and ice shape scaling methods (How can tunnel parameters be adjusted so that different combinations of parameters give comparable ice shapes?).

Additional recommendations were made to the FAA by members of the working group representing industry. They occur in subgroup reports which are not included in their entirety in this report. Although these recommendations were not included in the voting, extended discussions at the two meetings of the working group indicate substantial industry support for them. A key recommendation is for a process which is "clearly defined and endorsed by the FAA." Most of the other recommendations call for improvement to analytical tools by the research community, and acceptance of the tools by the FAA. These additional recommendations can be found in appendix J.

The working group hopes that its findings and recommendations will be useful to research organizations in formulating investment strategies for icing research.

5. REFERENCES.

1. FAA Aircraft Inflight Icing Plan, April 1997.

2. Olsen, William, Shaw, Robert, and Newton, James, "Ice Shapes and the Resulting Drag Increase for a NACA 0012 Airfoil," NASA TM 83556, January 1984. (E.122)

3. Bowden, D.T., "Effect of Pneumatic De-Icers and Ice Formations on Aerodynamic Characteristics of an Airfoil," NACA TN 3564, February 1956. (E.19)

4. Gray, V.H., "Correlations Among Ice Measurements, Impingement Rates, Icing Conditions and Drag of a 65A004 Airfoil," NACA TN 4151, February 1958. (E.60)

5. Kim, H.S. and Bragg, M.B., "Effects of Leading-Edge Ice Accretion Geometry on Airfoil Performance," AIAA-99-03150, June-July 1999. (E.98)

6. Papadakis, Michael, Alansatan, Sait, and Seltmann, Michael, "Experimental Study of Simulated Ice Shapes on a NACA 0011 Airfoil," AIAA-99-0096, January 1999. (E.126)

7. Addy, Harold E., Jr., Potapczuk, Mark G., and Sheldon, David W., "Modern Airfoil Ice Accretions," AIAA-97-0174 and NASA TM 107423, January 1997. (E.5)

8. Bragg, M.B., "Experimental Aerodynamic Characteristics of an NACA 0012 Airfoil With Simulated Glaze Ice," J. Aircraft, Vol. 25, No. 9, September 1988, pp 849-854. (E.24)

9. Bragg, Michael B., "An Experimental Study of the Aerodynamics of a NACA 0012 Airfoil With a Simulated Glaze Ice Accretion – Volume II," NASA CR 191007, March 1993. (E.25)

10. Bragg, M.B. and Coirier, W.J., "Detailed Measurements of the Flow Field in the Vicinity of an Airfoil with Glaze Ice," AIAA-85-0409, January 1985. (E.28)

11. Bragg, M.B. and Coirier, W.J., "Aerodynamic Measurements of an Airfoil With Simulated Glaze Ice," AIAA-86-0484, January 1986. (E.29)

12. Flemming, Robert J. and Lednicer, David A., "High Speed Ice Accretion on Rotorcraft Airfoils," NASA CR 3910, August 1985. (E.56)

13. Shin, Jaiwon and Bond, Thomas H., "Results of an Icing Test on a NACA 0012 Airfoil in The NASA Lewis Icing Research Tunnel," AIAA-92-0647 and NASA TM 105374, January 1992. (E.150)

14. Shin, Jaiwon and Bond, Thomas H., "Experimental and Computational Ice Shapes and Resulting Drag Increase for a NACA 0012 Airfoil," NASA TM 105743, January 1992. (E.151)

15. Abbott, Ira H. and von Doenhoff, Albert E., "Theory of Wing Sections," Dover, New York, 1959. (E.3)

16. Gray, V.H., "Prediction of Aerodynamic Penalties Caused by Ice Formations on Various Airfoils," NASA TN D-2166, 1964. (E.61)

17. Gray, V.H., "Correlation of Airfoil Ice Formations and Their Aerodynamic Effects With Impingement and Flight Conditions," SAE Preprint No. 225. (E.62)

18. Gray, Vernon H. and von Glahn, Uwe H., "Effect Of Ice and Frost Formations on Drag of NACA 651-212 Airfoil for Various Modes of Thermal Ice Protection," NACA RM E53C10, NACA TN 2962, June 1953. (E.63)

19. Gray, V.H. and von Glahn, U.H., "Aerodynamic Effects Caused by Icing of an Unswept NACA 65A-004 Airfoil," NACA TN 4155, February 1958. (E.64)

20. Bragg, M.B., "Rime Ice Accretion and Its Effect on Airfoil Performance," NASA CR 165599, March 1982. (E.21)

21. Ruff, G. and Anderson, D., "Quantification of Ice Accretions for Ice Scaling Evaluations," AIAA-98-0195, January 1998.

22. Brun, R. J., Gallagher, H. M., and Vogt, D. E., "Impingement of Water Droplets on NACA 65A004 Aerofoil [?] and Effect of Change in Airfoil Thickness From 12 to 4 Percent at 4° Angle of Attack," NACA TN 3047, November 1953.

23. Jacobs, Eastman N., "Airfoil Section Characteristics as Affected by Protuberances," NACA TR 446, 1933. (E.52)

24. Johnson, Clarence L., "Wing Loading, Icing and Associated aspects of Modern Transport Design," J Aeron Sci., Vol. 8, No. 2, December 1940, pp 43-54. (E.86)

APPENDIX A—TASK 12A IN FAA IN-FLIGHT AIRCRAFT ICING PLAN

ICE ACCRETION AND ITS EFFECTS ON PERFORMANCE/STABILITY AND CONTROL.

Task 12. Develop guidance material on ice accretion shapes and roughness and resultant effects on performance/stability and control. This material will be relevant to the identification and evaluation of critical ice shape features such as ice thickness, horn size, horn location, shape, and roughness.

A. The Federal Aviation Administration (FAA), along with industry and research organizations, shall form a working group to explore categories of ice accretions that represent potential safety problems on aircraft.

PLAN DETAILS, TASK 12A.

The certification process requires identification and evaluation of critical ice accretions. Criticality of possible ice accretions is not well understood, and guidance information is needed for compliance with established requirements. The working group will evaluate numerous ice shapes to help define areas of concern about the effects of ice accretion on airfoil performance and aircraft stability, control, and handling characteristics.

These ice accretion categories would include (but would not be limited to):

1. "Sandpaper" ice (a thin layer of ice composed of roughness elements)
2. Residual ice (ice remaining after a deicer cycle)
3. Rime ice
4. Glaze ice
5. Large-droplet ice (spanwise step accretions beyond the "normal" impingement zone)
6. Beak ice (single horn ice shape on the upper surface)
7. Intercycle ice (ice accumulated between deicer cycles)

These categories of ice would be considered during various phases of flight such as takeoff, landing, climb, hold, etc., for:

1. Operational ice protection systems
2. Failed ice protections systems
3. Unprotected surfaces

Responsible Parties. Aircraft Certification Service, FAA William J. Hughes Technical Center, NASA LeRC, Industry, Academia.

Schedule. December 1997: Publish a plan.

APPENDIX B—12A WORKING GROUP MEMBERS AND ATTENDEES

Name	Affiliation	Telephone Fax	E-mail Address
Harold Addy, Jr.	NASA Glenn Research	(216) 977-7467 (216)977-7469	h.e.addy@grc.nasa.gov
David Anderson	Ohio Aerospace Institute	(440)236-3596 (440)236-6652	105553.2676@compuserve.com
James Bettcher	Airline Pilots Association	(817)428-7654 (817)788-4760	Jimbettcher@compuserve.com
Thomas Bond	NASA Glenn Research Center	(216)433-3900 (216)977-7469	Tom.bond@grc.nasa.gov
Michael Bragg	University of Illinois-Dept. of Aeronautical & Astronautical Engineering	(217)244-5551 (217)244-0720	Mbragg@uiuc.edu
John Dow, Sr.	Federal Aviation Administration	(816) 426-6932 (816) 426-2169	John_dow@faa.gov
Eric Duvivier	JAA/DGAC-F	33 1 45526280 33 1 45526176	DUVIVIER_Eric@sfact.dgac.fr
Norman Ellis	De Havilland, Inc.	(416)375-3186 (416)375-7361	Nellis@dehavilland.ca
Colin Fender	Federal Aviation Administration	(425)227-2191 (425)227-1100	colin.fender@faa.dot.gov
Robert Flemming	Sikorsky Aircraft	(203)386-5789 (203)386-5925	rflemming@sikorsky.com
Steve Green	Air Line Pilots Association	(802)899-5471	72153.1651@compuserve.com
Dana Herring	Beech	(316)676-6718 (316)676-8889	Dana_Herring@Raytheon.com
Eugene Hill	Federal Aviation Administration	(425)227-1293 (425)227-1181	eugene.hill@faa.gov
Kathi Ishimaru	Federal Aviation Administration	(425)227-2674 (425)227-1100	kathi.ishimaru@faa.gov
Kichio Ishimitsu	Boeing	(206)234-1058 (206)237-8281	kichio.k.ishimitsu@boeing.com
Abdi Khodadoust	Boeing	(562) 593-9353 (562) 593-7593	abdollah.khodadoust@boeing.com
Michael Papadakis	Wichita State University	(316)978-5936 (316)978-3307	Papadaki@twsuvm.uc.twsu.edu
Mark Potapczuk	NASA Glenn Research	(216)433-3919 (216)977-7469	mark.g.potapczuk@grc.nasa.gov
James Riley	Federal Aviation Administration	(609)485-4144 (609)485-4005	James.t.riley@tc.faa.gov
Anil Shah	Boeing Commercial Airplane	(425)234-5908 (425)237-1313	anil.d.shah@boeing.com
David Sweet	BFGoodrich Aerospace-Ice Protection Systems	(330)374-3707 (330)374-2299	dsweet@bfgips.com

APPENDIX C—FAA IN-FLIGHT AIRCRAFT ICING PLAN SURVEY QUESTIONNAIRE, PART 1

(This survey primarily addresses airframe icing. It is not intended to address propulsion system or engine icing issues or propeller icing.)

1. If artificial (simulated) ice shapes are used to demonstrate compliance with in-flight icing certification requirements.

    1.1. How are the shapes and their attributes determined (details requested)?

    1.2. How are the ice accretion impingement limits determined and validated?

    1.3. Are current artificial ice shape definition processes satisfactory? What tools are employed to determine ice accretions (e.g., icing wind tunnel, computer code, etc.)? What are needed improvements?

    1.4. What rationale is used to select the shape used for certification?

2. Are critical ice shapes defined?

    2.1. How?

    2.2. Are intermediate ice features which may have smaller dimensions, more angular features or more adverse textures (such as granular roughness), but greater adverse aerodynamic effects considered?

    2.3. Are different ice shapes established to determine the most adverse effect on different aerodynamic characteristics, such as the handling qualities and performance?

    2.4. What are the flying qualities considered?

    2.5. What are the flight regimes and aircraft configurations considered?

    2.6. What types of ice are considered for each of the above cases?

    2.7. With the high lift surfaces extended, are ice accumulations on these surfaces considered?

    2.8. Is the effect on airplane performance and handling characteristics of ice accreted in one airplane configuration considered for subsequent airplane configurations?, e.g., is the effect of ice accreted in holding with flaps retracted considered when the flaps are extended for approach and landing?

    2.9. How are artificial (simulated) ice shapes validated?

3. To what extent are the effects of artificial (simulated) ice shapes on airplane performance and handling characteristics corroborated by flight testing in natural icing conditions.

APPENDIX D—DISCUSSION OF CURRENT METHODOLOGY–CRITICAL ICE SHAPES

D.1. INTRODUCTORY.

This appendix is based primarily upon industry response to the survey questions reproduced in appendix C of this report. They describe various methods used in the determination of critical ice shapes in certification of a commercial aircraft. The emphasis is on transport aircraft, but much of the material is applicable to other classes of aircraft.

A broad range of tools is used to determine ice shapes, including icing tunnels, dry wind tunnels, ice accretion codes, and heat transfer computer codes. Code of Federal (14 CFR Parts 23 and 25) allow use of these engineering tools, complementing flight testing in natural icing conditions, to verify the adequacy of aircraft ice protection systems for safe in-flight icing operations. However, these methodologies discussed in the following should not be construed as certification methods generally accepted by the Federal Aviation Administration (FAA) or other airworthiness authorities. Methodologies used to determine critical ice shapes should be included in regulation compliance plans that are negotiated with and accepted by airworthiness authorities for specific aircraft models.

The discussion employs the following definitions, based mainly on Society of Automotive Engineers Aerospace Information Report (SAE AIR) 1667.

Natural Icing – Icing that occurs during a flight in a cloud formed by natural processes in the atmosphere.

Artificial Icing – Icing that results in the formation of ice which is "real" ice, but which is formed by "artificial" means, that is, any means other than flight in atmospheric icing conditions. Such means include use of a spray rig on the ground (in a tunnel or other indoor or outdoor facility) or on a tanker.

Simulated Ice – Ice shapes that are fabricated from wood, epoxy, or other materials by any construction technique.

Computed (calculated) Ice – Ice shapes that are generated from computational fluid dynamics (CFD) tools.

Critical Ice Shape – See page 11 of the main text.

D.2. REVIEW OF METHODS—DETERMINATION OF ICE SHAPES.

The industry survey responses outlined various methods of determining the ice shapes. They are grouped into three methods and discussed below.

D.3. METHOD A: COMPUTATIONAL/ANALYTICAL.

Ice shapes are established using computer codes for the icing conditions defined in FAR Part 25 Appendix C. Unless the critical conditions are already known from prior evaluations, the ice shape analysis is done for a range of aircraft operational and icing conditions to search for

critical conditions. These calculations are performed for lifting surfaces, including wings and horizontal and vertical tail sections. Each protected and unprotected part of a lifting surface exposed to icing is analyzed. Each operational flight condition, such as takeoff, climb, cruise, hold, descent, and approach, is considered when selecting a critical ice shape.

The ice shape analysis is normally performed on a two-dimensional (2D) section normal to the leading edge, but three-dimensional (3D) codes may be used for some parts of certification analysis, if accepted by the authorities. In a 2D icing code used for a 3D problem the effective 2D angle-of-attack (AOA) is computed using a 3D flow code to take into account the 3D effects; then the resultant velocity and AOA are used for input to the 2D ice accretion code. The most prominent publicly available 3D ice accretions codes are not actually fully 3D, in that they use a 3D flow field generated by a commercially available solver, but incorporate ice accretion modeling which remains 2D. Accordingly they are sometimes referred to as quasi-2D or 2.5D.

Computed ice shapes generally correlated well to experimental ice shapes for cold temperature and low liquid water content (LWC) conditions. It has been generally accepted that ice accretion codes are less accurate in predicting ice shapes for warm temperatures and high LWCs. However, National Aeronautic and Space Administration (NASA) Glenn, the FAA 11A Working Group, and other organizations are currently engaged in more systematic assessment of ice accretion code performance that will permit more precise characterization of capabilities.

Two-dimensional codes may not be suitable to define shapes on some aircraft surfaces, such as protrusions (antennas, strakes, wing fences), and components that have a complex 3D geometry, such as fairing intersections, scoops, vents, radomes, and windshields. The residual ice from anti-ice and deice system operation typically are not predicted by such codes. Combinations of computer runs and photographs from tanker flights and natural icing encounters are used to approximate shapes for many areas on the aircraft that may accrete ice shapes, which are believed to not yet be predicted with sufficient accuracy by computer codes for certification work.

Ice accretion codes are not currently used to predict ice shapes on highly swept surfaces because they are not believed to be capable of representing the true effects of leading edge sweep on ice formations. Furthermore, codes are not used to predict the shapes of run-back ice in the case of a heated leading edge, because no code is believed to be capable of predicting run-back ice realistically. In this case, other methods, including the use of icing tunnels and tankers, have been used.

On a highly swept wing, the actual ice shape that would accrete would be a "lobster tail" shape. In certification practice, several 2D predictions at different span locations are combined to develop a simulated (fabricated) ice accretion that varies somewhat in size along the span, but is a solid shape, not a lobster tail shape with gaps between the ice sections. The case for the conservatism of this approach rests on the contention that the solid (no-gap) simulated shape would have a more severe aerodynamic effect than the lobster tail shape with gaps. Aerodynamic experts generally accept this view although there is relatively little data that bears directly on the question.

D.4. METHOD B: EXPERIMENTAL.

D.4.1 ICING TUNNELS.

Shapes have been determined by tests of full-scale leading-edge specimens of wings and other aircraft surfaces in an icing wind tunnel. Based mainly on photographic evidence, simulated (fabricated) ice shapes derived from tunnels are claimed to approximate the shapes produced during in-flight natural icing conditions. Quantitative comparison is difficult for a number of reasons, and has not been done in certification; nor have research organizations published much in this area.

Ice shape scaling and aerodynamic scaling of ice shape effects are sometimes necessary in the icing certification process, since the sizes of existing icing tunnels impose limitations on model size, and also since a tunnel may be unable to provide the desired icing conditions. Manufacturers provided little information on the scaling methods they employ, and discussions in the 12A Working Group meetings suggest that there is no consensus in industry as to the most suitable methods.

For a large wing section, a hybrid model with full-scale leading edge and a truncated aft section and trailing edge flap may be acceptable to the authorities if it is judged to produce a leading-edge flow field, resulting in essentially the same leading-edge impingement pattern as would occur on a full-scale model.

D.4.2 AIRBORNE ICING TANKERS.

Flying the test aircraft in an icing cloud generated behind an icing tanker is used to determine location and qualitative features of shapes. This method has been used to determine simulated (fabricated) shapes for nonlifting surfaces, (not airfoil-type geometries) or areas where theoretical methods for calculation of ice shapes may not be validated or accepted (for example, highly swept wings and other 3D geometries resulting in highly 3D flow). If this method is used to define simulated (fabricated) shapes on lifting surfaces, special care should be taken in calibration of the icing cloud.

D.4.3 NATURAL ICING FLIGHT TESTS.

In most icing certification programs, flight in natural icing conditions is done at the conclusion of the certification program, after flight testing with simulated ice shapes has already been completed. However, the natural icing tests mentioned here are additional flights, done earlier in the certification program for the purpose of determining the simulated (fabricated) shapes on noncritical parts of the aircraft for subsequent flight testing with simulated (fabricated) ice shapes. Natural encounters have been accepted by the authorities to define ice shapes for areas that are shown not to be critical for flight. The test aircraft is flown into the known icing conditions and the shapes are observed, photographed, and recorded by the video camera, and this documentation is used in fabricating the simulated ice shape for flight testing. This method is direct, but it is costly and time consuming.

D.5. METHOD C: EMPIRICAL.

This approach may combine Method A, Method B, and the applicant's engineering practices. One manufacturer uses only the water droplet trajectory impingement results from Method A to derive the impingement characteristics of the surface geometry. The ice shapes are then determined using icing tunnel-based correlations, relating icing conditions to ice shape features. Some aircraft manufacturers can draw on a broad databank of experience with ice shapes from icing tunnel tests and flight tests in natural icing conditions during past aircraft certification programs.

"Empirical" shapes such as sandpaper, rope, and beak ice shapes have been required by the FAA in some certification programs. For a short exposure, small amounts of simulated ice with a roughness height of 1 mm and a particle density of 8 to 10 grains per cm^2 has been used in some certification programs. For longer exposures simulated ice with a roughness height 3 mm with the same particle density has been used.

D.6. VALIDATION/SUBSTANTIATION OF METHODS.

When a code is proposed for use in a certification program, the applicant is responsible for providing validation data to the authorities to justify the use of the code.

The quantity and type of validation required may vary with the application and with the past experience of the responsible Aircraft Certification Office (ACO). The applicant works with the ACO to determine what kind of data is used, what kinds of quality checks are done, and how much data is examined in order to "validate" the code for a particular certification application. Historically, icing tunnel test data have been used to corroborate prediction capabilities. There is very little high-quality data available from natural icing flight tests to compare with an analysis. Basically, natural icing tests provide only qualitative ice shape information. The natural icing observations and photographs provide only the orientation, location, roughness, and the extent of the ice accretions at best.

A systematic validation approach for certification work has not been defined for analytical codes or icing facilities. The FAA has formed an 11A Working Group to identify formulate acceptance criteria for icing test facilities and analytical codes.

D.7. DETERMINATION OF CRITICAL ICE SHAPES.

Two scenarios for flight in icing conditions are considered in defining critical ice shapes to be flight tested: (a) normal system operation, and (b) failed system scenario. Experience has shown that glaze ice shapes usually have greatest aerodynamic impact. However, very rough accretions (represented by fabricated roughness) have sometimes been found to have an even greater impact for some maneuvers and classes of aircraft because the roughness can induce lifting surface stall.

One approach that has been followed in the determination of a critical ice shape is as follows:

The first step is the determination of the droplet diameter that will provide the highest accretion rate on the airfoil within the FAR Part 25 Appendix C conditions. The droplet size which results in the largest water catch rate is selected for ice shape development. Ambient temperatures selected are those which produce a total temperature near freezing for fixed wing aircraft. The

temperature for rotary wing aircraft will be that temperature associated with full-span icing. Ice shape sensitivities to altitude are included within the ice shape selection matrix.

The second step consists in determining, for each flight phase, the combination of flight and icing conditions that satisfy the following:

- highest accretion rate
- double horn ice shapes or beak ice shapes (essentially for total temperature close to 0°C for a fixed wing aircraft) as suggested within JAR AMJ 25.1419
- longest exposure time

The purpose of the "normal system operation" scenario is to produce the ice accretion on the unprotected areas of the aircraft which would result from takeoff, climb, descent and holding in FAR Part 25 Appendix C "Continuous Maximum" icing conditions for an appropriate exposure duration with normal ice protection system operation. The protected surfaces are considered to be free from any ice accretion, while the unprotected surfaces, in general, are exposed to icing conditions for up to 45 minutes.

The purpose of the "failed system" scenario is to define the ice shape that results from a single failure in the ice protection system. The icing exposure for the protected surfaces is taken as the time to exit the icing condition after the system failure. Certification programs have used 50 percent of the exposure in holding operation of the aircraft for the failed system scenario. That is, the exposure has been taken to be as much as 22.5 minutes in icing conditions.

Flight conditions such as airspeed and angle of attack are specified for the aircraft at maximum design landing gross weight to determine the ice shape. Average values for aircraft angle of attack are typically used. Airfoil sections are selected for ice accretion analysis and include, but are not limited to, the root and tip sections of the wing and the tail. In addition, unprotected lifting and nonlifting sections are identified to account for aerodynamic and/or drag effects.

For the wing and horizontal tail in holding conditions, the calculated shapes are examined to determine the most critical, which is often the one having the largest horn projection height on the lifting surface. Shapes on other surfaces are calculated for the same condition.

Shapes are derived for all flight conditions in which it is considered possible to encounter ice. Both rime and glaze shapes are reviewed. Based on engineering experience, judgment supported with wind tunnel tests and including knowledge of the influence on lift and drag from aerodynamic disturbances on airfoils, the shapes are chosen to represent the critical ice shapes. Also, the selected ice shapes are evaluated with respect to criteria that will disturb flow conditions the most. Glaze shapes with horn lengths protruding normal to the local flow direction have been shown to produce large drag penalties. If there is any question as to which shape is more critical, each shape in question is tested. New analytical methods are currently being developed to estimate maximum lift and drag to help make this determination.

The trimming condition that gives the worst horn shape on the lower surface may be selected for the tailplane. The worst horn positions from an aerodynamic perspective are assumed to be those that are farthest around the lifting surface measured from the leading edge.

D.8. FABRICATION OF 3D SIMULATED ICE SHAPES FOR ATTACHMENT TO AIRCRAFT SURFACES.

The simulated (fabricated) ice shapes used on the aircraft are actual or simplified envelopes of ice forms determined for various spanwise sections of the airfoil. The shape definitions in terms of characteristic dimensions are used to fabricate the simulated shapes. Intermediate positions are defined by linear interpolation between sections and extrapolation to the root and the tip. Surface textures of these simulated ice shapes are defined according to the aircraft manufacturer's experience and AMJ 25.1419 (JAR 25) requirements. One manufacturer has used crushed walnut shells for the surface texture on the flight test shapes. These shapes are fastened to the wing leading edge and used for handling and for performance testing.

D.9. CONCLUDING REMARKS.

An aircraft may be certified using a combination of the methods discussed above, drawing upon the strengths of each. The aircraft manufacturer conducts a detailed study to determine the airplane performance for combinations of ice shape and airplane configuration. This type of analysis usually includes results from wind tunnel studies, a review of ancestral data for that airplane type (if it exists), and flight test verification of combinations considered most critical. Despite the improvements that has been made in the various methods in recent years, critical ice shapes can be highly configuration dependent, and their determination can be highly dependent on both engineering judgment and actual flight test experience.

As an example, for T-tail aircraft, one manufacturer has found that the pushover maneuver is considered a good indication of stick force availability to control the aircraft in the longitudinal axis. This test is therefore conducted with a combination of ice shapes on the horizontal tail (and the wing, if required) to determine the stick force margin available for airplane controllability. For one T-tail aircraft type this could be, for example, a 30-min ice shape on the horizontal tail at landing flaps, while for another T-tail aircraft type the critical shape might be a 15-min ice shape on the wing at takeoff flaps. Airplanes with conventional tail design usually have the engines mounted under the wings. The performance of this type of design could be assessed differently with ice shapes (on the wings and/or tail).

Another example is the assessment of anti-icing failure modes and the probability of occurrence for each failure mode. The critical ice shape would then be the cyclical ice shape generated as a result of the part-time anti-icing system operation for a given flap setting, during approach or takeoff.

This appendix has emphasized the heavy reliance on engineering judgment in determination of critical ice shapes in current certification practice. As in other areas of certification where this is the case, this may necessitate a conservative approach in order to ensure safety. A goal of the FAA, NASA, other research organizations, and industry is to reduce reliance on engineering judgment through the development, validation, and acceptance of improved icing simulation methods, particularly analytical computer codes. Although it is not anticipated that significant reliance on engineering judgment will be eliminated from icing certification work, reducing reliance upon it through acceptance of simulation tools is the most promising path to better standardization and guidance in determination of critical ice shapes.

APPENDIX E—BIBLIOGRAPHY OF AERODYNAMIC EFFECTS

1. Abbott, Frank T., Jr. and Turner, Harold R., Jr., "The Effects of Roughness at High Reynolds Numbers on the Lift and Drag Characteristics of Three Thick Airfoils," NACA ACR No. L4H21, August 1944 (Wartime Report No. L-46).

2. Abbott, Ira H., "The Drag of Two Streamline Bodies as Affected by Protuberances and Appendages," NACA TR 451, September 1932.

3. Abbott, Ira H. and von Doenhoff, Albert E., *Theory of Wing Sections*, Dover, New York, 1959.

4. Abbott, Ira H., von Doenhoff, Albert E., and Stivers, L.S., "Summary of Airfoil Data," NACA Report 824, 1945.

5. Addy, Harold E., Jr, Potapczuk, Mark G., and Sheldon, David W., "Modern Airfoil Ice Accretions," AIAA-97-0174 and NASA TM 107423, January 1997.

6. Ashenden, Russell, "Airfoil Performance Degradation by Supercooled Cloud, Drizzle, and Rain Drop Icing," M.S. Thesis, Dept. of Atmospheric Science, Univ. of Wyoming, Laramie, WY, 1996

7. Ashenden, Russell, Lindberg, William, Marwitz, John D., and Hoxie, Benjamin, "Airfoil Performance Degradation by Supercooled Cloud, Drizzle, and Rain Drop Icing," J. Aircraft, Vol. 33, No. 6, November-December 1996, pp. 1040-1046.

8. Ashenden, Russell, Lindberg, William and Marwitz, John D., "Two-Dimensional Airfoil Performance Degradation Because of Simulated Freezing Drizzle," J. Aircraft, Vol. 35, No. 6, November-December 1998, pp. 905-911.

9. Ashenden, Russell and Marwitz, John D., "Turboprop Aircraft Performance Response to Various Environmental Conditions," J. Aircraft, Vol. 34, No. 3, May-June 1997, pp. 278-287.

10. Bartlett, C.S., "The Effect of Experimental Uncertainties on Icing Test Results," AIAA-90-0665, January 1990.

11. Bezos, Gaudy M., "Results of Aerodynamic Testing of Large-Scale Wing Sections in a Simulated Natural Rain Environment," AIAA-90-0486, January 1990.

12. Bilanin, A., "Scaling Laws for Testing of High Lift Airfoils Under Heavy Rainfall," AIAA-85-0257, January 1985.

13. Bilanin, A.J. and Chua, K., "Mechanisms Resulting in Accreted Ice Roughness," AIAA-92-0287, January 1992.

14. Bilanin, A.J., Quackenbush, T.R., and Feo, A., "Feasibility of Predicting Performance Degradation of Airfoils in Heavy Rain," NASA CR 181842, June 1989.

15. Bleeker, W., "Einige Bemerkungen über Eisansatz an Flugzeugen," Meteorologische Zeitschrift, September 1932, pp. 349-354. (Also available as NACA TM 1027.)

16. Boer, J.N. and van Hengst, J., "Aerodynamic Degradation Due to Distributed Roughness on High Lift Configuration," AIAA-93-0028, January 1993.

17. Boermans, L.M.M. and Selen, H.J.W., "Design and Tests of Airfoils for Sailplanes With Application to the ASW-19b," ICAS-82-5.2.2, 1982.

18. Bond, Thomas H., Flemming, Robert J., and Britton, Randall K., "Icing Tests of a Model Main Rotor," Proceedings of the 46th Annual American Helicopter Society Forum, Volume 1, May 1990.

19. Bowden, D.T., "Effect of Pneumatic Deicers and Ice Formations on Aerodynamic Characteristics of an Airfoil," NACA TN 3564, February 1956.

20. Bowden, D.T., Gensemer, A.E., and Speen, C.A., "Engineering Summary of Airframe Icing Technical Data," FAA, FAA-ADS-4, 1964.

21. Bragg, M.B., "Rime Ice Accretion and Its Effect on Airfoil Performance," NASA CR 165599, March 1982.

22. Bragg, M.B., "Effect of Geometry on Airfoil Icing Characteristics," J. Aircraft, Vol. 21, No. 7, July 1984, pp. 505-511.

23. Bragg, Michael B., "An Experimental Study of the Aerodynamics of a NACA 0012 Airfoil With a Simulated Glaze Ice Accretion," NASA CR 179571, January 1987.

24. Bragg, M.B., "Experimental Aerodynamic Characteristics of an NACA 0012 Airfoil With Simulated Glaze Ice," J. Aircraft, Vol. 25, No. 9, September 1988, pp. 849-854.

25. Bragg, Michael B., "An Experimental Study of the Aerodynamics of a NACA 0012 Airfoil With a Simulated Glaze Ice Accretion-Volume II," NASA CR 191007, March 1993.

26. Bragg, M.B., "Aircraft Aerodynamic Effects Due to Large-Droplet Ice Accretions," AIAA-96-0932, January 1996.

27. Bragg, M.B., "Aerodynamics of Supercooled Large-Droplet Ice Accretions and the Effect on Aircraft Control," Proceedings of the FAA International Conference on Aircraft Inflight Icing, Springfield, VA, DOT/FAA/AR-96/81, II, 1996, pp. 387-399.

28. Bragg, M.B. and Coirier, W.J., "Detailed Measurements of the Flow Field in the Vicinity of an Airfoil With Glaze Ice," AIAA-85-0409, January 1985.

29. Bragg, M.B. and Coirier, W.J., "Aerodynamic Measurements of an Airfoil With Simulated Glaze Ice," AIAA-86-0484, January 1986.

30. Bragg, M.B., Cummings, M.J., Lee, S., and Henze, C.M., "Boundary Layer and Heat-Transfer Measurements on an Airfoil with Simulated Ice Roughness," AIAA-96-0866, January 1996.

31. Bragg, M.B. and Gregorek, G.M., "Aerodynamic Characteristics of Airfoil With Ice Accretions," AIAA-82-0282, January 1982.

32. Bragg, M.B. and Gregorek, G.M., "Environmentally Induced Surface Roughness on Laminar Flow Airfoils: Implications for Flight Safety," AIAA-89-2049, July-August 1989.

33. Bragg, M.B., Gregorek, G.M., and Lee, J.D., "Airfoil Aerodynamics in Icing Conditions," J. Aircraft, Vol. 23, No. 1, January 1986, pp. 76-81.

34. Bragg, M.B., Gregorek, G.M., and Shaw, R.J., "Wind Tunnel Investigation of Airfoil Performance Degradation Due to Icing," AIAA-82-0582, January 1982.

35. Bragg, M.B., Heinrich, D.C., Valarezo, W.O., and McGhee, R.J., "Effect of Underwing Frost on a Transport Aircraft Airfoil at Flight Reynolds Number," J. Aircraft, Vol. 31, No. 6, November–December 1994, pp. 1372-1379.

36. Bragg, M.B., Kerho, M.F., and Cummings, M.J., "Effect of Initial Ice Roughness on Airfoil Aerodynamics," AIAA-94-0800, January 1994.

37. Bragg, M.B., Kerho, M.F., and Cummings, M.J., "Airfoil Boundary Layer Due to Large Leading-Edge Roughness," AIAA-95-0536, January 1995.

38. Bragg, M.B., Kerho, M.F., and Khodadoust, A., "LDV Flow Field Measurements on a Straight and Swept Wing With a Simulated Ice Accretion," AIAA-93-0300, January 1993.

39. Bragg, M.B., Khodadoust, A., and Kerho, M., "Aerodynamics of a Finite Wing With Simulated Ice," Computational and Physical Aspects of Aerodynamic Flows, Long Beach, CA, January 1992.

40. Bragg, M.B., Khodadoust, A., and Spring, S.A., "Measurements in a Leading-Edge Separation Bubble Due to a Simulated Airfoil Ice Accretion," AIAA Journal, Vol. 30, No. 6, June 1992, pp. 1462-1467.

41. Britton, Randall K., "Ongoing Development of a Computer Jobstream to Predict Helicopter Main Rotor Performance in Icing Conditions," NASA CR 187076, February 1991.

42. Britton, Randall K., "Development of an Analytical Method to Predict Helicopter Main Rotor Performance in Icing Conditions," AIAA-92-0418, January 1992.

43. Brumby, R.E., "Wing Surface Roughness, Cause and Effect," DC Flight Approach, January 1979.

44. Brumby, R.E., "The Effects of Wing Contamination on Essential Flight Characteristics," Douglas Paper No. 8127, presented at the SAE Aircraft Ground Deicing Conference, Denver, September 20-22, 1988.

45. Brumby, R.E., "The Effect of Wing Ice Contamination on Essential Flight Characteristics," Paper 2, AGARD CP-496, Effects of Adverse Weather on Aerodynamics, Proceedings of the 68th AGARD Fluid Dynamics Panel Specialists Meeting, April–May 1991.

46. Calay, Rajnish K., Holdø, Arne E., Mayman, Philip, and Lun, Isaac, "Experimental Simulation of Runback Ice," J. Aircraft, Vol. 34, No. 2, March–April 1997, pp. 206–212.

47. Carbonaro, M., "Aerodynamic Effects of De/Anti-Icing Fluids, and Description of a Facility and Test Technique for Their Assessment," Paper 18, AGARD CP-496, Effects of Adverse Weather on Aerodynamics, Proceedings of the 68th AGARD Fluid Dynamics Panel Specialists Meeting, April–May 1991.

48. Cebeci, T., "Effects of Environmentally Imposed Roughness on Airfoil Performance," NASA CR 179639, June 1987.

49. Cooper, W.A., Sand, W.R., Politovich, M.K., and Veal, D.L., "Effects of Icing on Performance of a Research Airplane," J. Aircraft, Vol. 21, No. 9, September 1984, pp. 708–715.

50. Dryden, H.L., "Review of Published Data on the Effect of Roughness on Transition From Laminar to Turbulent Flow," J. Aeron. Sci., Vol. 20, No. 7, July 1953, pp. 477–482.

51. Dunham, R. Earl, Jr., Bezos, Gaudy M., Gentry, Garl L., Jr., and Melson, Edward Jr., "Two-Dimensional Wind Tunnel Tests of a Transport-Type Airfoil in a Water Spray," AIAA-85-0258, January 1985.

52. Dunham, Dana J., Dunham, R.Earl, Jr., and Bezos, Gaudy M., "A Summary of NASA Research on Effects of Heavy Rain on Airfoils," Paper 15, AGARD CP-496, Effects of Adverse Weather on Aerodynamics, Proceedings of the 68th AGARD Fluid Dynamics Panel Specialists Meeting, April–May 1991.

53. Dunn, Timothy A. and Loth, Eric, "Effects of Simulated-Spanwise-Ice Shapes on Airfoils: Computational Investigation," AIAA-99-0093, January 1999.

54. Flemming, Robert J., Bond, Thomas H., and Britton, Randall K., "Results of a Sub-Scale Model Rotor Icing Test," AIAA-91-0660, January 1991.

55. Flemming, Robert J., Britton, Randall K., and Bond, Thomas H., "Model Rotor Icing Tests in the NASA Lewis Icing Research Tunnel," Paper 9, AGARD CP-496, Effects of Adverse Weather on Aerodynamics, Proceedings of the 68th AGARD Fluid Dynamics Panel Specialists Meeting and NASA TM 104351, April–May 1991.

56. Flemming, Robert J. and Lednicer, David A., "High Speed Ice Accretion on Rotorcraft Airfoils," NASA CR 3910, August 1985.

57. Ferguson, S., Mullins, B., Jr., Smith, D., and Korkan, K., "Full-Scale Empennage Wind Tunnel Test to Evaluate Effects of Simulated Ice on Aerodynamic Characteristics," AIAA-95-0451, January 1995.

58. Fiddes, S.P., Kirby, D.A., Woodward, D.S., and Peckham, D.H., "Investigation Into the Effects of Scale and Compressibility on Lift and Drag in the RAE 5m Pressurized Low-Speed Wind Tunnel," Aeronautical Journal, Paper No. 1302, March 1985.

59. Gelder, T.F., Lewis, J.P., and Koutz, S.L., "Icing Protection for a Turbojet Transport Airplane: Heating Requirements, Methods of Protection, and Performance Penalties," NACA TN 2866, January 1953.

60. Gray, V.H., "Correlations Among Ice Measurements, Impingement Rates, Icing Conditions and Drag of a 65A004 Airfoil," NACA TN 4151, February 1958.

61. Gray, V.H., "Prediction of Aerodynamic Penalties Caused by Ice Formations on Various Airfoils," NASA TN D-2166, 1964.

62. Gray, V.H., "Correlation of Airfoil Ice Formations and Their Aerodynamic Effects With Impingement and Flight Conditions," SAE Preprint No. 225.

63. Gray, Vernon H. and von Glahn, Uwe H., "Effect of Ice and Frost Formations on Drag of NACA 651-212 Airfoil for Various Modes of Thermal Ice Protection," NACA RM E53C10, NACA TN 2962, June 1953.

64. Gray, V.H. and von Glahn, U.H., "Aerodynamic Effects Caused by Icing of an Unswept NACA 65A-004 Airfoil," NACA TN 4155, February 1958.

65. Grigson, C.W.B., "Nikuradse's Experiment," AIAA Journal, Vol. 22, No. 7, July 1984, pp. 999–1001.

66. Gulick, Beverly G., "Effects of Simulated Ice Formation on the Aerodynamic Characteristics of an Airfoil," NACA WR L-292, May 1938.

67. Haines, P.A. and Luers, J.K., "Aerodynamic Penalties of Heavy Rain on a Landing Aircraft," NASA CR 156885, July 1982.

68. Hansman, R.J., "Microphysical Factors Which Influence Ice Accretion," Proceedings of the First Bombardier International Workshop on Aircraft Icing/Boundary-Layer Stability and Transition, Montreal, Canada, 1993, pp. 86–103.

69. Hansman, R.J., Jr. and Barsotti, M.F., "The Aerodynamic Effect of Surface Wetting Characteristics on a Laminar Flow Airfoil in Simulated Heavy Rain," AIAA-85-0260, January 1985.

70. Hansman, R.J., Breuer, K.S., Hazan, D., Reehorst, A., and Vargas, M., "Close-Up Analysis of Aircraft Ice Accretion," AIAA-93-0029, January 1993.

71. Hansman, R.J., Reehorst, A., and Sims, J., "Analysis of Surface Roughness Generation in Aircraft Ice Accretion," AIAA-92-0298, January 1992.

72. Hansman, R.J. and Turnock, S.R., "Investigation of Surface Water Behavior During Glaze Ice Accretion," J. Aircraft, Vol. 26, No. 2, February 1989, pp. 140-147.

73. Hastings, Earl C., Jr. and Manuel, Gregory S., "Measurements of Water Film Characteristics on Aircraft Surfaces From Wind Tunnel Tests," AIAA-85-0259, January 1985.

74. Hill, E.G. and Zierten, T.A., "Aerodynamic Effects of Aircraft Ground De/Anti-Icing Fluids," J. Aircraft, Vol. 30, No. 1, January-February 1993, pp. 24-34.

75. Hoerner, S.F., Fluid-Dynamic Lift, published by the author, 1965.

76. Hoerner, S.F. and Borst, H.V., Fluid-Dynamic Lift, published by the author, 1975.

77. Holmes, E., Obara, C. and Yip, L., "Natural Laminar Flow Experiments on Modern Airplane Surfaces," NASA Technical Paper 2256, June 1984.

78. Hooker, Ray W., "The Aerodynamic Characteristics of Airfoils as Affected by Surface Roughness," NACA TN 457, April 1933.

79. Hoxie, B., "Experimental Study of the Effect of Ice Accretion on Wing Performance," Research Experiences in Fluid Mechanics, Department of Mechanical Engineering, University of Wyoming, August 1995.

80. Ingelman-Sundberg, M., Trunov, O.K., and Ivaniko, A., "Methods for Prediction of the Influence of Ice on Aircraft Flying Characteristics," Report JR-1, a joint report from the Swedish-Soviet Working Group on Scientific-Technical Cooperation in the Field of Flight Safety, 6th Meeting, 1977.

81. Jackson, Darren G. and Bragg, Michael B., "Aerodynamic Performance of an NLF Airfoil With Simulated Ice," AIAA-99-0373, January 1999.

82. Jacobs, Eastman N., "Airfoil Section Characteristics as Affected by Protuberances," NACA TR 446, 1933.

83. Jacobs, Eastman N. and Abbott, Ira H., "The NACA Variable-Density Wind Tunnel," NACA TR 416, 1932.

84. Jacobs, Eastman N. and Sherman, Albert, "Wing Characteristics as Affected by Protuberances of Short Span," NACA TR 449, 1933.

85. Jeck, R., "A Workable, Aircraft-Specific Icing Severity Scheme," AIAA-98-0094, January 1998.

86. Johnson, Clarence L., "Wing Loading, Icing and Associated aspects of Modern Transport Design," J Aeron Sci., Vol. 8, No. 2, December 1940, pp. 43-54.

87. Jones, R. and Williams, D.H., "The Effect of Surface Roughness on the Characteristics of the Aerofoils NACA 0012 and RAF 34," British ARC, R&M No. 1708, 1936.

88. Kerho, M.F., "Effect of Large Distributed Roughness Near an Airfoil Leading Edge on Boundary-Layer Development and Transition," Ph.D. Dissertation, Dept. of Aeronautical and Astronautical Engineering, University of Illinois at Urbana-Champaign, Urbana, IL, 1995.

89. Kerho, M.F. and Bragg M.B., "Effect of Large Distributed Leading-Edge Roughness on Boundary-Layer Development and Transition," AIAA-95-1803, January 1995.

90. Kerho, M.F. and Bragg, M.B., "Airfoil Boundary-Layer Development and Transition With Large Leading-Edge Roughness," AIAA Journal, Vol. 35, No. 1, January 1997, pp. 75-84.

91. Kerho, M.F., Bragg, M.B., and Shin, J., "Helium Bubble Flow Visualization of the Spanwise Separation on a NACA 0012 With Simulated Glaze Ice," AIAA-92-0413 and NASA TM 105742, January 1992.

92. Khodadoust, Abdollah, "A Flow Visualization Study of the Leading-Edge Separation Bubble on a NACA 0012 Airfoil With Simulated Glaze Ice," M.S. Thesis, Ohio State University, June 1987 and NASA CR 180846, January 1988.

93. Khodadoust, A., "Effect of a Simulated Glaze Ice Shape on the Aerodynamic Performance of a Rectangular Wing," AIAA-92-4042, 1992.

94. Khodadoust, A. and Bragg, M.B., "Aerodynamics of a Finite Wing With Simulated Ice," J. Aircraft, Vol. 32, No. 1, January-February 1995, pp. 137-144.

95. Khodadoust, A., Bragg, M.B. and Kerho, M., "LDV Measurements on a Rectangular Wing With a Simulated Glaze Ice Accretion," AIAA-92-2690, 1992.

96. Khodadoust, A., Bragg, M.B., Kerho, M., Wells, S., and Soltani, M. R., "Finite Wing Aerodynamics With Simulated Glaze Ice," AIAA-92-0414, January 1992.

97. Khodadoust, A., Dominik, C. J., Shin, J., and Miller, D., "Effect of In-Flight Ice Accretion on the Performance of a Multi-Element Airfoil," Proceedings of the Aircraft Icing Symposium, Montreal, Canada, September 1995.

98. Kim, H.S. and Bragg, M.B., "Effects of Leading-Edge Ice Accretion Geometry on Airfoil Performance," AIAA-99-03150, June-July 1999.

99. Kind, R.J. and Lawrysyn, M.A., "Effects of Frost on Wing Aerodynamics and Takeoff Performance," Paper 8, AGARD CP-496, Effects of Adverse Weather on Aerodynamics, Proceedings of the 68th AGARD Fluid Dynamics Panel Specialists Meeting, April–May 1991.

100. Kind, R.J. and Lawrysyn, MA., "Performance Degradation Due to Hoar Frost on Lifting Surfaces," Canadian Aeronautics and Space Journal, Vol. 38, No. 2, June 1992, pp. 62-70.

101. Kind, R.J. and Lawrysyn, M.A., "Aerodynamic Characteristics of Hoar Frost Roughness," AIAA Journal, Vol. 30, No. 7, July 1992, pp. 1703-1707.

102. Kirby, Mark S. and Hansman, R. John, "An Experimental and Theoretical Study of the Ice Accretion Process During Artificial and Natural Icing Conditions," NASA CR 182119, and DOT/FAA/CT-87/17, April 1988.

103. Kirchner, R.D., "Water Bead Formation in Glaze Icing Conditions," AIAA-95-0539, January 1995.

104. Korkan, K.D., Dadone, L. and Shaw, R.J., "Performance Degradation of Helicopter Rotor Systems in Forward Flight Due to Rime Ice Accretions," AIAA-83-0029, January 1983.

105. Kuethe, A. and Chow, C., "Foundations of Aerodynamics," 5th ed., John Wiley & Sons, Inc., New York, 1998.

106. Langmuir, Irving and Blodgett, Katharine B., "A Mathematical Investigation of Water Droplet Trajectories," Army Airforce Technical Report No. 5418, 1946 and General Electric Report No. RL-225, June 1949.

107. Laschka, E. and Jesse, R.E., "Determination of Ice Shapes and Their Effect on the Aerodynamic Characteristics for the Unprotected Tail of the A 300," proceedings of ICAS, Haifa, Israel, August 1974, pp. 409-418.

108. Leckman, P.R., "Qualification of Light Aircraft for Flight in Icing Conditions," SAE Paper 710394, 1971.

109. Lee, S. and Bragg, M., "Effects of Simulated-Spanwise-Ice Shapes on Airfoils: Experimental Investigation," AIAA-99-0092, January 1999.

110. Lee, S., Dunn, T., Gurbacki, H.M., Bragg, M.B., and Loth, E., "An Experimental and Computational Investigation of Spanwise-Step-Ice Shapes on Airfoil Aerodynamics," AIAA-98-0490, January 1998.

111. Leurs, J.K. and Haines, P.A., "Experimental Measurements of Rain Effects on Aircraft Aerodynamics," AIAA-83-0275, January 1983.

112. Lewis William and Perkins, Porter J., "A Flight Evaluation and Analysis of the Effect of Icing Conditions on the PG-2 Airship," NACA TN 4220, April 1958.

113. Ljungstroem, B.L.G., "Wind Tunnel Investigation of Simulated Hoar Frost on a Two-Dimensional Wing Section With and Without High-Lift Devices," Report FFA-AU-902, Aeronautical Research Institute of Sweden (FFA), April 1972.

114. Lynch, Frank T., Valarezo, Walter O., and McGhee, Robert J., "The Adverse Aerodynamic Impact of Very Small Leading-Edge Ice (Roughness) Buildup on Wings and Tails," Paper 12, AGARD CP-496, Effects of Adverse Weather on Aerodynamics, Proceedings of the 68th AGARD Fluid Dynamics Panel Specialists Meeting, April-May 1991.

115. McMasters, J.H. Roberts, W.H., and Payne, F.M., "Recent Air-Freon Tests of a Transport Airplane in High Lift Configurations," AIAA-88-2034, 1988.

116. Maresh, J.L. and Bragg, M.B., "The Role of Geometry in Minimizing the Effect of Insect Contamination of Laminar Flow Sections," AIAA-84-2170, August 1984.

117. Messinger, B.L., "Equilibrium Temperature of an Unheated Icing Surface as a Function of Airspeed," J. Aeron. Sci., Vol. 20, No. 1, January 1953, pp. 29-42.

118. Miller, T.L., Korkan, K.D., and Shaw, R.J., "Statistical Study of an Airfoil Glaze Ice Drag Coefficient Correlation," SAE Paper 830753, April 1983.

119. Morelli, J.P., "Flight Test Wing Surface Roughness Effects for Development of an Airfoil Surface Contamination Detection System," McDonnell Douglas Corporation Report No. MDC-96K9377, Long Beach, CA, December 1996.

120. Morgan, Harry L., Jr., Ferris, James C., and McGhee, Robert J., "A Study of High-Lift Airfoils at High Reynolds Numbers in the Langley Low-Turbulence Pressure Tunnel," NASA TM 89125, June 1987.

121. Mullins, B.R., Smith, D.E., and Korkan, K.D. ,"Effects of Icing on the Aerodynamics of a Flapped Airfoil," AIAA-95-0449, January 1995.

122. Olsen, William, Shaw, Robert, and Newton, James, "Ice Shapes and the Resulting Drag Increase for a NACA 0012 Airfoil," NASA TM 83556, January 1984.

123. Olsen, W. and Walker, E., "Experimental Evidence for Modifying the Current Physical Model for Ice Accretion on Aircraft Surfaces," NASA TM 87184, May 1986.

124. Oolbekkink, B. and Volkers, D.F., "Aerodynamic Effects of Distributed Roughness on a NACA 632-015 Airfoil," AIAA-91-0443, January 1991.

125. Orr, D.J., Breuer, K.S., Torres, E.E., and Hansman, R.J., "Spectral Analysis and Experimental Modeling of Ice Accretion Roughness," AIAA-96-0865, January 1996.

126. Papadakis, Michael, Alansatan, Sait, and Seltmann, Michael, "Experimental Study of Simulated Ice Shapes on a NACA 0011 Airfoil," AIAA-99-0096, January 1999.

127. Papadakis, Michael, Vu, Giao T., Hung, Eric K., Bidwell, Colin S., Bencic, Timothy, and Breer, Marlin D., "Progress in Measuring Water Impingement Characteristics on Aircraft Surfaces," AIAA-98-0488, January 1998.

128. Politovich, Marcia K., "Aircraft Icing Caused by Large Supercooled Droplets," J Appl Meteorology, Vol. 28, No. 9, September 1989, pp. 856–868.

129. Politovich, Marcia K., "Response of a Research Aircraft to Icing and Evaluation of Severity Indices," J. Aircraft, Vol. 33, No. 2, March–April 1996, pp. 291–297.

130. Potapczuk, Mark G., Al-Khalil, Kamel, M., and Velazquez, Matthew T., "Ice Accretion and Performance Degradation Calculations With LEWICE/NS," AIAA-93-0173 and NASA TM 105972, January 1993.

131. Potapczuk, Mark G. and Berkowitz, Brian M., "An Experimental Investigation of Multi-Element Airfoil Ice Accretion and Resulting Performance Degradation," AIAA-89-0752 and NASA TM 101441, January 1989.

132. Potapczuk, M.G. and Berkowitz, B.M., "Experimental Investigation of Multielement Airfoil Ice Accretion and Resulting Performance Degradation," J. Aircraft, Vol. 27, No. 8, August 1990, pp. 679-691.

133. Potapczuk, M.G., Bragg, M.B., Kwon, O.J. and Sankar, L.N., "Simulation of Iced Wing Aerodynamics," Paper 7, AGARD CP-496, Effects of Adverse Weather on Aerodynamics, Proceedings of the 68th AGARD Fluid Dynamics Panel Specialists Meeting and NASA TM 104362, April–May 1991.

134. Preston, G.M. and Blackman, C.C., "Effects of Ice Formations on Airplane Performance in Level Cruising Flight," NACA TN 1598, May 1948.

135. Ranaudo, R.J., Batterson, J.G., Reehorst, A.L., Bond, T.H., and O'Mara, T.M., "Effects of Horizontal Tail Ice on Longitudinal Aerodynamic Derivatives," J. Aircraft, Vol. 28, No. 3, March 1991, pp. 193-199.

136. Ratvasky, T.P. and Ranaudo, R.J., "Icing Effects on Aircraft Stability and Control Determined From Flight Data," AIAA-93-0398 and NASA TM 105977, January 1993.

137. Ratvasky, Thomas P. and Van Zante, Judith Foss, "In-Flight Aerodynamic Measurements of an Iced Horizontal Tailplane," AIAA-99-0638 and NASA TM-1999-208902, January 1999.

138. Reehorst, Andrew, Potapczuk, Mark, Ratvasky, Thomas, and Gile Laflin, Brenda, "Wind Tunnel Measured Effects on a Twin-Engine Short-Haul Transport Caused by Simulated Ice Accretions," AIAA-96-0871 and NASA TM 107143, January 1996.

139. Reehorst, Andrew, Potapczuk, Mark, Ratvasky, Thomas, and Gile Laflin, Brenda, "Wind Tunnel Measured Effects on a Twin-Engine Short-Haul Transport Caused by Simulated Ice Accretions," NASA TM 107419, May 1997.

140. Reehorst, A., Chung, J., Potapczuk, M., Choo, Y., Wright, W., and Langhals, T., "An Experimental and Numerical Study of Icing Effects on the Performance and Controllability of a Twin Engine Aircraft," AIAA-99-0374, NASA TM-1999-208896, and ICOMP-99-02, January 1999.

141. Runyan, L.J., Zierten, T.A., Hill, E.G., and Addy Jr., H.E., "Lewis Icing Research Tunnel Test of the Aerodynamic Effects of Aircraft Ground Deicing/Ani-Icing Fluids," NASA TP 3238, August 1992.

142. Schlichting, H., *Boundary-Layer Theory*, 7th ed., McGraw-Hill, New York, 1979.

143. Schrenk, O., "Effect of Roughness on Properties of Airfoils," NACA TM 375, August 1926. Translated from "Vorlaufige Mitteilungen der Aerodynamischen Versuchsanstalt zu Göttingen," No. 4, November 1925.

144. Scott, J.N. and Hankey, W.L., "Navier-Stokes Solutions of Flow Fields About Ice Shapes," presentation made at Aircraft Icing Workshop, NASA Lewis Research Center, Cleveland, Ohio, 1987.

145. Shah, A.D., Patnoe, M.W., and Berg, E.L., "Droplet Size Distribution and Ice Shapes," AIAA-98-0487, January 1998.

146. Shaw, Robert J., Potapczuk, Mark G., and Bidwell, Colin S., "Predictions of Airfoil Aerodynamic Performance Degradation Due to Icing," NASA TM 101434, January 1989.

147. Shaw, R.J., Sotos, R.G., and Solano, F.R., "An Experimental Study of Airfoil Icing Characteristics," NASA TM 82790, January 1982.

148. Shin, J. "Characteristics of Surface Roughness Associated With Leading-Edge Ice Accretion," J. Aircraft, Vol. 33, No. 2, March–April 1996, pp. 316–321.

149. Shin, Jaiwon, Berkowitz, Brian, Chen, Hsun, and Cebeci, Tuncer, "Prediction of Ice Shapes and Their Effect on Airfoil Drag," J. Aircraft, Vol. 31, No. 2., March–April 1994, pp. 263–270.

150. Shin, Jaiwon and Bond, Thomas H., "Results of an Icing Test on a NACA 0012 Airfoil in The NASA Lewis Icing Research Tunnel," AIAA-92-0647 and NASA TM 105374, January 1992.

151. Shin, Jaiwon and Bond, Thomas H., "Experimental and Computational Ice Shapes and Resulting Drag Increase for a NACA 0012 Airfoil," NASA TM 105743, January 1992.

152. Shin, J., Wilcox, P., Chin, V., and Sheldon, D., "Icing Test Results on an Advanced Two-Dimensional High-Lift Multi-Element Airfoil," AIAA-94-1869 and NASA TM 106620, June 1994.

153. Sigal, A. and Danberg, J., "New Correlation of Roughness Density Effect on the Turbulent Boundary Layer," AIAA Journal, Vol. 28, No. 3, March 1990, pp. 554-556.

154. Simpson, R.L., "A Generalized Correlation of Roughness Density Effects on the Turbulent Boundary Layer," AIAA Journal, Vol. 11, No. 2, February 1973, pp. 242-244.

155. Smith, A.M.O. and Kaups, Kalle, "Aerodynamics of Surface Roughness and Imperfections," SAE Paper 680198, April 1968.

156. Spring, Samuel A., "An Experimental Mapping of the Flow Field Behind a Glaze Ice Shape on a NACA 0012 Airfoil," M.S. Thesis, Ohio State University, June 1987 and NASA CR 180847, January 1988.

157. Strash, D.J. and Summa, J.M., "Development of a Three-Dimensional Flow Code Package to Predict Performance and Stability of Aircraft With Leading-Edge Ice Contamination," NASA CR 198519 and AMI Report No. 9408, September 1996.

158. Tang, F.C., "Experimental Investigation of Heavy Rainfall Effect on a 2-D High-Lift Airfoil," Paper 17, AGARD CP-496, Effects of Adverse Weather on Aerodynamics, Proceedings of the 68th AGARD Fluid Dynamics Panel Specialists Meeting, April-May 1991.

159. Teymourazov, R. and Kofman, V., "The Effect of Ice Accretion on the Wing and Stabilizer on Aircraft Performance," Interstate Aviation Committee, no date given.

160. Tezok, F., Brahimi, M.T., and Paraschiviou, I., "Investigation of the Physical Processes Underlying the Ice Accretion Phenomena," AIAA-98-0484, January 1998.

161. Tezok, F. and Kafyeke, F., "Classification of Wing Leading Edge Roughness," Proceedings of the 6th Aerodynamics Symposium, April 28-30, 1997, Toronto, Canada.

162. Thompson, Brian E. and Jang, Juneho, "Aerodynamic Efficiency of Wings in Rain," J. Aircraft, Vol. 33, No. 6, November-December 1996, pp. 1047-1053.

163. Thompson, B.E., Jang, J., and Dion, J.L., "Wing Performance in Moderate Rain," J. Aircraft, Vol. 32, No. 5, September-October 1995, pp. 1034-1039.

164. Thoren, R.L., "Icing Flight Tests on the Lockheed P2V," ASME Paper No. 48-SA-41, 1948.

165. Trunov, O.K. and Ingelman-Sundberg, M., "On the Problem of Horizontal Tail Stall Due to Ice," Report JR-3, a joint report from the Swedish-Soviet Working Group on Flight Safety, February 1985.

166. Valarezo, W.O., "Effects of Roughness on Aircraft Performance," Ohio Aerospace Institute Aircraft Icing Short Course, September 4, 1992, Brook Park, Ohio.

167. Valarezo, W.O., "Maximum Lift Degradation Due to Wing Upper Surface Contamination," Proceedings of the 1st Bombardier International Workshop on Aircraft Icing/Boundary-Layer Stability and Transition, September 21-21, 1993, Montreal, Canada, pp. 104-112.

168. Valarezo, Walter O. and Chin, Vincent D., "Method for the Prediction of Wing Maximum Lift," J. Aircraft, Vol. 31, No. 1, January-February 1994, pp. 103-109.

169. Valarezo, W.O., Lynch, F.T., and McGhee, R.J., "Aerodynamic Performance Effects Due to Small Leading-Edge Ice (Roughness) on Wings and Tails," J. Aircraft, Vol. 30, No. 6, November-December 1993, pp. 807-812.

170. van Dam, C.P. and Holmes, B.J., "Boundary-Layer Transition Effects on Airplane Stability and Control," AIAA-86-2229, August 1986.

171. van Hengst, J., "Aerodynamic Effects of Ground De/Anti-Icing Fluids on Fokker 50 and Fokker 100," J. Aircraft, Vol. 30, No. 1, January-February 1993, pp. 35-40.

172. van Hengst, J. and Boer, J.N., "The Effect of Hoar-Frosted Wings on the Fokker 50 Take-Off Characteristics," Paper 13, AGARD CP-496, Effects of Adverse Weather on Aerodynamics, Proceedings of the 68th AGARD Fluid Dynamics Panel Specialists Meeting, April-May 1991.

173. Van Zante, Judith Foss and Ratvasky, Thomas P., "Investigation of Dynamic Flight Maneuvers With an Iced Tailplane," AIAA-99-0371 and NASA TM-1999-208849, January 1999.

174. von Glahn, Uwe H. and Gray, Vernon H., "Effect of Ice Formations on Section Drag of Swept NACA 63a-009 Airfoil With Partial-Span Leading-Edge Slat for Various Modes of Thermal Ice Protection," NACA RME53J30, March 1954.

175. White, F., *Viscous Fluid Flow*, McGraw-Hill, New York, 1974.

176. Wickens, R.H. and Nguyen, V.D., "Wind Tunnel Investigation of a Wing-Propeller Model Performance Degradation Due to Distributed Upper-Surface Roughness and Leading-Edge Shape Modification," Paper 11, AGARD CP-496, Effects of Adverse Weather on Aerodynamics, Proceedings of the 68th AGARD Fluid Dynamics Panel Specialists Meeting, April-May 1991.

177. Winkler, J.F. and Bragg, M.B., "Local Flow Field About Large Distributed Roughness in the Initial Ice Accretion Process," AIAA-96-0868, January 1996.

178. Zaman, K.B.M.Q. and Potapczuk, M.G., "The Low Frequency Oscillation in the Flow Over a NACA 0012 Airfoil With an Iced Leading Edge," NASA TM 102018, June 1989.

179. Zierten, Thomas A. and Hill, E.G., "Effects of Wing Simulated Ground Frost on Aircraft Performance," von Karman Institute for Fluid Dynamics Lecture Series, Influence of Environmental Factors on Aircraft Wing Performance, Brussels, Belgium, February 16-19, 1987.

180. Zierten, Thomas A. and Hill, E.G., "Wind Tunnel Investigation of the Aerodynamic Effects of Aircraft Ground Deicing/Anti-Icing Fluids and Criteria for Aerodynamic Acceptance," Paper 19, AGARD CP-496, Effects of Adverse Weather on Aerodynamics, Proceedings of the 68th AGARD Fluid Dynamics Panel Specialists Meeting, April–May 1991.

APPENDIX F—SUMMARY OF PUBLISHED STUDIES

TABLE F-1. SUMMARY OF PUBLISHED STUDIES

Ref. No.	Authors	Source	Facility	Model	Contamination	Aero Performance Data
1	Abbott (Frank) and Turner	NACA ACR No. L4H21, 1944	NACA Langley Low-Turbulence Pressure Tunnel	unswept, single-element, 3-ft chord (1) NACA 63(420)-422 (2) NACA 65(223)-422 (3) 22%-thick Davis airfoil	roughness at leading edge and at various chord-wise locations	C_l *vs* α, C_d *vs* C_l
2	Abbott (Ira)	NACA TR 451, 1932	NACA Variable-Density	scale model of Goodyear "Akron" airship	protuberances and appendages	C_d *vs* Re ΔC_d *vs* Re
3	Abbott (Ira) and von Doenhoff	*Theory of Wing Sections*, Dover Publications, 1959	NACA Langley LTPT (see p 125)	various NACA airfoils	roughness	C_l *vs* α C_m *vs* α C_d *vs* C_l C_m *vs* C_l
4	Abbott (Ira), von Doenhoff, and Stivers	NACA TR 824, 1945	wind tunnels flight	various NACA airfoils	roughness	C_l *vs* α C_m *vs* α C_d *vs* C_l C_m *vs* C_l
5	Addy, Potapczuk, and Sheldon	AIAA-97-0174 and NASA TM 107423, 1997	NASA Lewis Icing Research Tunnel	unswept, single-element, 36-in-chord (1) business jet wing section (2) commercial transport wing section	rime, glaze ice	C_d *vs* α C_l *vs* α

TABLE F-1. SUMMARY OF PUBLISHED STUDIES (Continued)

Ref. No.	Authors	Source	Facility	Model	Contamination	Aero Performance Data
7	Ashenden, Lindberg, Marwitz, and Hoxie	*J. Aircraft*, vol. 33, no. 6, 1996, pp1040-1046	U. Wyoming low-speed tunnel	unswept, single-element 8-in-chord NACA 23012	glaze, freezing drizzle, freezing rain and pnematic-boot residual ice shapes predicted by LEWICE	ΔC_l ΔC_d *vs* α C_m *vs* α
8	Ashenden, Lindberg, and Marwitz	*J. Aircraft*, vol. 35, no. 6, 1998, pp 905-911	U. Wyoming low-speed tunnel	unswept, single-element 8-in-chord NACA 23012	simulations of LEWICE-predicted cloud, drizzle and freezing rain ice accretions, spar-strap, roughness	C_l *vs* α C_d *vs* C_l C_m *vs* α L/D *vs* α
9	Ashenden and Marwitz	*J. Aircraft*, vol. 34, no. 3, 1997, pp 278-287	U. Wyoming King Air in flight	Beechcraft Super King Air	freezing drizzle, cloud ice, mixed-phase with freezing drizzle	ΔC_d Change in Rate of Climb
11	Bezos	AIAA-90-0486, 1990	NASA Langley Aircraft Landing Dynamics Facility	unswept 10-ft-chord NACA 64-210 wing section (1) cruise config. (single-element) (2) landing config. (multi-element)	heavy rain	C_l *vs* α
14	Bilanin, Quackenbush, and Feo	NASA CR 181842, 1989	analytical with droplet-splashing studies	NA	heavy rain	none

TABLE F-1. SUMMARY OF PUBLISHED STUDIES (Continued)

Ref. No.	Authors	Source	Facility	Model	Contamination	Aero Performance Data
16	Boer and van Hengst	AIAA-93-0028, 1993	Dutch Nat'l Aerospace (NLR) Low Speed Windtunnel	unswept, .6-m-chord, 60%-span cross section of Fokker F-28 wing (1) flap only (18°) (2) flap at 18° and slat at 15°	distributed roughness	$\Delta C_{l,max}$ *vs* k/c $\Delta\alpha_{Cl,max}$ *vs* k/c
18	Bond, Flemming, and Britton	Proc. of the 46th AHS Forum, 1990	NASA Lewis IRT	rotorcraft	glaze and rime ice	lift and torque coeff change in lift and thrust coeffs. with time
19	Bowden	NACA TN 3564, 1956	NASA Lewis IRT	unswept, single-element NACA 0011	residual from pneumatic boot, rime and glaze ice, spoilers at various *s/c*	C_l *vs* α C_d *vs* time and *vs* C_l ΔC_d *vs* time ΔC_m *vs* time ΔC_l *vs* time
20	Bowden, Gensemer, and Speen	FAA-ADS-4, 1964	(survey of published data)	various fixed- and rotary-wing airframes	in-flight icing	C_l *vs* C_d effect of icing on ROC airspeed *vs* horsepower ΔC_d *vs* α
21	Bragg	NASA CR 165599, 1982	(1) analytical (2) OSU 6x22 Transonic Airfoil Wind Tunnel	NACA 65A413 NACA 64-215 NACA 65A004	rime ice	C_l *vs* α, C_l *vs* C_d C_m *vs* C_l c_p *vs* x/c

TABLE F-1. SUMMARY OF PUBLISHED STUDIES (Continued)

Ref. No.	Authors	Source	Facility	Model	Contamination	Aero Performance Data
22	Bragg	*J. Aircraft*, vol. 21, no. 7, 1984, pp 505 -511	analytical	various	(droplet impingement study)	(study of effect of airfoil geometry on droplet impingement)
24	Bragg	*J. Aircraft*, vol. 25, no. 9, 1988, pp 849-854	OSU 3-ft x 5-ft subsonic wind tunnel	unswept, single-element NACA 0012	(1) IRT glaze (artificial simulation) (2) LEWICE glaze (artificial sim.) (3) 36-grit sandpaper (k/c=.0011) on (1) & (2)	c_p vs x/c C_l vs α C_d vs α C_m vs α
25	Bragg	NASA CR 191007, 1993	OSU 3-ft x 5-ft subsonic wind tunnel	unswept, single-element NACA 0012	(1) IRT glaze (artificial simulation) (2) LEWICE glaze (artificial sim.) (3) 60-grit sandpaper (k/c=.00057) on (1) & (2) (4) 36-grit sandpaper (k/c=.0011) on (1) & (2)	c_p vs x/c C_l vs α C_d vs α C_m vs α velocity profiles
26	Bragg	AIAA-96-0932, 1996	(reviews results by Jacobs, TR 446, 1932)	unswept, single-element NACA 0012	protuberances at various locations	C_l vs α C_l vs C_d C_m vs α calculated effects on aircraft hinge moment.
27	Bragg	DOT/FAA/AR-96/81, II, 1996, pp 387-399	(reviews results by Jacobs, TR 446, 1932)	unswept, single-element NACA 0012	protuberances at various locations	C_l vs α C_l vs C_d C_m vs α calculated effects on aircraft hinge moment.

TABLE F-1. SUMMARY OF PUBLISHED STUDIES (Continued)

Ref. No.	Authors	Source	Facility	Model	Contamination	Aero Performance Data
28	Bragg and Coirier	AIAA-85-0409, 1985	OSU 3-ft x 5-ft subsonic wind tunnel	unswept, single-element NACA 0012	artificial ice simulating IRT glaze accretion	C_l *vs* α C_d *vs* α C_m *vs* α
29	Bragg and Coirier	AIAA-86-0484, 1986	OSU 3-ft x 5-ft subsonic wind tunnel	unswept, single-element NACA 0012	artificial ice simulating IRT glaze accretion	C_l *vs* α C_d *vs* α C_m *vs* α
30	Bragg, Cummings, Lee, and Henze	AIAA-96-0866, 1996	UIUC 3-ft x 4-ft subsonic wind tunnel	unswept, single-element NACA 0012	simulated distributed roughness using two sizes of hemispherical shapes: (1) 0.35 mm high, (2) 0.75 mm high	turb. intensity and intermittency C_l *vs* α C_l *vs* C_d effect of free-stream turbulence heat-transfer profiles
32	Bragg and Gregorek	AIAA-89-2049, 1989	various (paper reviews previous studies)	unswept, single-element, various (paper reviews previous studies)	roughness, frost, rain, glaze ice, insect (paper reviews previous studies)	C_l *vs* α C_l *vs* C_d $C_{l,max}$ *vs* k/c $C_{l,max}$ *vs* NACA std roughness $C_{d,min}$ *vs* NACA std roughness
33	Bragg, Gregorek, and Lee	*J. Aircraft*, vol. 23, no. 1, 1986, pp 76-81	(1) NASA Lewis IRT (2) Fluidyne 65-in transonic tunnel	unswept, single-element, NACA 63A415	(1) artificial rime and glaze based on IRT accretions (2) artificial shapes based on helicopter spray rig moulds (3) sim. roughness on smooth shapes	C_l *vs* α C_d *vs* α C_l *vs* C_d

TABLE F-1. SUMMARY OF PUBLISHED STUDIES (Continued)

Ref. No.	Authors	Source	Facility	Model	Contamination	Aero Performance Data
34	Bragg, Gregorek, and Shaw	AIAA-82-0582, 1982	NASA Lewis IRT	unswept NACA 63A415 with flap fixed in cruise configuration	artificial simulations of IRT-accreted ice: (1) climb glaze (2) climb rime (3) cruise glaze (4) cruise rime	C_l *vs* α ΔC_d *vs* α C_m *vs* C_l
35	Bragg, Heinrich, Valarezo, and McGhee	*J. Aircraft*, vol. 31, no. 6, 1994, pp 1372-1379	NASA Langley LTPT	unswept, supercritical high-lift transport airfoil	Simulated frost on pressure surface	C_l *vs* α C_l *vs* C_d
36	Bragg, Kerho, and Cummings	AIAA-94-0800, 1994	UIUC 3-ft x 4-ft subsonic wind tunnel	unswept, single-element NACA 0012	isolated hemispherical roughness elements to simulate ice roughness	boundary-layer parameters
37	Bragg, Kerho, and Cummings	AIAA-95-0536, 1995	UIUC 3-ft x 4-ft subsonic wind tunnel	unswept, single-element, NACA 0012	simulated roughness: (1) single hemispherical elements 0.5 mm high, (2) distributed elements 0.35 mm high	turbulence intensity and intermittency
38	Bragg, Kerho, and Khodadoust	AIAA-93-0300, 1993	UIUC 3-ft x 4-ft subsonic wind tunnel	unswept and swept, single-element NACA 0012	artificial ice simulating IRT glaze-ice accretion	LDV-measured local velocities

TABLE F-1. SUMMARY OF PUBLISHED STUDIES (Continued)

Ref. No.	Authors	Source	Facility	Model	Contamination	Aero Performance Data
40	Bragg, Khodadoust, and Spring	*AIAA Journal*, vol. 30, no. 6, 1992, pp 1462-1467	OSU 3-ft x 5-ft subsonic wind tunnel	NACA 0012	artificial ice simulating IRT glaze-ice accretion	pressure distribution and velocity profiles in separation bubble, b.l. momentum and displacement thicknesses
41	Britton	NASA CR 187076, 1991	analytical approach to predicting effect of ice on rotorcraft performance	rotorcraft	IRT ice	C_d *vs* α (exper) compared with predictions
42	Britton	AIAA-92-0418, 1992	analytical approach to predicting effect of ice on rotorcraft performance	rotorcraft	IRT ice	C_d *vs* α experiment compared with predictions Torque rise with time ΔC_l *vs* α ΔC_d *vs* α
45	Brumby	AGARD CP-496, paper 2, 1991	wind tunnel	various	frost, roughness, protuberances	C_l *vs* α C_d *vs* C_l C_m *vs* α (generic results) $\Delta C_{l,max}$ *vs* k/c (correlation) $\Delta\alpha_{Cl,max}$ *vs* $\Delta C_{l,max}$
46	Calay, Holdo, Mayman, and Lun	*J. Aircraft*, vol. 34, no. 2, 1997, pp 206-212	U. Hertfordshire low-speed wind tunnel	unswept, single-element NACA 0012	ice simulated with wedges of various size and shape and at various positions on airfoil	c_p *vs* x/c C_l *vs* α ΔC_l

TABLE F-1. SUMMARY OF PUBLISHED STUDIES (Continued)

Ref. No.	Authors	Source	Facility	Model	Contamination	Aero Performance Data
48	Cebeci	NASA CR 179639, 1987	various (review of previous studies); computational	various (review of previous studies)	rain, insect and ice roughness, glaze ice	C_l *vs* α (calculated) C_d *vs* C_l
49	Cooper, Sand, Politovich, and Veal	*J. Aircraft*, vol. 21, no. 9, 1984, pp 708-715	U. Wyoming King Air in flight	Beechcraft Super King Air	in-flight icing	rate of climb *vs* airspeed
50	Dryden	*J. Aeron Sci*, vol. 20, no. 7, 1953, pp 477-482	various (review of previous studies)	various (review of previous studies)	roughness	Transition *Re vs* roughness size
51	Dunham, Bezos, Gentry, and Melson	AIAA-85-0258, 1985	Langley 4-m x 7-m	unswept, multielement NACA 64-210	rain	C_l *vs* α (calculated) C_l *vs* C_d
52	Dunham, Dunham, and Bezos	AGARD CP-496, paper 15, 1991	Langley 14 x 22 ft subsonic tunnel with rain, track test with rain	various	heavy rain	C_l *vs* α C_l *vs* C_d $\alpha_{Cl,max}$ *vs* rain rate $\Delta C_{l,max}$ *vs* rain rate

TABLE F-1. SUMMARY OF PUBLISHED STUDIES (Continued)

Ref. No.	Authors	Source	Facility	Model	Contamination	Aero Performance Data
53	Dunn and Loth	AIAA-99-0093	analytical study using NSU2D code	unswept NACA 23012 airfoil with simple flap	quarter-round to simulate spanwise step-ice from SLD encounter	C_l *vs* α C_l *vs* C_d C_m *vs* α C_h *vs* α
54	Flemming, Bond, and Britton	AIAA-91-0660, 1991	NASA Lewis IRT	(1) OH-58 tail rotor, (2) powered-force model with fully articulated head, four 4.88-in-chord blades	glaze, rime	$\Delta C_{l,max}$ *vs* time Δ torque coef. *vs* time
55	Flemming, Britton, and Bond	AGARD CP-496, paper 9 and NASA TM 104351, 1991	NASA Lewis IRT	(1) OH-58 tail rotor, (2) powered-force model with fully articulated head, four 4.88-in-chord blades	glaze, rime	
56	Flemming and Lednicer	NASA CR 3910, 1985	(1) NRC High-Speed Icing Wind Tunnel (2) OSU 6 x 22 Transonic Airfoil Facility	unswept, single-element airfoils with 2.69- to 6.38-in chord; forms: NACA 0012, SC1095, SC1094 R8, SC1012 R8, SSC-A09, VR-7, OH-58 Tail Rotor Blade and NACA 0011.5	rime, mixed and glaze ice	C_l *vs* α C_d *vs* C_l C_m *vs* C_l
57	Ferguson, Mullins, Smith, and Korkan	AIAA-95-0451, 1995	Texas A&M Low-Speed Wind Tunnel	2 full-size, half-span, swept horizontal stabilizers with boots	artificial ice simulating light rime and residual step based on LEWICE predictions	C_l *vs* α C_d *vs* α C_m *vs* α

TABLE F-1. SUMMARY OF PUBLISHED STUDIES (Continued)

Ref. No.	Authors	Source	Facility	Model	Contamination	Aero Performance Data
60	Gray	NACA TN 4151, 1958	NASA Lewis IRT	unswept, single-element NACA 65A004	rime and glaze ice	correlation of C_d with icing conditions
61	Gray	NASA TN D-2166, 1964	NASA Lewis IRT	unswept, single-element airfoils: (1) NACA 65A004 (2) NACA 63A009 (3) NACA 0011 (4) NACA 651-212 (5) NACA 652-015	rime and glaze ice	ΔC_d, C_d correlation with icing conditions
63	Gray and von Glahn	NACA RM E53C10 and NACA TN 2962, 1953	NASA Lewis IRT	unswept, single-element NACA 651-212	rime, glaze ice, frost, residual from thermal IP (runback), protuberances at various locations	C_d *vs* time ΔC_d *vs* protub. height ΔC_d *vs* protub. location ΔC_d *vs* α
64	Gray and von Glahn	NACA TN 4155, 1958	NASA Lewis IRT	unswept, single-element NACA 65A004	rime, glaze ice	ΔC_d *vs* time ΔC_l *vs* time ΔC_m *vs* time C_d *vs* α C_l *vs* α C_m *vs* α
66	Gulick	NACA WR L-292, 1938	NACA Full-Scale Wind Tunnel	unswept, single-element, 6-ft chord NACA 0012	Simulated boot residual	C_l *vs* α Increment in stall speed *vs* wing loading

TABLE F-1. SUMMARY OF PUBLISHED STUDIES (Continued)

Ref. No.	Authors	Source	Facility	Model	Contamination	Aero Performance Data
67	Haines and Luers	NASA CR 156885, 1982	analytical	single- and multielement wing sections	heavy rain simulated by surface roughness	C_l *vs* α C_d *vs* C_l ΔC_d *vs* rain rate $\Delta C_{l,max}$ *vs* rain rate $\Delta\alpha_{Cl,max}$ *vs* rain rate
69	Hansman and Barsotti	AIAA-85-0260, 1985	MIT 1-ft x 1-ft low-speed tunnel	6-in-chord Wortmann FX-67-K-170 NLF airfoil	simulated heavy rain	C_l *vs* α lift-to-drag ratio *vs* α C_d *vs* a
74	Hill and Zierten	*J. Aircraft*, vol. 30, no. 1, 1993, pp 24-34	(1) flight (2) NASA Lewis IRT	(1) Boeing 737-200ADV aircraft (2) unswept 1.5-ft-chord 737-200ADV airfoil at 65% semispan (3) 0.091-scale half model of 737-200ADV	ground deicing and anti-icing fluids	$C_{l,max}$ *vs* temperature $\Delta C_{l,max}$ *vs* temperature ΔC_l *vs* temperature at 8°AOA C_d *vs* temperature
78	Hooker	NACA TN 457, 1933	NASA Langley variable-density tunnel	unswept, single-element airfoils: (1) 5-in-chord NACA 0012 (2) 5-in-chord NACA 4412 (3) 6-in-chord RAF 30	roughness	C_l *vs* α C_d *vs* α C_m *vs* α C_d *vs* C_l
80	Ingelman-Sundberg, Trunov, and Ivaniko	Swedish-Soviet Working Group Report JR-1, 1977	(1) 1.5- x 2-m ejector-driven tunnel (2) flight testing	(1) unswept, multielement, 0.65-m-chord NACA 652-A215 wing section (2) An-12 aircraft	simulated hoar frost, artificial glaze and rime ice	C_l *vs* α $C_{l,max}$ *vs* ice shape C_d *vs* ice shape C_d *vs* C_l C_l *vs* C_d (flight)

TABLE F-1. SUMMARY OF PUBLISHED STUDIES (Continued)

Ref. No.	Authors	Source	Facility	Model	Contamination	Aero Performance Data
81	Jackson and Bragg	AIAA-99-0373, 1999	(1) NASA Lewis IRT (ice-accretion tests) (2) UIUC LSLT wind tunnel (aero tests)	NLF(1)-0414F airfoil	stereo-lithographed shapes from IRT tracings with and without roughness to simulate: (1) glaze ice for IPS failure (2) intercycle ice for 4 IPS operating modes	C_l *vs* α C_d *vs* α C_m *vs* α C_h *vs* α
82	Jacobs	NACA TR 446, 1933	NACA Langley variable-density tunnel	unswept, single-element NACA 0012	protuberances (full-span strips)	C_l *vs* α C_d *vs* α C_m *vs* α
83	Jacobs and Abbott (Ira)	NACA TR 416, 1932	NACA Langley variable-density tunnel	NA	NA	(description of variable-density tunnel)
84	Jacobs and Sherman	NACA TR 449, 1933	NACA Langley variable-density tunnel	unswept, single-element airfoils: (1) NACA 0012 (2) NACA 4412	protuberances (partial-span strips)	C_l *vs* α C_m *vs* α C_d *vs* C_l
86	Johnson	*J. Aeron Sci*, vol. 8, no. 2, 1940, pp 43-54	wind tunnel and flight experience; data from wind tunnel tests (tunnel not identified)	aircraft not identified	(1) simulated ice on leading edge (2) simulated ice behind boots	C_l *vs* α (for full aircraft) C_l *vs* C_d (for full aircraft) C_l *vs* C_m (for full aircraft) C_l *vs* C_r (for full aircraft) data from ref. 82 for wings

TABLE F-1. SUMMARY OF PUBLISHED STUDIES (Continued)

Ref. No.	Authors	Source	Facility	Model	Contamination	Aero Performance Data
92	Khodadoust	NACA CR 180846, 1988	OSU subsonic wind tunnel	unswept, single-element NACA 0012	simulated glaze ice	(Flow visualization study)
98	Kim and Bragg	AIAA-99-03150, 1999	UIUC 3-ft x 4-ft subsonic wind tunnel	unswept, 18-in-chord NLF(1)-0414F with flap at 0°	geometrical shapes to simulate glaze horns	C_l *vs* α C_d *vs* α C_m *vs* α C_h *vs* α
99	Kind and Lawrysyn	AGARD CP-496, paper 8, 1991	(1) "a low-speed wind tunnel" (2) computations	(1) flat plate (2) 2-D sections of: (a) NACA 2412 (b) BGK1	natural frost	measured: b.l. velocity profiles C_l *vs* α (computed) C_d *vs* α (computed) takeoff distance
100	Kind and Lawrysyn	*Can Aeron and Space Journal*, vol. 38, no. 2, 1992, pp 62-70	(1) "a low-speed wind tunnel" (2) computations	(1) flat plate (2) 2-D sections of: (a) NACA 2412 (b) BGK1	natural frost	measured: b.l. velocity profiles C_l *vs* α (computed) C_d *vs* α (computed) takeoff distance
101	Kind and Lawrysyn	*AIAA Journal*, vol. 30, no. 7, 1992, pp 1703-1707	0.51- x 0.76-m closed-return wind tunnel	flat plate	natural frost	boundary-layer velocity profiles

TABLE F-1. SUMMARY OF PUBLISHED STUDIES (Continued)

Ref. No.	Authors	Source	Facility	Model	Contamination	Aero Performance Data
108	Leckman	SAE paper 710394, 1971	(analysis using a method to estimate effects of ice)	(1) Cessna Turbo Centurion T210K (2) Cessna Turbo Super Skymaster T337F	glaze ice	rate of climb BHP *vs* speed stall speed *vs* flap deflection C_l *vs* C_d thrust *vs* airspeed
110	Lee, Dunn, Gurbacki, Bragg, and Loth	AIAA-98-0490, 1998	(1) UIUC 3-ft x 4-ft subsonic wind tunnel (2) computations	unswept, modified NACA 23012 with simple flap	full-span step	C_l *vs* α C_l *vs* C_d C_m *vs* α C_h *vs* α C_l *vs* flap deflection
111	Leurs and Haines	AIAA-83-0275, 1983	water-spray rig and wing attached to moving vehicle	uswept, single-element, 15-in-chord NACA 0018 (approximation)	heavy rain	C_l *vs* α
112	Lewis and Perkins	NACA TN 4220, 1958	flight	ZPG-2 airship	icing encounters in flight	observations described (vibration, shedding, etc)
114	Lynch, Valarezo, and McGhee	AGARD CP-496, paper 12, 1991	NASA Langley LTPT	unswept single- and multielement airfoil	leading-edge roughness	$\Delta C_{l,max}$ *vs* k/c $\Delta C_{l,max}$ *vs* Re C_l *vs* α

TABLE F-1. SUMMARY OF PUBLISHED STUDIES (Continued)

Ref. No.	Authors	Source	Facility	Model	Contamination	Aero Performance Data
116	Maresh and Bragg	AIAA-84-2170, 1984	analytical review	various	insect impingement	C_l *vs* α C_l *vs* C_d ΔC_d *vs* α
120	Morgan, Ferris, and McGhee	NASA TM 89125, 1987	NASA Langley LTPT	unswept, multielement airfoil	simulated frost simulated glaze ice	$C_{l,max}$ *vs* Re
122	Olsen, Shaw, and Newton	NASA TM 83556, 1984	NASA Lewis IRT	unswept, single-element NACA 0012	rime and glaze ice	C_d *vs* test parameters
123	Olsen and Walker	NASA TM 87184, 1986	NASA Lewis IRT	unswept, single-element NACA 0012	glaze ice	(close-up motion pictures of accretion development)
124	Oolbekkink and Volkers	AIAA-91-0443, 1991	0.84- x 1.2-m closed-loop tunnel at the Polytechnical Institute of Haarlem	unswept, single-element 0.24-m-chord NACA 632-015	distributed roughness	C_l *vs* α ΔC_l *vs* roughness starting point correlation of lift loss with b.l. thickness

TABLE F-1. SUMMARY OF PUBLISHED STUDIES (Continued)

Ref. No.	Authors	Source	Facility	Model	Contamination	Aero Performance Data
125	Papadakis, Alansatan, and Seltmann	AIAA-99-0096, 1999	WSU Beech Memorial low-speed wind tunnel	unswept, single-element, 12-in- and 24-in-chord NACA 0011 airfoils	full-span spoilers	C_l *vs* α C_d *vs* α C_m *vs* α c_p *vs* x/c
129	Politovich	*J. Aircraft*, vol. 33, no. 2, 1996, pp 291-297	U. Wyoming King Air in flight	Beechcraft Super King Air	natural icing, including rime, glaze and SLD	C_l *vs* *LWC*, temp, *MVD*, accumulation C_d *vs* *LWC*, temp, *MVD*, potential accumulation ΔROC *vs* *LWC*, temp, *MVD*, potential accumulation
130	Potapczuk, Al-Khalil, and Velazquez	AIAA-93-0173 and NASA TM 105972, 1993	LEWICE/NS calculations	unswept, single-element NACA 0012	rime, mixed and glaze ice	C_d *vs* temp (comparison with Olsen, Shaw, and Newton, NASA TM 83556, 1984)
131	Potapczuk and Berkowitz	AIAA-89-0752 and NASA TM 101441, 1989	NASA Lewis IRT	unswept, multielement Boeing 737-200 ADV wing section	rime, mixed and glaze ice	C_l *vs* α and time C_d *vs* α and time C_m *vs* α and time
132	Potapczuk and Berkowitz	*J. Aircraft*, vol. 27, no. 8, 1990, pp 679-691	NASA Lewis IRT	unswept, multielement Boeing 737-200 ADV wing section	rime, mixed and glaze ice	C_l *vs* α and time C_d *vs* α and time C_m *vs* α and time

TABLE F-1. SUMMARY OF PUBLISHED STUDIES (Continued)

Ref. No.	Authors	Source	Facility	Model	Contamination	Aero Performance Data
133	Potapczuk, Bragg, Kwon, and Sankar	AGARD CP-496, paper 7 and NASA TM 104362, 1991	3D NS Flow solver, OSU subsonic wind tunnel	unswept and swept single-element NACA 0012	artificial glaze ice	C_p *vs* x/c C_l *vs* span position
134	Preston and Blackman	NACA TN 1598, 1948	"twin-engine airplane" in flight	propellers, wings, empennage, engine cowlings, and misc unprotected surfaces	rime, mixed and glaze ice	Propeller efficiency loss, propeller unbalance, drag increase
135	Ranaudo, Batterson, Reehorst, Bond, and O'Mara	*J. Aircraft*, vol. 28, no. 3, 1991, pp 193-199	NASA Lewis Twin Otter in flight	DHC-6 Twin Otter horizontal tail	artificial ice shapes simulating glaze ice accretion	Vertical force coefficient derivative vs speed pitching moment coefficient derivative vs speed
136	Ratvasky and Ranaudo	AIAA-93-0398 and NASA TM 105977, 1993	NASA Lewis Twin Otter in flight	DHC-6 Twin Otter horizontal and vertical tail	artificial ice shapes simulating glaze ice accretion	Stability and control parameters
137	Ratvasky and Van Zante	AIAA-99-0638 and NASA TM-1999-208902, 1999	NASA Lewis Twin Otter in flight	DHC-6 Twin Otter horizontal tail	artificial ice shapes simulating glaze ice accretion	aircraft dynamics tail C_l *vs* speed elevator deflection *vs* speed elevator hinge moment *vs* speed

TABLE F-1. SUMMARY OF PUBLISHED STUDIES (Continued)

Ref. No.	Authors	Source	Facility	Model	Contamination	Aero Performance Data
138	Reehorst, Potapczuk, Ratvasky, and Laflin	AIAA-96-0871 and NASA TM 107143, 1996	NASA Langley 14- x 22-ft Subsonic Tunnel	1/8-scale twin-engine subsonic transport aircraft with multi-element wings	artificial ice shapes simulating glaze ice accretion	C_l vs α C_m vs α C_l vs C_d visualization of flow along wing
139	Reehorst, Potapczuk, Ratvasky, and Laflin	NASA TM 107419, 1997	NASA Langley 14- x 22-ft Subsonic Tunnel	1/8-scale twin-engine subsonic transport aircraft with multi-element wings	artificial ice shapes simulating glaze ice accretion	C_l vs α C_m vs α C_l vs C_d visualization of flow along wing
141	Runyan, Zierten, Hill, and Addy	NASA TP 3238, 1992	NASA Lewis IRT	(1) unswept 1.5-ft-chord 737-200ADV airfoil at 65% semispan, with and without flaps (2) .091-scale half model of 737-200ADV	ground deicing and anti-icing fluids	$C_{l,max}$ and $\Delta C_{l,max}$ vs parameters C_l vs test parameters ΔC_m vs fluid C_d and ΔC_d vs test parameters aircraft performance parameters
143	Schrenk	NACA TM 375, 1926	unknown	wing "profile No. 449"	0.5-mm iron-wire gauze (1) on entire surface (2) on pressure surface (3) on suction surface, distrib.and in 40-mm bands (4) near l.e. (5) near mid chord (6) near trailing edge	C_l vs C_d
145	Shah, Patnoe, and Berg	AIAA-98-0487, 1998	computations with LEWICE code	typical jet transport wing, 2.46-m chord	rime, mixed and glaze ice from SLD	(predicted ice shapes only)

TABLE F-1. SUMMARY OF PUBLISHED STUDIES (Continued)

Ref. No.	Authors	Source	Facility	Model	Contamination	Aero Performance Data
146	Shaw, Potapczuk, and Bidwell	NASA TM 101434, 1989	IRT, ARC2D code, IBL code	unswept, single-element NACA 0012	artificial glaze ice	c_p *vs* x/c C_l *vs* α CD *vs* α
147	Shaw, Sotos, and Solano	NASA TM 82790, 1982	NASA Lewis IRT	unswept, single-element 1.34-m-chord NACA 63_2-A415	rime and glaze ice	ΔC_d *vs* icing time ΔC_d *vs* α
148	Shin	*J. Aircraft*, vol. 33, no. 2, 1996, pp 316-321	NASA Lewis IRT	unswept, single-element NACA 0012	initial ice roughness	(roughness characterization study)
149	Shin, Berkowitz, Chen, and Cebeci	*J. Aircraft*, vol. 31, no. 2, 1994, pp 263-270	analytical study using LEWICE, IBL	unswept, single-element NACA 0012	rime and glaze ice	C_d *vs* temperture C_d *vs* α. (Code predictions are compared with Olsen, et al [TM 83556, 1984] measurements in IRT)
150	Shin and Bond	AIAA-92-0647 and NASA TM 105374, 1992	NASA Lewis IRT	unswept, single-element 21-in-chord NACA 0012	rime and glaze ice	clean a/f C_d *vs* α for several studies compared, repeatability of C_d for individual icing tests in IRT

TABLE F-1. SUMMARY OF PUBLISHED STUDIES (Continued)

Ref. No.	Authors	Source	Facility	Model	Contamination	Aero Performance Data
151	Shin and Bond	NASA TM 105743, 1992	(1) NASA Lewis IRT (2) computations using LEWICE/IBL	unswept, single-element 21-in-chord NACA 0012	rime and glaze ice	C_d *vs* total temperature
152	Shin, Wilcox, Chin, and Sheldon	AIAA-94-1869 and NASA TM 106620, 1994	NASA Lewis IRT	unswept, multielement MDA	rime and glaze ice	C_l *vs* α c_p *vs* x/c
154	Simpson	*AIAA Journal*, vol. 11, no. 2, 1973, pp 242-244	analytical	NA	roughness	correlation of boundary-layer velocity with roughness height
155	Smith and Kaups	SAE paper 680198, 1968	analytical	NA	roughness	methods to calculate drag and drag increase due to roughness
156	Spring	NASA CR 180847, 1988	OSU subsonic wind tunnel	unswept, single-element NACA 0012	artificial shapes simulating glaze ice	c_p *vs* x/c C_l *vs* α C_d *vs* α

TABLE F-1. SUMMARY OF PUBLISHED STUDIES (Continued)

Ref. No.	Authors	Source	Facility	Model	Contamination	Aero Performance Data
157	Strash and Summa	NASA CR 198519 and AMI Report 9408, 1996	VSAERO 3-D flow code analysis	B 727-200 aircraft	ice	C_m *vs* body α C_l *vs* body α C_m *vs* C_l
162	Thompson and Jang	*J. Aircraft*, vol. 33, no. 6, 1996, pp 1047-1053	Rensselaer 4- by 6-foot subsonic wind tunnel	unswept, single-element, 6-in-chord NACA 4412	rain on various surface treatments: (1) wettable, (2) commercial aircraft paint, (3) nonwettable	Lift/drag (wet) divided by lift/drag (dry) *vs* α; lift/moment (wet) divided by lift/moment (dry) *vs* α; moment/drag (wet) divided by moment/drag (dry) *vs* α
163	Thompson, Jang, and Dion	*J. Aircraft*, vol. 32, no. 5, 1995, pp 1034-1039	Rensselaer 4- by 6-foot subsonic wind tunnel	unswept, single-element, 6-in-chord NACA 4412	rain on clean, wire-tripped and grit-tripped wings	ΔC_l *vs* α ΔC_d *vs* α ΔC_m *vs* α
165	Trunov and Ingelman-Sundberg	Swedish-Soviet Working Group Report JR-3, 1985	(1) "a Soviet icing wind tunnel" (2) "a Swedish wind tunnel" (3) flight	(1) 44° swept NACA 64-009 tailplane (2) unswept tailplane with 8% thickness (3) model (1) with sim. NACA 0012 l.e. (4) various aircraft	artificial shapes cast from icing tunnel accretions of rime and glaze ice	Lift and hinge moment, stick force
168	Valarezo and Chin	*J. Aircraft*, vol. 31, no. 1, 1994, pp 103-109	RAE 11.5- x 8.5-ft low-speed wind tunnel and analysis (prediction method)	various airfoil configurations	none	C_l and $C_{l,max}$ *vs* flap angle, flap deflection, slat deflection, α, *Re*

TABLE F-1. SUMMARY OF PUBLISHED STUDIES (Continued)

Ref. No.	Authors	Source	Facility	Model	Contamination	Aero Performance Data
169	Valarezo, Lynch, and McGhee	*J. Aircraft*, vol. 30, no. 6, 1993, pp 807-812	LTPT, ONERA F-1 and IBL code	(1) unswept, multi-element airfoil (2) 3-D tail single-element airfoil	artificial distributed roughness	$\Delta C_{l,max}$ *vs* Re $\Delta C_{l,max}$ *vs* k/c $c_{p,max}$ *vs* α C_l *vs* α $\Delta\alpha_{stall}$ *vs* k/c
170	van Dam and Holmes	AIAA-86-2229, 1986	Dragonfly aircraft in flight (NLF wings) and analysis	various NLF airfoils	none: correlate results with location of transition	C_l *vs* C_d C_l *vs* α C_m *vs* α pitch-control characteristics longitud. dynamic stab. char.
171	van Hengst	*J. Aircraft*, vol. 30, no. 1, 1993, pp 35-40	Flight (takeoff) tests of Fokker 50 and Fokker 100 aircraft	Fokker 50 and Fokker 100 wings	ground de- and anti-icing fluids	C_l *vs* α takeoff times pitch response
174	von Glahn and Gray	NACA RME53J30, 1954	NASA Lewis IRT	swept, multielement 6.9-ft-chord NACA 63A-009 airfoil with thermal ice protection	accreted ice, residual ice, runback ice	C_d *vs* α C_d *vs* time in icing
176	Wickens and Nguyen	AGARD CP-496, paper 11, 1991	wind tunnel (not described)	nacelle and 4-bladed, 2-ft-diameter, powered propeller attached to wing	distributed roughness artificial rime and glaze ice	C_l *vs* α C_l *vs* C_d C_m *vs* α prop thrust *vs* α prop normal force *vs* α prop C_m *vs* α

TABLE F-1. SUMMARY OF PUBLISHED STUDIES (Continued)

Ref. No.	Authors	Source	Facility	Model	Contamination	Aero Performance Data
178	Zaman and Potapczuk	NASA TM 102018, 1989	low-speed wind tunnel analysis with 2-D NS code	LRN(1)-1007 and NACA 0012 airfoils	artificial glaze ice (on NACA 0012 only)	C_l *vs* time C_l *vs* α C_d *vs* α C_m *vs* α
180	Zierten and Hill	AGARD CP-496, paper 19, 1991	NASA Lewis IRT	(1) unswept 1.5-ft-chord 737-200ADV airfoil at 65% semispan (2) 0.091-scale half model of 737-200ADV	ground deicing and anti-icing fluids	$C_{l,max}$ *vs* temperature $\Delta C_{l,max}$ *vs* temperature C_l *vs* temperature at 8°AOA ΔC_l *vs* temperature at 8°AOA C_d *vs* temperature

APPENDIX G—EFFECT OF GLAZE ON DRAG AND LIFT

TABLE G-1. EFFECT OF GLAZE ICE ON DRAG AND LIFT (Studies Using Protuberances)

Ref. No.	Authors	Reference	Figure or Table No.	Airfoil		Protuberance				Performance Data				
											Drag		Lift	
				Description	c, in	Description	h/c	x/c	θ, °	Re, 10^6	α, °	ΔC_d at α	$\Delta\alpha$ at $C_{l,max}$	$\Delta C_{l,max}$
19	Bowden	NACA TN 3564, 1956	Figure 28 (a)	NACA 0011	87.4	1/4-in-high spoiler	0.003	0.010	8.4	(not report-ed for these data)	0.0	0.002		
											2.3	0.004		
											4.6	0.012		
											6.9	0.028		
											9.2	0.063		
19	Bowden	NACA TN 3564, 1956	Figure 28 (a)	NACA 0011	87.4	1/4-in-high spoiler	0.003	0.025	21.4	(not report-ed for these data)	0.0	0.002		
											2.3	0.005		
											4.6	0.012		
											7.0	0.022		
											9.1	0.041		
19	Bowden	NACA TN 3564, 1956	Figure 28 (a)	NACA 0011	87.4	1/4-in-high spoiler	0.003	0.050	29.5	(not report-ed for these data)	0.0	0.004		
											2.4	0.006		
											4.6	0.008		
											7.0	0.012		
											9.3	0.016		
19	Bowden	NACA TN 3564, 1956	Figure 28 (b)	NACA 0011	87.4	1/2-in-high spoiler	0.006	0.025	21.4	(not report-ed for these data)	0.0	0.005		
											2.3	0.010		
											4.7	0.021		
											6.9	0.039		
											9.0	0.075		
46	Calay, Holdo, Mayman, and Lun	J. Aircraft, v 34, 1997, pp 206-212	Figures 8 and 10	NACA 0012	39.4	SS (front-facing step)	0.014	0.057	-2.8	1.25	0.0	0.010	-1.5	0.26
						SF (triangular ramp)	0.008	0.057	9.8	1.25	0.0	0.011	-1.5	0.17
						SR (rear-facing step)	0.004	0.057	73.2	1.25	0.0	0.008	-0.5	0.21

TABLE G-1. EFFECT OF GLAZE ICE ON DRAG AND LIFT
(Studies Using Protuberances (Continued))

Ref. No.	Authors	Reference	Figure or Table No.	Airfoil		Protuberance				Performance Data				
											Drag		Lift	
				Description	c, in	Description	h/c	x/c	θ, °	Re, 10^6	α, °	ΔC_d at α	$\Delta\alpha$ at $C_{l,max}$	$\Delta C_{l,max}$
82	Jacobs	NACA TR 446, 1933	Figure 2	NACA 0012	5.0	protuberance at l.e.	0.000	0	0	3.1	0.0	0.000	3.1	0.21
											3.1	0.000		
											6.1	0.000		
											9.2	0.000		
82	Jacobs	NACA TR 446, 1933	Figure 2	NACA 0012	5.0	protuberance at l.e.	0.001	0	0	3.1	0.0	0.000	4.3	0.37
											3.1	0.001		
											6.0	0.001		
											9.2	0.003		
82	Jacobs	NACA TR 446, 1933	Figure 2	NACA 0012	5.0	protuberance at l.e.	0.002	0	0	3.1	0.1	0.000	5.1	0.41
											3.0	-0.001		
											6.0	0.003		
82	Jacobs	NACA TR 446, 1933	Figure 2	NACA 0012	5.0	protuberance at l.e.	0.005	0	0	3.1	-0.2	0.001	3.2	0.60
											2.8	0.002		
											3.5	0.001		
											6.1	0.004		
											6.4	0.003		
											9.2	0.015		
82	Jacobs	NACA TR 446, 1933	Figure 2	NACA 0012	5.0	protuberance at l.e.	0.013	0	0	3.1	0.1	0.000	3.5	0.64
											3.2	0.002		
											6.2	0.006		
											6.3	0.008		
82	Jacobs	NACA TR 446, 1933	Figure 10	NACA 0012	5.0	upper-surface protub. at x/c = 0.05	0.000	0.05	28.1	3.1	0.0	0.000	1.1	0.09
											3.1	0.000		
											6.1	0.000		
											9.2	0.001		

TABLE G-1. EFFECT OF GLAZE ICE ON DRAG AND LIFT
(Studies Using Protuberances (Continued))

Ref. No.	Authors	Reference	Figure or Table No.	Airfoil		Protuberance				Performance Data				
											Drag		Lift	
				Description	c, in	Description	h/c	x/c	θ, °	Re, 10^6	α, °	ΔC_d at α	$\Delta\alpha$ at $C_{l,max}$	$\Delta C_{l,max}$
82	Jacobs	NACA TR 446, 1933	Figure 10	NACA 0012	5.0	upper-surface protub. at x/c = 0.05	0.001	0.05	28.1	3.1	0.0	0.001	1.2	0.21
											3.1	0.002		
											6.2	0.003		
											9.2	0.004		
82	Jacobs	NACA TR 446, 1933	Figure 10	NACA 0012	5.0	upper-surface protub. at x/c = 0.05	0.002	0.05	28.1	3.1	0.1	0.003	1.7	0.44
											3.2	0.005		
											6.2	0.010		
											9.4	0.017		
82	Jacobs	NACA TR 446, 1933	Figure 10	NACA 0012	5.0	upper-surface protub. at x/c = 0.05	0.005	0.05	28.1	3.1	0.1	0.006	4.7	0.69
											3.1	0.013		
											6.3	0.026		
											9.7	0.055		
82	Jacobs	NACA TR 446, 1933	Figure 10	NACA 0012	5.0	upper-surface protub. at x/c = 0.05	0.013	0.05	28.1	3.1	0.0	0.018	6.3	1.02
											3.3	0.040		
											6.5	0.098		
98	Kim and Bragg	AIAA-99-03150, 1999	Figures 4 and 5	NLF(1)-0414F	18	Upper horn simulation; horn radius/base width = 0; s/c = 0.017	0.044	0.0060	40.0	1.8	0.1	0.020	8.2	0.59
											1.1	0.028		
											2.1	0.040		
											3.2	0.051		
											4.2	0.066		
											5.2	0.090		
											6.1	0.120		
											7.1	0.139		
											8.1	0.169		

TABLE G-1. EFFECT OF GLAZE ICE ON DRAG AND LIFT
(Studies Using Protuberances (Continued))

Ref. No.	Authors	Reference	Figure or Table No.	Airfoil		Protuberance				Performance Data				
											Drag		Lift	
				Description	c, in	Description	h/c	x/c	θ, °	Re, 10^6	α, °	ΔC_d at α	$\Delta\alpha$ at $C_{l,max}$	$\Delta C_{l,max}$
98	Kim and Bragg	AIAA-99-03150, 1999	Figures 4 and 5	NLF(1)-0414F	18	Upper horn simulation; horn radius/base width = 0.25; s/c = 0.017	0.044	0.0060	40.0	1.8	0.1	0.020	8.1	0.57
											1.1	0.028		
											2.1	0.036		
											3.2	0.047		
											4.2	0.062		
											5.2	0.085		
											6.1	0.112		
											7.1	0.140		
											8.1	0.161		
98	Kim and Bragg	AIAA-99-03150, 1999	Figures 4 and 5	NLF(1)-0414F	18	Upper horn simulation; horn radius/base width = 0.5; s/c = 0.017	0.044	0.0060	40.0	1.8	0.1	0.021	8.1	0.55
											1.1	0.028		
											2.1	0.036		
											3.2	0.046		
											4.2	0.059		
											5.2	0.081		
											6.2	0.107		
											7.1	0.133		
											8.1	0.153		
98	Kim and Bragg	AIAA-99-03150, 1999	Figures 7 and 8	NLF(1)-0414F	18	Upper horn simulation; horn radius/base width = 0.5; s/c = 0	0.022	0.0000	0.0	1.8	0.0	0.006	3.0	0.23
											1.1	0.007		
											2.1	0.007		
											3.1	0.004		
											4.1	0.003		
											5.2	0.004		
											6.2	0.009		
											7.2	0.012		
											8.2	0.014		

TABLE G-1. EFFECT OF GLAZE ICE ON DRAG AND LIFT
(Studies Using Protuberances (Continued))

Ref. No.	Authors	Reference	Figure or Table No.	Airfoil		Protuberance				Performance Data				
											Drag		Lift	
				Description	c, in	Description	h/c	x/c	θ, °	Re, 10^6	α, °	ΔC_d at α	$\Delta\alpha$ at $C_{l,max}$	$\Delta C_{l,max}$
98	Kim and Bragg	AIAA-99-03150, 1999	Figures 7 and 8	NLF(1)-0414F	18	Upper horn simulation; horn radius/base width = 0.5; s/c = 0	0.044	0.0000	0.0	1.8	0.0	0.008	4.0	0.26
											1.1	0.010		
											2.1	0.012		
											3.1	0.010		
											4.2	0.012		
											5.2	0.016		
											6.2	0.021		
											7.3	0.030		
											8.3	0.049		
98	Kim and Bragg	AIAA-99-03150, 1999	Figures 7 and 8	NLF(1)-0414F	18	Upper horn simulation; horn radius/base width = 0.5; s/c = 0	0.067	0.0000	0.0	1.8	0.0	0.009	4.0	0.25
											1.1	0.012		
											2.1	0.015		
											3.1	0.014		
											4.2	0.015		
											5.2	0.020		
											6.2	0.026		
											7.3	0.037		
											8.3	0.053		
98	Kim and Bragg	AIAA-99-03150, 1999	Figures 9 and 10	NLF(1)-0414F	18	Upper horn simulation; horn radius/base width = 0; s/c = 0.034	0.022	0.0200	60.0	1.8	0.1	0.021	8.2	0.63
											1.1	0.029		
											2.1	0.037		
											3.1	0.048		
											4.1	0.063		
											5.1	0.085		
											6.1	0.115		
											7.1	0.136		
											8.1	0.162		

TABLE G-1. EFFECT OF GLAZE ICE ON DRAG AND LIFT
(Studies Using Protuberances (Continued))

Ref. No.	Authors	Reference	Figure or Table No.	Airfoil		Protuberance				Performance Data				
											Drag		Lift	
				Description	c, in	Description	h/c	x/c	θ, °	Re, 10^6	α, °	ΔC_d at α	$\Delta\alpha$ at $C_{l,max}$	$\Delta C_{l,max}$
98	Kim and Bragg	AIAA-99-03150, 1999	Figures 9 and 10	NLF(1)-0414F	18	Upper horn simulation; horn radius/base width = 0; s/c = 0.034	0.044	0.0200	60.0	1.8	0.1	0.046	10.2	0.80
											1.1	0.060		
											2.1	0.077		
											3.1	0.100		
											4.1	0.124		
											5.0	0.142		
											6.0	0.155		
											7.0	0.168		
98	Kim and Bragg	AIAA-99-03150, 1999	Figures 9 and 10	NLF(1)-0414F	18	Upper horn simulation; horn radius/base width = 0; s/c = 0.034	0.067	0.0200	60.0	1.8	0.1	0.072	12.2	0.92
											1.1	0.096		
											2.0	0.115		
											3.0	0.135		
											4.0	0.150		
											5.0	0.169		
98	Kim and Bragg	AIAA-99-03150, 1999	Figure 12	NLF(1)-0414F	18	Upper horn simulation; horn radius/base width = 0.5; s/c = -0.012	0.022	0.0055	-50.0	1	0.0	0.003	0.0	-0.01
											1.1	0.001		
											2.1	0.001		
											3.1	0.003		
											4.1	0.001		
											5.2	0.000		
											6.2	-0.001		
											7.2	0.001		
											8.2	0.000		

TABLE G-1. EFFECT OF GLAZE ICE ON DRAG AND LIFT
(Studies Using Protuberances (Continued))

Ref. No.	Authors	Reference	Figure or Table No.	Airfoil		Protuberance					Performance Data			
											Drag		Lift	
				Description	c, in	Description	h/c	x/c	θ, °	Re, 10^6	α, °	ΔC_d at α	$\Delta\alpha$ at $C_{l,max}$	$\Delta C_{l,max}$
98	Kim and Bragg	AIAA-99-03150, 1999	Figure 12	NLF(1)-0414F	18	Upper horn simulation; horn radius/base width = 0.5; s/c = -0.012	0.044	0.0055	-50.0	1	0.0	0.006	1.0	-0.04
											1.0	0.002		
											2.1	0.005		
											3.1	0.004		
											4.1	0.001		
											5.2	0.001		
											6.2	0.000		
											7.2	0.000		
											8.2	-0.002		
98	Kim and Bragg	AIAA-99-03150, 1999	Figure 12	NLF(1)-0414F	18	Upper horn simulation; horn radius/base width = 0.5; s/c = -0.012	0.067	0.0055	-50.0	1	0.0	0.014	-2.1	-0.14
											1.0	0.013		
											2.1	0.010		
											3.1	0.006		
											4.1	0.003		
											5.1	0.002		
											6.2	0.000		
											7.2	-0.001		
											8.2	-0.002		
98	Kim and Bragg	AIAA-99-03150, 1999	Figures 13 and 14	NLF(1)-0414F	18	Upper horn simulation; horn radius/base width = 0.5; s/c = 0.034	0.044	0.0200	60.0	1.8	0.1	0.035	10.2	0.72
											1.1	0.049		
											2.1	0.062		
											3.1	0.079		
											4.1	0.104		
											5.1	0.129		
											6.1	0.148		
											7.1	0.165		
											8.0	0.190		

TABLE G-1. EFFECT OF GLAZE ICE ON DRAG AND LIFT
(Studies Using Protuberances (Continued))

Ref. No.	Authors	Reference	Figure or Table No.	Airfoil		Protuberance				Performance Data				
				Description	c, in	Description	h/c	x/c	θ, °	Re, 10^6	Drag α, °	Drag ΔC_d at α	Lift $\Delta\alpha$ at $C_{l,max}$	Lift $\Delta C_{l,max}$
98	Kim and Bragg	AIAA-99-03150, 1999	Figures 13 and 14	NLF(1)-0414F	18	Upper horn simulation; horn radius/base width = 0.5; s/c = 0.017	0.044	0.0060	40.0	1.8	0.1	0.021	8.1	0.55
											1.1	0.028		
											2.1	0.036		
											3.2	0.046		
											4.2	0.059		
											5.2	0.081		
											6.2	0.107		
											7.1	0.133		
											8.1	0.153		
98	Kim and Bragg	AIAA-99-03150, 1999	Figures 13 and 14	NLF(1)-0414F	18	Upper horn simulation; horn radius/base width = 0.5; s/c = 0.0085	0.044	0.0015	20.0	1.8	0.1	0.011	6.1	0.42
											1.1	0.015		
											2.1	0.022		
											3.2	0.025		
											4.2	0.030		
											5.2	0.045		
											6.2	0.061		
											7.2	0.084		
											8.2	0.114		
98	Kim and Bragg	AIAA-99-03150, 1999	Figures 13 and 14	NLF(1)-0414F	18	Upper horn simulation; horn radius/base width = 0.5; s/c = 0	0.044	0.0000	0.0	1.8	0.0	0.008	4.0	0.26
											1.1	0.010		
											2.1	0.012		
											3.1	0.010		
											4.2	0.012		
											5.2	0.016		
											6.2	0.021		
											7.3	0.030		
											8.3	0.049		

TABLE G-1. EFFECT OF GLAZE ICE ON DRAG AND LIFT
(Studies Using Protuberances (Continued))

Ref. No.	Authors	Reference	Figure or Table No.	Airfoil		Protuberance					Performance Data			
											Drag		Lift	
				Description	c, in	Description	h/c	x/c	θ, °	Re, 10^6	α, °	ΔC_d at α	$\Delta\alpha$ at $C_{l,max}$	$\Delta C_{l,max}$
98	Kim and Bragg	AIAA-99-03150, 1999	Figures 13 and 14	NLF(1)-0414F	18	Upper horn simulation; horn radius/base width = 0.5; s/c = -0.006	0.044	0.0014	-25.0	1.8	0.0	0.010	0.0	0.09
											1.0	0.010		
											2.1	0.009		
											3.1	0.006		
											4.1	0.004		
											5.2	0.006		
											6.2	0.007		
											7.2	0.008		
											8.2	0.010		
98	Kim and Bragg	AIAA-99-03150, 1999	Figures 13 and 14	NLF(1)-0414F	18	Upper horn simulation; horn radius/base width = 0.5; s/c = -0.006	0.044	0.0014	-25.0	1.8	0.0	0.012	0.0	-0.01
											1.0	0.012		
											2.1	0.011		
											3.1	0.006		
											4.1	0.003		
											5.2	0.002		
											6.2	0.002		
											7.2	0.002		
											8.2	0.002		
110	Lee, Dunn, Gurbacki, Bragg, and Loth	AIAA-98-0490, 1998	Figure 10	NACA 23012m	18.0	0.25-in qtr round at x/c = 0.02, no b.l. trip	0.020	0.031	9.8	1.8	0.0	0.009	8.4	0.93
											1.1	0.014		
											2.1	0.018		
											3.1	0.025		
											4.1	0.033		
											5.2	0.044		
											6.2	0.075		
											7.2	0.109		
											8.1	0.141		

TABLE G-1. EFFECT OF GLAZE ICE ON DRAG AND LIFT
(Studies Using Protuberances (Continued))

Ref. No.	Authors	Reference	Figure or Table No.	Airfoil Description	Airfoil c, in	Protuberance Description	h/c	x/c	θ, °	Re, 10^6	Drag α, °	Drag ΔC_d at α	Lift $\Delta\alpha$ at $C_{l,max}$	Lift $\Delta C_{l,max}$
110	Lee, Dunn, Gurbacki, Bragg, and Loth	AIAA-98-0490, 1998	Figure 10	NACA 23012m	18.0	0.25-in qtr round at x/c = 0.10, trip at x/c = 0.05	0.020	0.114	33.1	1.8	0.0	0.050	7.4	0.98
											1.0	0.063		
											2.0	0.076		
											3.1	0.089		
											4.0	0.097		
											5.0	0.112		
											6.0	0.128		
											7.1	0.144		
											8.0	0.159		
110	Lee, Dunn, Gurbacki, Bragg, and Loth	AIAA-98-0490, 1998	Figure 10	NACA 23012m	18.0	0.25-in qtr round at x/c = 0.20, trip at x/c = 0.05	0.020	0.214	43.2	1.8	0.0	0.044	5.4	0.87
											1.1	0.052		
											2.0	0.059		
											3.1	0.068		
											4.1	0.077		
											5.0	0.084		
											6.1	0.097		
											7.1	0.107		
											8.1	0.119		
110	Lee, Dunn, Gurbacki, Bragg, and Loth	AIAA-98-0490, 1998	Figure 11	NACA 23012m	18.0	0.15-in qtr round at x/c = 0.10, trip at x/c = 0.05	0.012	0.108	32.6	1.8	0.1	0.025	5.4	0.84
											1.1	0.029		
											2.1	0.037		
											3.1	0.059		
											4.1	0.077		
											5.1	0.089		
											6.1	0.093		
											7.2	0.103		
											8.1	0.123		

TABLE G-1. EFFECT OF GLAZE ICE ON DRAG AND LIFT
(Studies Using Protuberances (Continued))

Ref. No.	Authors	Reference	Figure or Table No.	Airfoil		Protuberance				Performance Data				
											Drag		Lift	
				Description	c, in	Description	h/c	x/c	θ, °	Re, 10^6	α, °	ΔC_d at α	$\Delta\alpha$ at $C_{l,max}$	$\Delta C_{l,max}$
110	Lee, Dunn, Gurbacki, Bragg, and Loth	AIAA-98-0490, 1998	Figure 11	NACA 23012m	18.0	0.25-in qtr round at x/c = 0.10, t trip at x/c = 0.05	0.020	0.114	33.1	1.8	0.1	0.050		
											1.1	0.064		
											2.1	0.076		
											3.1	0.089		
											4.1	0.096		
											5.1	0.111		
											6.1	0.127		
											7.2	0.144		
											8.1	0.159		
126	Papadakis, Alansatan, and Seitman	AIAA-99-0096, 1999	Tables 4 through 6	NACA 0011	24.0	full-span spoiler	0.063	0.02	10.0	2.46	0.0	0.021		
											4.0	0.078		
											14.0	0.232		
										1.86	0.0	0.020		
											4.0	0.066		
											14.0	0.236		
										1.36	0.0	0.021		
											4.0	0.058		
											14.0	0.236		
126	Papadakis, Alansatan, and Seitman	AIAA-99-0096, 1999	Tables 4 through 6	NACA 0011	24.0	full-span spoiler	0.063	0.02	50.0	2.46	0.0	0.057		
											4.0	0.115		
											14.0	0.258		
										1.86	0.0	0.055		
											4.0	0.116		
											14.0	0.256		
										1.36	0.0	0.057		
											4.0	0.114		
											14.0	0.255		

TABLE G-1. EFFECT OF GLAZE ICE ON DRAG AND LIFT
(Studies Using Protuberances (Continued))

Ref. No.	Authors	Reference	Figure or Table No.	Airfoil		Protuberance				Performance Data				
											Drag		Lift	
				Description	c, in	Description	h/c	x/c	θ, °	Re, 10^6	α, °	ΔC_d at α	$\Delta\alpha$ at $C_{l,max}$	$\Delta C_{l,max}$
126	Papadakis, Alansatan, and Seitman	AIAA-99-0096, 1999	Tables 4 through 6	NACA 0011	24.0	full-span spoiler	0.063	0.02	90.0	2.46	0.0	0.071		
											4.0	0.120		
											14.0	0.254		
										1.86	0.0	0.074		
											4.0	0.126		
											14.0	0.252		
										1.36	0.0	0.073		
											4.0	0.128		
											14.0	0.251		
126	Papadakis, Alansatan, and Seitman	AIAA-99-0096, 1999	Tables 4 through 6	NACA 0011	24.0	full-span spoiler	0.063	0.02	130.0	2.46	0.0	0.043		
											4.0	0.094		
											14.0	0.210		
										1.86	0.0	0.046		
											4.0	0.100		
											14.0	0.212		
										1.36	0.0	0.045		
											4.0	0.098		
											14.0	0.206		
126	Papadakis, Alansatan, and Seitman	AIAA-99-0096, 1999	Figure 7	NACA 0011	24.0	full-span spoiler	0.063	0.02	10.0	2.46	-0.2	0.021		
											0.9	0.030		
											1.9	0.041		
											3.8	0.076		
											5.9	0.117		
											7.9	0.148		
											9.9	0.174		

TABLE G-1. EFFECT OF GLAZE ICE ON DRAG AND LIFT
(Studies Using Protuberances (Continued))

Ref. No.	Authors	Reference	Figure or Table No.	Airfoil		Protuberance					Performance Data			
											Drag		Lift	
				Description	c, in	Description	h/c	x/c	θ, °	Re, 10^6	α, °	ΔC_d at α	$\Delta\alpha$ at $C_{l,max}$	$\Delta C_{l,max}$
126	Papadakis, Alansatan, and Seitman	AIAA-99-0096, 1999	Figure 7	NACA 0011	24.0	Full-span spoiler	0.063	0.02	50.0	2.46	-0.2	0.056		
											0.8	0.070		
											1.9	0.088		
											3.9	0.116		
											5.8	0.143		
											7.8	0.169		
											9.8	0.198		
126	Papadakis, Alansatan, and Seitman	AIAA-99-0096, 1999	Figure 7	NACA 0011	24.0	full-span spoiler	0.063	0.02	90.0	2.46	-0.2	0.071		
											0.8	0.083		
											1.9	0.097		
											3.8	0.118		
											5.8	0.142		
											7.8	0.171		
											9.8	0.194		
126	Papadakis, Alansatan, and Seitman	AIAA-99-0096, 1999	Figure 7	NACA 0011	24.0	full-span spoiler	0.063	0.02	130.0	2.46	-0.2	0.042		
											0.9	0.054		
											1.8	0.067		
											3.9	0.094		
											5.9	0.116		
											7.8	0.137		
											9.9	0.161		

TABLE G-1. EFFECT OF GLAZE ICE ON DRAG AND LIFT
(Studies Using Protuberances (Continued))

Ref. No.	Authors	Reference	Figure or Table No.	Airfoil		Protuberance				Performance Data				
											Drag		Lift	
				Description	c, in	Description	h/c	x/c	θ, °	Re, 10^6	α, °	ΔC_d at α	$\Delta\alpha$ at $C_{l,max}$	$\Delta C_{l,max}$
126	Papadakis, Alansatan, and Seitman	AIAA-99-0096, 1999	Figure 8	NACA 0011	24.0	full-span spoiler	0.063	0.02	10.0	1.36	-0.2	0.019		
											0.9	0.025		
											1.8	0.032		
											3.9	0.056		
											5.9	0.097		
											7.9	0.143		
											9.8	0.167		
126	Papadakis, Alansatan, and Seitman	AIAA-99-0096, 1999	Figure 8	NACA 0011	24.0	full-span spoiler	0.063	0.02	50.0	1.36	-0.2	0.047		
											0.8	0.061		
											1.9	0.077		
											3.8	0.109		
											5.8	0.142		
											7.8	0.170		
											9.8	0.196		
126	Papadakis, Alansatan, and Seitman	AIAA-99-0096, 1999	Figure 8	NACA 0011	24.0	full-span spoiler	0.063	0.02	90.0	1.36	-0.2	0.071		
											0.8	0.085		
											1.8	0.101		
											3.8	0.123		
											5.8	0.148		
											7.8	0.174		
											9.8	0.202		

TABLE G-1. EFFECT OF GLAZE ICE ON DRAG AND LIFT
(Studies Using Protuberances (Continued))

Ref. No.	Authors	Reference	Figure or Table No.	Airfoil		Protuberance				Performance Data				
											Drag		Lift	
				Description	c, in	Description	h/c	x/c	θ, °	Re, 10^6	α, °	ΔC_d at α	$\Delta\alpha$ at $C_{l,max}$	$\Delta C_{l,max}$
126	Papadakis, Alansatan, and Seitman	AIAA-99-0096, 1999	Figure 8	NACA 0011	24.0	full-span spoiler	0.063	0.02	130.0	1.36	-0.2	0.044		
											0.8	0.055		
											1.8	0.069		
											3.8	0.096		
											5.8	0.119		
											7.8	0.145		
											9.8	0.161		
126	Papadakis, Alansatan, and Seitman	AIAA-99-0096, 1999	Figure 9	NACA 0011	24.0	full-span spoiler	0.125	0.02	10.0	1.36	-0.1	0.052		
											0.8	0.066		
											1.8	0.084		
											3.8	0.118		
											5.9	0.151		
											7.8	0.173		
											9.9	0.210		
126	Papadakis, Alansatan, and Seitman	AIAA-99-0096, 1999	Figure 9	NACA 0011	24.0	full-span spoiler	0.125	0.02	50.0	1.36	-0.1	0.095		
											0.9	0.107		
											1.8	0.120		
											3.8	0.150		
											5.8	0.183		
											7.9	0.210		
											9.8	0.238		

TABLE G-1. EFFECT OF GLAZE ICE ON DRAG AND LIFT
(Studies Using Protuberances (Continued))

				Airfoil		Protuberance				Performance Data				
											Drag		Lift	
Ref. No.	Authors	Reference	Figure or Table No.	Description	c, in	Description	h/c	x/c	θ, °	Re, 10^6	α, °	ΔC_d at α	$\Delta\alpha$ at $C_{l,max}$	$\Delta C_{l,max}$
126	Papadakis, Alansatan, and Seitman	AIAA-99-0096, 1999	Figure 9	NACA 0011	24.0	full-span spoiler	0.125	0.02	90.0	1.36	-0.2	0.125		
											0.7	0.137		
											1.8	0.150		
											3.8	0.171		
											5.8	0.194		
											7.8	0.221		
											9.8	0.248		
126	Papadakis, Alansatan, and Seitman	AIAA-99-0096, 1999	Figure 9	NACA 0011	24.0	full-span spoiler	0.125	0.02	130.0	1.36	-0.2	0.096		
											0.7	0.107		
											1.8	0.116		
											3.8	0.134		
											5.8	0.152		
											7.8	0.168		
											9.8	0.190		
126	Papadakis, Alansatan, and Seitman	AIAA-99-0096, 1999	Figure 10	NACA 0011	24.0	full-span spoiler	0.063	0.02	90.0	1.86	-0.2	0.068		
											0.8	0.082		
											1.8	0.098		
											3.8	0.121		
											5.8	0.146		
											7.8	0.168		
											9.9	0.197		

TABLE G-1. EFFECT OF GLAZE ICE ON DRAG AND LIFT
(Studies Using Protuberances (Continued))

Ref. No.	Authors	Reference	Figure or Table No.	Airfoil		Protuberance					Performance Data			
											Drag		Lift	
				Description	c, in	Description	h/c	x/c	θ, °	Re, 10^6	α, °	ΔC_d at α	$\Delta\alpha$ at $C_{l,max}$	$\Delta C_{l,max}$
126	Papadakis, Alansatan, and Seitman	AIAA-99-0096, 1999	Figure 10	NACA 0011	24.0	full-span spoiler	0.063	0.04	90.0	1.86	-0.2	0.087		
											0.8	0.098		
											1.7	0.108		
											3.8	0.132		
											5.8	0.154		
											7.8	0.179		
											9.9	0.200		
126	Papadakis, Alansatan, and Seitman	AIAA-99-0096, 1999	Figure 11	NACA 0011	24.0	full-span spoiler	0.063	0.02	90.0	1.36	-0.2	0.071		
											0.8	0.085		
											1.8	0.101		
											3.8	0.123		
											5.8	0.148		
											7.8	0.174		
											9.8	0.202		
126	Papadakis, Alansatan, and Seitman	AIAA-99-0096, 1999	Figure 11	NACA 0011	24.0	full-span spoiler	0.063	0.04	90.0	1.36	-0.2	0.092		
											0.8	0.103		
											1.8	0.116		
											3.8	0.139		
											5.8	0.161		
											7.8	0.178		
											9.8	0.204		

TABLE G-1. EFFECT OF GLAZE ICE ON DRAG AND LIFT
(Studies Using Protuberances (Continued))

Ref. No.	Authors	Reference	Figure or Table No.	Airfoil		Protuberance					Performance Data			
											Drag		Lift	
				Description	c, in	Description	h/c	x/c	θ, °	Re, 10^6	α, °	ΔC_d at α	$\Delta\alpha$ at $C_{l,max}$	$\Delta C_{l,max}$
126	Papadakis, Alansatan, and Seitman	AIAA-99-0096, 1999	Figure 12	NACA 0011	24.0	full-span spoiler	0.063	0.02	90.0	1.36	-0.2	0.071		
											0.8	0.085		
											1.8	0.101		
											3.8	0.123		
											5.8	0.148		
											7.8	0.174		
											9.8	0.202		
126	Papadakis, Alansatan, and Seitman	AIAA-99-0096, 1999	Figure 12	NACA 0011	24.0	full-span spoiler	0.125	0.02	90.0	1.36	-0.2	0.125		
											0.7	0.137		
											1.8	0.150		
											3.8	0.171		
											5.8	0.194		
											7.8	0.221		
											9.8	0.248		
126	Papadakis, Alansatan, and Seitman	AIAA-99-0096, 1999	Figure 13	NACA 0011	24.0	full-span spoiler	0.063	0.04	90.0	1.36	-0.3	0.093		
											0.8	0.104		
											1.8	0.117		
											3.8	0.139		
											5.8	0.161		
											7.8	0.178		
											9.8	0.205		

TABLE G-1. EFFECT OF GLAZE ICE ON DRAG AND LIFT
(Studies Using Protuberances (Continued))

Ref. No.	Authors	Reference	Figure or Table No.	Airfoil		Protuberance				Performance Data				
											Drag		Lift	
				Description	c, in	Description	h/c	x/c	θ, °	Re, 10^6	α, °	ΔC_d at α	$\Delta\alpha$ at $C_{l,max}$	$\Delta C_{l,max}$
126	Papadakis, Alansatan, and Seitman	AIAA-99-0096, 1999	Figure 13	NACA 0011	24.0	full-span spoiler	0.125	0.04	90.0	1.36	-0.3	0.133		
											0.7	0.144		
											1.8	0.156		
											3.7	0.175		
											5.7	0.202		
											7.8	0.229		
											9.8	0.251		
126	Papadakis, Alansatan, and Seitman	AIAA-99-0096, 1999	Figure 14	NACA 0011	24.0	full-span spoiler	0.063	0.02	50.0	1.36	-0.2	0.047		
											0.8	0.061		
											1.9	0.077		
											3.8	0.109		
											5.8	0.142		
											7.8	0.170		
											9.8	0.196		
126	Papadakis, Alansatan, and Seitman	AIAA-99-0096, 1999	Figure 14	NACA 0011	24.0	full-span spoiler	0.063	0.02	50.0	1.86	-0.2	0.050		
											0.8	0.066		
											1.8	0.080		
											3.8	0.112		
											5.8	0.138		
											7.8	0.163		
											9.8	0.198		

TABLE G-1. EFFECT OF GLAZE ICE ON DRAG AND LIFT
(Studies Using Protuberances (Continued))

Ref. No.	Authors	Reference	Figure or Table No.	Airfoil Description	Airfoil c, in	Protuberance Description	h/c	x/c	θ, °	Re, 10^6	Drag α, °	Drag ΔC_d at α	Lift $\Delta\alpha$ at $C_{l,max}$	Lift $\Delta C_{l,max}$
126	Papadakis, Alansatan, and Seitman	AIAA-99-0096, 1999	Figure 14	NACA 0011	24.0	full-span spoiler	0.063	0.02	50.0	2.46	-0.2	0.056		
											0.8	0.070		
											1.9	0.088		
											3.9	0.116		
											5.8	0.143		
											7.8	0.169		
											9.8	0.198		
126	Papadakis, Alansatan, and Seitman	AIAA-99-0096, 1999	Figure 15	NACA 0011	24.0	full-span spoiler	0.063	0.02	90.0	1.36	-0.2	0.071		
											0.8	0.085		
											1.8	0.101		
											3.8	0.123		
											5.8	0.148		
											7.8	0.174		
											9.8	0.202		
126	Papadakis, Alansatan, and Seitman	AIAA-99-0096, 1999	Figure 15	NACA 0011	24.0	full-span spoiler	0.063	0.02	90.0	1.86	-0.2	0.068		
											0.8	0.082		
											1.8	0.098		
											3.8	0.121		
											5.8	0.146		
											7.8	0.168		
											9.9	0.197		

TABLE G-1. EFFECT OF GLAZE ICE ON DRAG AND LIFT
(Studies Using Protuberances (Continued))

Ref. No.	Authors	Reference	Figure or Table No.	Airfoil		Protuberance				Performance Data				
											Drag		Lift	
				Description	c, in	Description	h/c	x/c	θ, °	Re, 10^6	α, °	ΔC_d at α	$\Delta\alpha$ at $C_{l,max}$	$\Delta C_{l,max}$
126	Papadakis, Alansatan, and Seitman	AIAA-99-0096, 1999	Figure 15	NACA 0011	24.0	full-span spoiler	0.063	0.02	90.0	2.46	-0.2	0.071		
											0.8	0.083		
											1.9	0.097		
											3.8	0.118		
											5.8	0.142		
											7.8	0.171		
											9.8	0.194		
126	Papadakis, Alansatan, and Seitman	AIAA-99-0096, 1999	Figure 16	NACA 0011	24.0	full-span spoiler	0.063	0.02	130.0	1.36	-0.2	0.044		
											0.8	0.055		
											1.8	0.069		
											3.8	0.096		
											5.8	0.119		
											7.8	0.145		
											9.8	0.161		
126	Papadakis, Alansatan, and Seitman	AIAA-99-0096, 1999	Figure 16	NACA 0011	24.0	full-span spoiler	0.063	0.02	130.0	1.86	-0.2	0.043		
											0.9	0.055		
											1.8	0.066		
											3.8	0.095		
											5.8	0.117		
											7.9	0.142		
											9.8	0.164		

TABLE G-1. EFFECT OF GLAZE ICE ON DRAG AND LIFT
(Studies Using Protuberances (Continued))

Ref. No.	Authors	Reference	Figure or Table No.	Airfoil		Protuberance				Performance Data				
											Drag		Lift	
				Description	c, in	Description	h/c	x/c	θ, °	Re, 10^6	α, °	ΔC_d at α	$\Delta\alpha$ at $C_{l,max}$	$\Delta C_{l,max}$
126	Papadakis, Alansatan, and Seitman	AIAA-99-0096. 1999	Figure 16	NACA 0011	24.0	full-span spoiler	0.063	0.02	130.0	2.46	-0.2	0.042		
											0.9	0.054		
											1.8	0.067		
											3.9	0.094		
											5.9	0.116		
											7.8	0.137		
											9.9	0.161		
126	Papadakis, Alansatan, and Seitman	AIAA-99-0096, 1999	Figure 17	NACA 0011	24.0	full-span spoiler	0.063	0.04	90.0	1.36	-0.2	0.092		
											0.8	0.103		
											1.8	0.116		
											3.8	0.139		
											5.8	0.161		
											7.8	0.178		
											9.8	0.204		
126	Papadakis, Alansatan, and Seitman	AIAA-99-0096, 1999	Figure 17	NACA 0011	24.0	full-span spoiler	0.063	0.04	90.0	1.86	-0.2	0.087		
											0.8	0.098		
											1.7	0.108		
											3.8	0.132		
											5.8	0.154		
											7.8	0.179		
											9.9	0.200		

TABLE G-1. EFFECT OF GLAZE ICE ON DRAG AND LIFT
(Studies Using Protuberances (Continued))

Ref. No.	Authors	Reference	Figure or Table No.	Airfoil		Protuberance				Performance Data				
											Drag		Lift	
				Description	c, in	Description	h/c	x/c	θ, °	Re, 10^6	α, °	ΔC_d at α	$\Delta\alpha$ at $C_{l,max}$	$\Delta C_{l,max}$
126	Papadakis, Alansatan, and Seitman	AIAA-99-0096, 1999	Figure 18	NACA 0011	24.0	full-span spoiler	0.063	0.02	50.0	1.36	-0.2	0.047		
											0.8	0.061		
											1.9	0.077		
											3.8	0.109		
											5.8	0.142		
											7.8	0.170		
											9.8	0.196		
126	Papadakis, Alansatan, and Seitman	AIAA-99-0096, 1999	Figure 19	NACA 0011	24.0	full-span spoiler	0.063	0.02	90.0	1.36	-0.2	0.071		
											0.8	0.085		
											1.8	0.101		
											3.8	0.123		
											5.8	0.148		
											7.8	0.174		
											9.8	0.202		
126	Papadakis, Alansatan, and Seitman	AIAA-99-0096, 1999	Figure 20	NACA 0011	24.0	full-span spoiler	0.063	0.04	50.0	1.36	-0.2	0.074		
											0.8	0.089		
											1.8	0.104		
											3.8	0.134		
											5.8	0.156		
											7.8	0.181		
											9.9	0.206		

TABLE G-1. EFFECT OF GLAZE ICE ON DRAG AND LIFT
(Studies Using Protuberances (Continued))

Ref. No.	Authors	Reference	Figure or Table No.	Airfoil		Protuberance				Performance Data				
											Drag		Lift	
				Description	c, in	Description	h/c	x/c	θ, °	Re, 10^6	α, °	ΔC_d at α	$\Delta\alpha$ at $C_{l,max}$	$\Delta C_{l,max}$
126	Papadakis, Alansatan, and Seitman	AIAA-99-0096, 1999	Figure 21	NACA 0011	24.0	full-span spoiler	0.063	0.04	90.0	1.36	-0.2	0.092		
											0.8	0.103		
											1.8	0.116		
											3.8	0.139		
											5.8	0.161		
											7.8	0.178		
											9.8	0.204		

TABLE G-2.1. STUDIES USING ACCRETED OR SIMULATED ICE
(Ref. 5, Addy, Potapaczuk, and Sheldon, AIAA-97-0174, 1997
36-in-Chord Commercial Transport and Business Jet Airfoils
Performance Data From Figures 7 through 12)

Ice shape identity	Icing Conditions						Ice shape (coordinates normalized with respect to chord)	Upper horn			Performance Data				
	α, °	V, mph	t_{tot}, °F	LWC, g/m^3	MVD, µm	time, min		h/c	x/c	θ, °	Re, 10^6	α, °	ΔC_d at α	$\Delta\alpha$ at $C_{l,max}$	$\Delta C_{l,max}$
run 106 Comm. Transp.	0	288	10.5	0.34	15	5.9	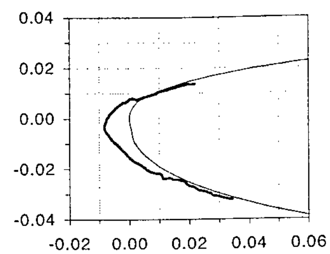	-	-	-	8.6	0	0.003		
run 112 Comm. Transp.	0	288	20.8	0.34	20	5.7	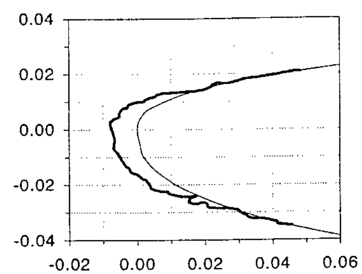	0.0081	0.0166	-2	8.3	0	0.006	1.14	0.178
run 124 Comm. Transp.	0	288	29.5	0.56	21	4.9	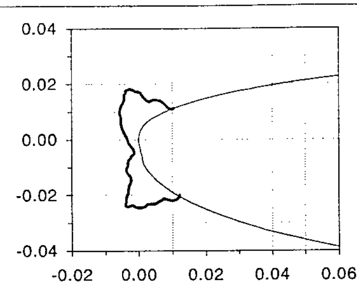	0.0144	0.0098	33	8.0	0	0.018	2.15	0.329

TABLE G-2.1. STUDIES USING ACCRETED OR SIMULATED ICE
(Ref. 5, Addy, Potapaczuk, and Sheldon, AIAA-97-0174, 1997
36-in-Chord Commercial Transport and Business Jet Airfoils
Performance Data From Figures 7 Through 12 (Continued))

Ice shape identity	Icing Conditions						Ice shape (coordinates normalized with respect to chord)	Upper horn			Performance Data				
	α,°	V, mph	t_{tot}, °F	LWC, g/m^3	MVD, µm	time, min		h/c	x/c	θ, °	Re, 10^6	α,°	ΔC_d at α	$\Delta\alpha$ at $C_{l,max}$	$\Delta C_{l,max}$
run 127 Comm. Transp.	0	288	29.5	0.56	21	18.5	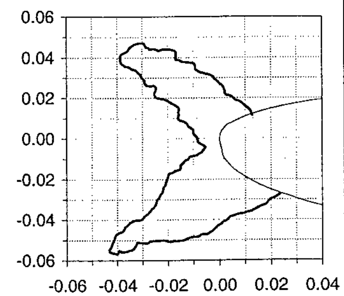	0.0563	0.0128	39	8.0	0	0.131	3.51	0.485
run 129 Comm. Transp.	0	288	29.5	0.56	21	2	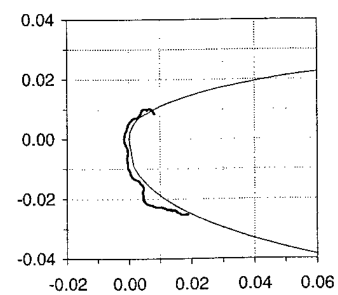	0.0033	0.0078	10	8.0	0	0.007	1.15	0.270
run 202 Business Jet	6	201	30.6	0.54	20	2	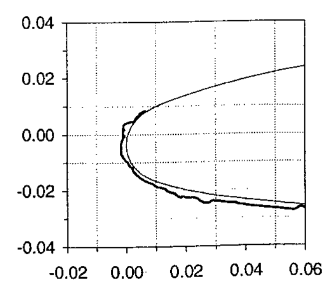	0.0036	0.0029	-11	5.9	6	0.020	1.59	0.180

TABLE G-2.1. STUDIES USING ACCRETED OR SIMULATED ICE
(Ref. 5, Addy, Potapaczuk, and Sheldon, AIAA-97-0174, 1997
36-in-Chord Commercial Transport and Business Jet Airfoils
Performance Data From Figures 7 Through 12 (Continued))

Ice shape identity	Icing Conditions						Ice shape (coordinates normalized with respect to chord)	Upper horn			Performance Data				
	α,°	V, mph	t_{tot}, °F	LWC, g/m^3	MVD, µm	time, min		h/c	x/c	θ, °	Re, 10^6	α,°	ΔC_d at α	$\Delta\alpha$ at $C_{l,max}$	$\Delta C_{l,max}$
run 203 Business Jet	6	201	30.6	0.54	20	6	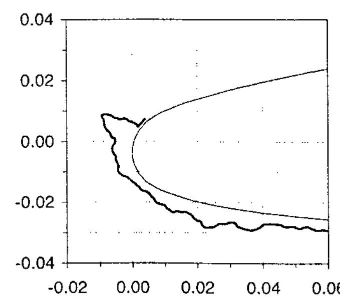	0.0133	0.0030	18	5.9	6	0.049	2.68	0.220
run 204 Business Jet	6	201	30.6	0.54	20	22.5	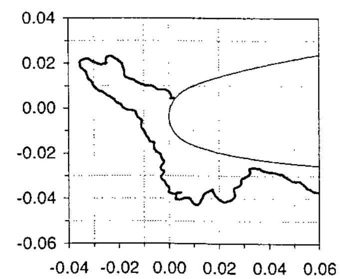	0.0402	0.0023	28	5.9	6	0.101	4.53	0.304
run 208 Business Jet	6	201	21.4	0.43	20	6	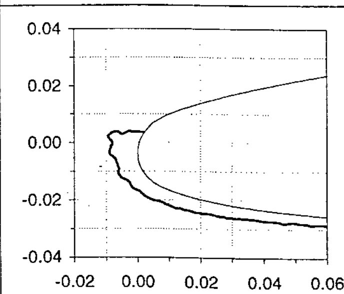	0.0107	0.0023	1	6.1	6	0.021	1.37	0.221

TABLE G-2.1. STUDIES USING ACCRETED OR SIMULATED ICE
(Ref. 5, Addy, Potapaczuk, and Sheldon, AIAA-97-0174, 1997
36-in-Chord Commercial Transport and Business Jet Airfoils
Performance Data From Figures 7 Through 12 (Continued))

Ice shape identity	Icing Conditions						Ice shape (coordinates normalized with respect to chord)	Upper horn			Performance Data				
	α,°	V, mph	t_{tot}, °F	LWC, g/m^3	MVD, µm	time, min		h/c	x/c	θ, °	Re, 10^6	α,°	ΔC_d at α	$\Delta\alpha$ at $C_{l,max}$	$\Delta C_{l,max}$
run 211 Business Jet	6	201	12.7	0.30	20	4.4	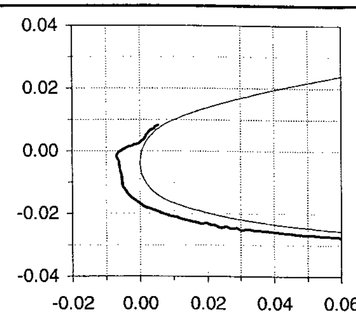	0.0105	0.0022	-26	6.3	6	0.014	2.16	0.188

TABLE G-2.2. STUDIES USING ACCRETED OR SIMULATED ICE
(Ref. 24 and 25, Bragg; Ref. 28 and 29, Bragg and Coirier, NACA 0012 Airfoil, c = 21 in)

Ref. 24, Bragg, *J. Aircraft*, vol. 25, 1988, Performance Data From Figures 8 and 12
Ref. 25, Bragg, NASA CR 191007, 1993, Performance Data From Tabulations, pp 9 and 10 and 315 - 317
Ref. 28. Bragg and Coirier, AIAA-85-0409, Performance Data From Figures 7 and 8
Ref. 29, Bragg and Coirier, AIAA-86-0484, Performance Data From Figures 11 and 12

Ice shape identity	Icing Conditions						Ice shape (coordinates normalized with respect to chord)	Upper horn			Performance Data				
	α,°	V, mph	t_{tot}, °F	LWC, g/m^3	MVD, µm	time, min		h/c	x/c	θ, °	Re, 10^6	α,°	ΔC_d at α	$\Delta\alpha$ at $C_{l,max}$	$\Delta C_{l,max}$
LEWICE (smooth) Ref. 24							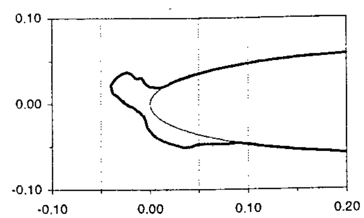	0.040	0.011	33	1.5	0.0	0.014	6.2	0.59
												1.0	0.016		
												2.1	0.017		
												3.2	0.022		
												4.3	0.031		
												6.2	0.066		
												7.2	0.102		
												8.2	0.127		
LEWICE (36-grit, k/c = 0.0011) Ref. 24							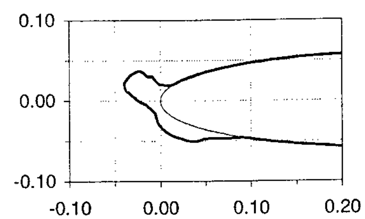	0.040	0.011	33	1.5	0.6	0.018	6.5	0.59
												1.7	0.020		
												2.7	0.023		
												3.7	0.028		
												4.9	0.039		
												6.0	0.053		
												6.8	0.087		
												7.8	0.111		

TABLE G-2.2. STUDIES USING ACCRETED OR SIMULATED ICE
(Ref. 24 and 25, Bragg; Ref. 28 and 29, Bragg and Coirier, NACA 0012 Airfoil, c = 21 in (Continued))

Ice shape identity	Icing Conditions						Ice shape (coordinates normalized with respect to chord)	Upper horn			Performance Data				
	α,°	V, mph	t_{tot}, °F	LWC, g/m^3	MVD, µm	time, min		h/c	x/c	θ, °	Re, 10^6	α,°	ΔC_d at α	$\Delta\alpha$ at $C_{l,max}$	$\Delta C_{l,max}$
simulated (smooth) Ref. 24							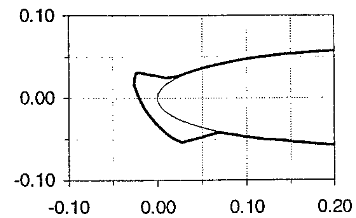	0.043	0.018	12	1.5	0.0	0.017	6.3	0.66
												1.1	0.018		
												2.1	0.019		
												3.1	0.024		
												4.2	0.030		
												5.3	0.043		
												6.3	0.063		
												7.3	0.099		
												8.0	0.125		
simulated (36-grit, k/c = 0.0011) Ref. 24							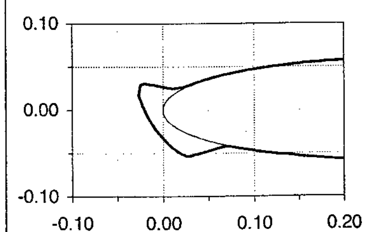	0.043	0.018	12	1.5	-0.1	0.021	6.3	0.66
												0.9	0.021		
												2.0	0.023		
												3.1	0.028		
												4.1	0.034		
												5.2	0.046		
												6.2	0.068		
												7.3	0.095		
												8.1	0.114		

TABLE G-2.2. STUDIES USING ACCRETED OR SIMULATED ICE
(Ref. 24 and 25, Bragg; Ref. 28 and 29, Bragg and Coirier, NACA 0012 Airfoil, c = 21 in (Continued))

Ice shape identity	Icing Conditions						Ice shape (coordinates normalized with respect to chord)	Upper horn			Performance Data				
	α,°	V, mph	t_{tot}, °F	LWC, g/m^3	MVD, µm	time, min		h/c	x/c	θ, °	Re, 10^6	α,°	ΔC_d at α	$\Delta\alpha$ at $C_{l,max}$	$\Delta C_{l,max}$
LEWICE (smooth) Ref. 25							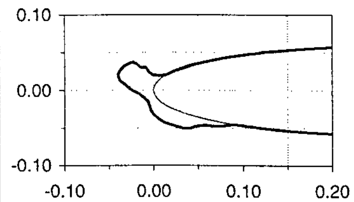	0.040	0.011	33	1.6	0.0	0.015	6.2	0.59
												1.0	0.015		
												2.1	0.017		
												3.1	0.022		
												4.2	0.031		
												5.2	0.044		
												5.2	0.044		
												6.2	0.066		
												7.2	0.095		
												7.2	0.102		
												8.1	0.128		
LEWICE (36-grit, k/c = 0.0011) Ref. 25							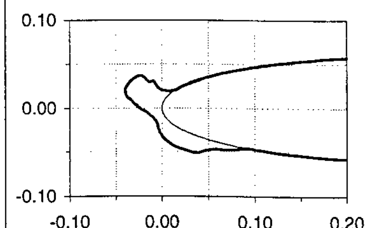	0.040	0.011	33	1.6	-0.4	0.018		
												0.7	0.018		
												1.7	0.019		
												2.8	0.022		
												3.8	0.028		
												4.8	0.035		
												5.9	0.053		
												6.8	0.087		
												7.8	0.111		

TABLE G-2.2. STUDIES USING ACCRETED OR SIMULATED ICE
(Ref. 24 and 25, Bragg; Ref. 28 and 29, Bragg and Coirier, NACA 0012 Airfoil, c = 21 in (Continued))

Ice shape identity	Icing Conditions						Ice shape (coordinates normalized with respect to chord)	Upper horn			Performance Data				
	α,°	V, mph	t_{tot}, °F	LWC, g/m^3	MVD, µm	time, min		h/c	x/c	θ, °	Re, 10^6	α,°	ΔC_d at α	$\Delta\alpha$ at $C_{l,max}$	$\Delta C_{l,max}$
simulated (smooth) Ref. 25							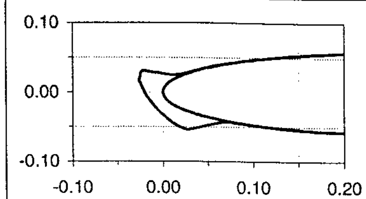	0.043	0.018	12	1.5	0.0	0.019		
												2.1	0.020		
												4.1	0.030		
												6.2	0.058		
												8.1	0.096		
simulated (36-grit, k/c = 0.0011) Ref. 25							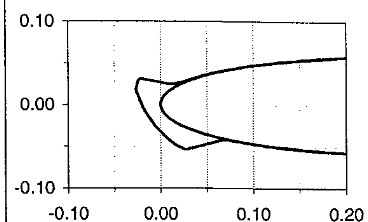	0.043	0.018	12	1.5	-0.01	0.021		
												1.01	0.021		
												2.05	0.023		
												3.09	0.027		
												4.11	0.033		
												5.15	0.045		
												6.15	0.067		
												7.13	0.095		
simulated (60-grit, k/c = 0.00057) Ref. 25							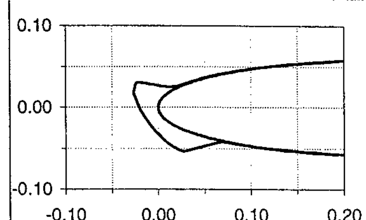	0.043	0.018	12	1.5	-0.01	0.022		
												1.01	0.021		
												2.05	0.023		
												3.08	0.026		
												4.12	0.035		
												4.12	0.035		
												5.15	0.048		
												6.15	0.070		
												6.15	0.079		
												7.12	0.112		

TABLE G-2.2. STUDIES USING ACCRETED OR SIMULATED ICE
(Ref. 24 and 25, Bragg; Ref. 28 and 29, Bragg and Coirier, NACA 0012 Airfoil, c = 21 in (Continued))

Ice shape identity	Icing Conditions						Ice shape (coordinates normalized with respect to chord)	Upper horn			Performance Data				
	α,°	V, mph	t_{tot}, °F	LWC, g/m^3	MVD, µm	time, min		h/c	x/c	θ, °	Re, 10^6	α,°	ΔC_d at α	$\Delta\alpha$ at $C_{l,max}$	$\Delta C_{l,max}$
5-min glaze Ref. 28							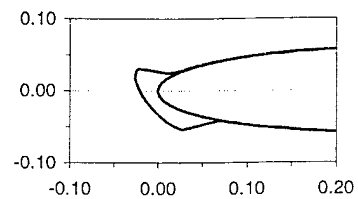	0.043	0.018	12	1.5	0.0	0.026	7.0	0.85
												0.9	0.026		
												1.9	0.026		
												2.9	0.030		
												3.9	0.038		
												4.9	0.052		
												5.9	0.066		
5-min glaze Ref. 29							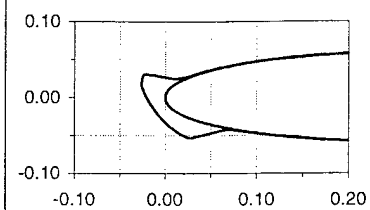	0.043	0.018	12	1.5	0.0	0.019	6.8	0.67
												1.0	0.018		
												2.0	0.019		
												3.1	0.024		
												4.1	0.030		
												5.1	0.043		
												6.1	0.064		
												7.1	0.099		

TABLE G-2.3. STUDIES USING ACCRETED OR SIMULATED ICE
(Ref. 34, Bragg, Gregorek, and Shaw, AIAA-82-0582, 1982, NACA 63_2-A415 Airfoil, c = 53.8 in
Performance Data From Figures 22 and 23)

Ice shape identity	Icing Conditions						Ice shape (coordinates normalized with respect to chord)	Upper horn			Performance Data				
	α,°	V, mph	t_{tot}, °F	LWC, g/m^3	MVD, µm	time, min		h/c	x/c	θ, °	Re, 10^6	α,°	ΔC_d at α	$\Delta\alpha$ at $C_{l,max}$	$\Delta C_{l,max}$
glaze 3 (cruise) smooth	2.6	114	25	1.5	15	15	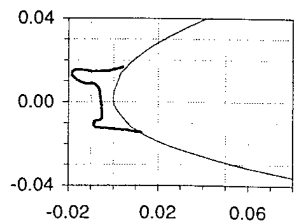	0.026	0.0071	-6	5.30	-0.4	0.004		
												2.6	0.007		
												5.6	0.025		
glaze 3 (cruise) rough	2.6	114	25	1.5	15	15	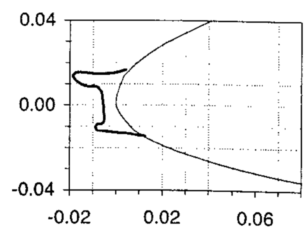	0.026	0.0071	-6	5.30	-0.4	0.006	1.9	0.15
												2.7	0.005		
												3.6	0.009		
												5.6	0.020		
glaze 7 (climb) smooth	6.6	89	25	2.9	20	15	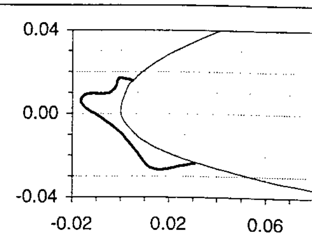	0.024	0.0056	-20	4.15	-0.3	0.006		
												2.7	0.005		
												4.7	0.010		

TABLE G-2.3. STUDIES USING ACCRETED OR SIMULATED ICE
(Ref. 34, Bragg, Gregorek, and Shaw, AIAA-82-0582, 1982, NACA 63_2-A415 Airfoil, c = 53.8 in
Performance Data From Figures 22 and 23 (Continued))

Ice shape identity	Icing Conditions						Ice shape (coordinates normalized with respect to chord)	Upper horn			Performance Data				
	α,°	V, mph	t_{tot}, °F	LWC, g/m^3	MVD, µm	time, min		h/c	x/c	θ, °	Re, 10^6	α,°	ΔC_d at α	$\Delta\alpha$ at $C_{l,max}$	$\Delta C_{l,max}$
glaze 7 (climb) rough	6.6	89	25	2.9	20	15	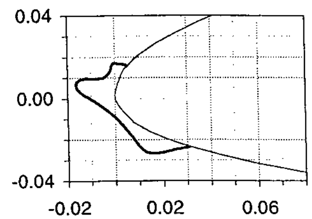	0.024	0.0056	-20	4.15	-0.3	0.006	0.9	0.05
												2.7	0.005		
												4.7	0.008		
												6.7	0.013		
rime 3 (cruise) smooth	2.6	114	-15	1.5	15	15	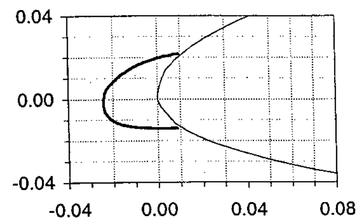	0.041	0.0115	-26	6.15	-0.35	0.00178		
												2.653	-6E-06		
												6.616	0.0013		
												8.632	0.00328		
												9.587	0.00481		
												10.61	0.0068		
												11.6	0.00935		
rime 3 (cruise) rough	2.6	114	-15	1.5	15	15	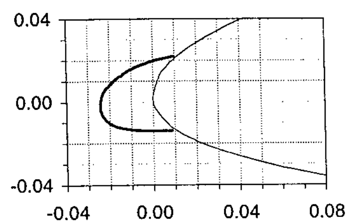	0.041	0.0115	-26	6.15	-0.35	0.00345	0.0	0.00
												4.634	0.00606		
												6.616	0.00979		
												8.597	0.01604		

TABLE G-2.3. STUDIES USING ACCRETED OR SIMULATED ICE
(Ref. 34, Bragg, Gregorek, and Shaw, AIAA-82-0582, 1982, NACA 63_2-A415 Airfoil, c = 53.8 in
Performance Data From Figures 22 and 23 (Continued))

Ice shape identity	Icing Conditions						Ice shape (coordinates normalized with respect to chord)	Upper horn			Performance Data				
	α,°	V, mph	t_{tot}, °F	LWC, g/m^3	MVD, µm	time, min		h/c	x/c	θ, °	Re, 10^6	α,°	ΔC_d at α	$\Delta\alpha$ at $C_{l,max}$	$\Delta C_{l,max}$
rime 7 (climb) smooth	6.6	89	-15	1.5	15	15	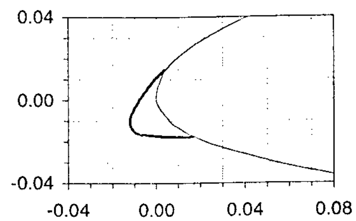	0.004	0.0314	-60	4.82	-0.43	0.00253	-0.2	0.90
												2.574	0.00037		
												4.616	0.0013		
												8.668	0.00342		
												10.68	0.00523		
rime 7 (climb) rough	6.6	89	-15	1.5	15	15	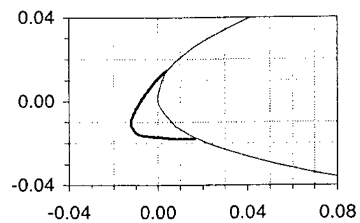	0.004	0.0314	-60	4.82	-0.36	0.00622		
												2.616	0.00528		
												4.661	0.00818		
												6.649	0.01305		

TABLE G-2.4(i). STUDIES USING ACCRETED OR SIMULATED ICE
(Ref. 56, Flemming and Lednicer, CR 3910, 1985, NACA 0012 Airfoil, c = 6 in
Ice Shapes From Figure 29, Performance Data From Appendices)

Ice shape identity	Icing Conditions						Ice shape (coordinates normalized with respect to chord)	Upper horn			Performance Data				
	α,°	V, mph	t_{tot}, °F	LWC, g/m^3	MVD, µm	time, min		h/c	x/c	θ, °	Re, 10^6	α,°	ΔC_d at α	$\Delta\alpha$ at $C_{l,max}$	$\Delta C_{l,max}$
run 2254	3.9	211	23.0	1.30	20	1.50	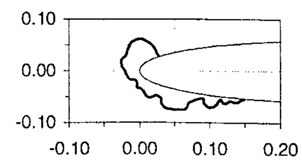	0.028	0.043	54	1.1	3.9	0.111		
run 2075	6.0	209	14.0	1.00	20	1.00	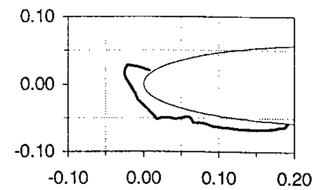	0.012	0.036	16	1.1	6.0	0.051		
run 2077	6.0	209	14.0	0.30	20	1.00	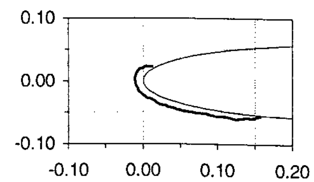	0.017	0.013	12	1.1	6.0	0.021		
run 2073	6.0	209	14.0	1.75	20	1.00	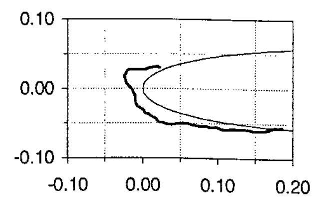	0.028	0.047	-1	1.1	6.0	0.050		

TABLE G-2.4(i). STUDIES USING ACCRETED OR SIMULATED ICE
(Ref. 56, Flemming and Lednicer, CR 3910, 1985, NACA 0012 Airfoil, c = 6 in
Ice Shapes From Figure 29, Performance Data From Appendices (Continued))

Ice shape identity	Icing Conditions						Ice shape (coordinates normalized with respect to chord)	Upper horn			Performance Data				
	α,°	V, mph	t_{tot}, °F	LWC, g/m^3	MVD, µm	time, min		h/c	x/c	θ, °	Re, 10^6	α,°	ΔC_d at α	$\Delta\alpha$ at $C_{l,max}$	$\Delta C_{l,max}$
run 2275	5.9	209	14.0	1.40	20	1.00	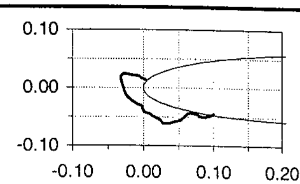	0.006	0.036	18	1.1	5.9	0.070		
run 2277	6.0	211	23.0	1.40	20	1.00	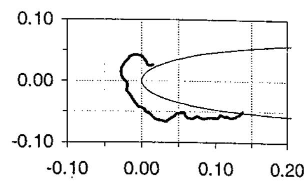	0.017	0.034	38	1.1	6.0	0.094		
run 2049	5.9	272	14.0	0.70	20	1.00	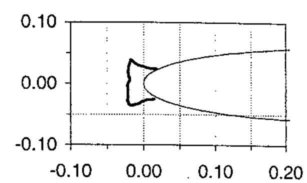	0.019	0.040	23	1.5	5.9	0.033		
run 1955	5.9	279	14.0	0.48	20	1.00	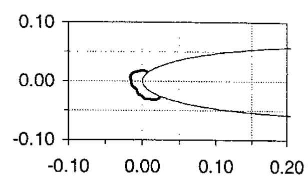	0.008	0.024	-11	1.4	5.9	0.030		

TABLE G-2.4(i). STUDIES USING ACCRETED OR SIMULATED ICE
(Ref. 56, Flemming and Lednicer, CR 3910, 1985, NACA 0012 Airfoil, c = 6 in
Ice Shapes From Figure 29, Performance Data From Appendices (Continued))

Ice shape identity	Icing Conditions						Ice shape (coordinates normalized with respect to chord)	Upper horn			Performance Data				
	α,°	V, mph	t_{tot}, °F	LWC, g/m^3	MVD, µm	time, min		h/c	x/c	θ, °	Re, 10^6	α,°	ΔC_d at α	$\Delta\alpha$ at $C_{l,max}$	$\Delta C_{l,max}$
run 2039	6.0	272	14.0	0.70	20	1.00	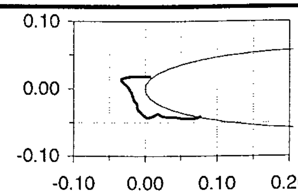	0.012	0.044	1	1.5	6.0	0.037		
run 2083	6.0	279	14.0	0.48	20	1.00	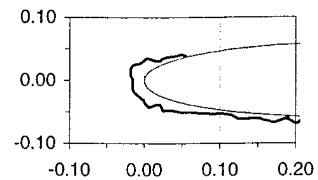	0.057	0.074	-10	1.4	6.0	0.032		
run 2106	6.0	279	14.0	0.48	20	1.00	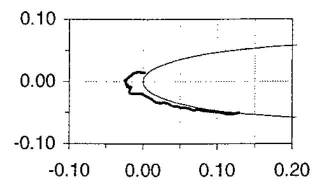	0.007	0.033	-22	1.4	6.0			
run 453	6.0	286	14.0	0.30	20	1.00	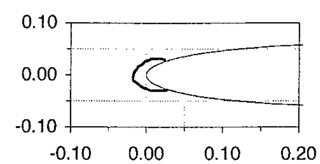	0.027	0.021	14	1.5	6.0	0.011		

TABLE G-2.4(i). STUDIES USING ACCRETED OR SIMULATED ICE
(Ref. 56, Flemming and Lednicer, CR 3910, 1985, NACA 0012 Airfoil, c = 6 in
Ice Shapes From Figure 29, Performance Data From Appendices (Continued))

Ice shape identity	Icing Conditions						Ice shape (coordinates normalized with respect to chord)	Upper horn			Performance Data				
	α,°	V, mph	t_{tot}, °F	LWC, g/m^3	MVD, µm	time, min		h/c	x/c	θ, °	Re, 10^6	α,°	ΔC_d at α	$\Delta\alpha$ at $C_{l,max}$	$\Delta C_{l,max}$
run 561	9.0	279	14.0	0.48	20	1.00	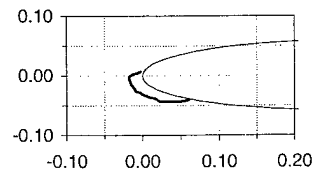	0.002	0.021	-25	1.4	9.0			
run 1153	3.0	415	14.0	0.58	20	0.75	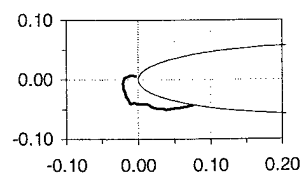	0.001	0.019	-2	2.0	3.0	0.024		
run 1953	5.9	279	14.0	0.48	20	1.00	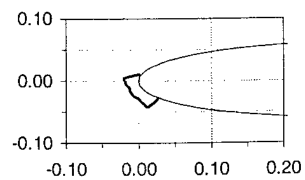	0.003	0.024	-17	1.4	5.9	0.033		
run 2256 CL	6.0	279	14.0	0.30	20	5.00	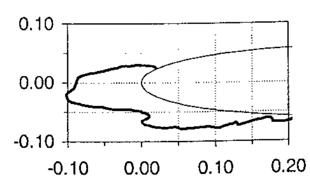	0.107	0.111	-9	1.4	6.0	0.016		

TABLE G-2.4(i). STUDIES USING ACCRETED OR SIMULATED ICE
(Ref. 56, Flemming and Lednicer, CR 3910, 1985, NACA 0012 Airfoil, c = 6 in
Ice Shapes From Figure 29, Performance Data From Appendices (Continued))

Ice shape identity	Icing Conditions						Ice shape (coordinates normalized with respect to chord)	Upper horn			Performance Data				
	α,°	V, mph	t_{tot}, °F	LWC, g/m^3	MVD, µm	time, min		h/c	x/c	θ, °	Re, 10^6	α,°	ΔC_d at α	$\Delta\alpha$ at $C_{l,max}$	$\Delta C_{l,max}$
run 2256 off CL	6.0	279	14.0	0.30	20	5.00	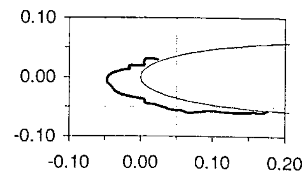	0.107	0.111	-9	1.4	6.0	0.016		
run 2071	6.0	341	14.0	0.53	20	0.75	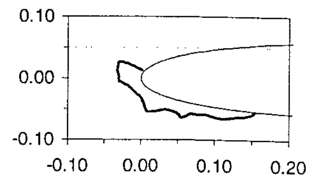	0.004	0.039	27	1.8	6.0	0.029		
run 2067	6.0	341	14.0	0.66	20	1.00	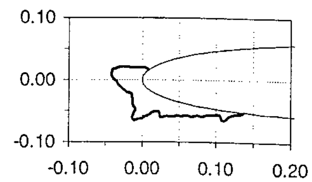	0.012	0.050	4	1.8	6.0	0.053		
run 2069	6.0	341	14.0	0.53	20	1.00	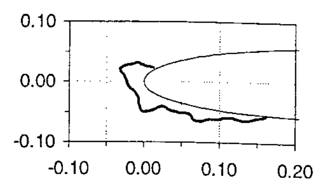	0.016	0.035	22	1.8	6.0	0.033		

TABLE G-2.4(i). STUDIES USING ACCRETED OR SIMULATED ICE
(Ref. 56, Flemming and Lednicer, CR 3910, 1985, NACA 0012 Airfoil, c = 6 in
Ice Shapes From Figure 29, Performance Data From Appendices (Continued))

Ice shape identity	Icing Conditions						Ice shape (coordinates normalized with respect to chord)	Upper horn			Performance Data				
	α,°	V, mph	t_{tot}, °F	LWC, g/m^3	MVD, µm	time, min		h/c	x/c	θ, °	Re, 10^6	α,°	ΔC_d at α	$\Delta\alpha$ at $C_{l,max}$	$\Delta C_{l,max}$
run 2250	6.1	348	14.0	0.94	20	0.75	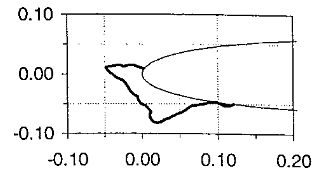	0.003	0.051	2	1.8	6.1	0.084		
run 2252	6.1	348	14.0	0.94	20	1.00	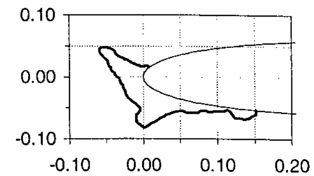	0.005	0.072	30	1.8	6.1	0.110		
run 2259	5.9	408	14.0	0.66	20	0.75	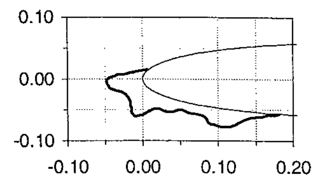	0.008	0.057	-14	2.0	5.9	0.011		
run 2271	6.0	412	23.0	0.66	20	0.75	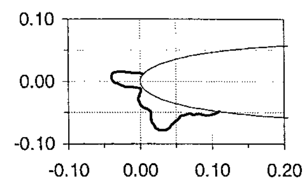	0.005	0.040	5	2.0	6.0	0.021		

TABLE G-2.4(i). STUDIES USING ACCRETED OR SIMULATED ICE
(Ref. 56, Flemming and Lednicer, CR 3910, 1985, NACA 0012 Airfoil, c = 6 in
Ice Shapes From Figure 29, Performance Data From Appendices (Continued))

Ice shape identity	Icing Conditions						Ice shape (coordinates normalized with respect to chord)	Upper horn			Performance Data				
	α,°	V, mph	t_{tot}, °F	LWC, g/m^3	MVD, µm	time, min		h/c	x/c	θ, °	Re, 10^6	α,°	ΔC_d at α	$\Delta\alpha$ at $C_{l,max}$	$\Delta C_{l,max}$
run 2280	6.0	416	32.0	0.66	20	0.75	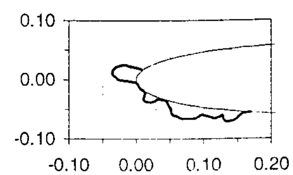	0.010	0.034	14	1.9	6.0	0.029		
run 2263	5.9	415	14.0	0.94	20	0.33	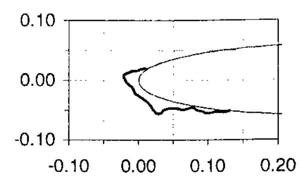	0.014	0.037	-18	2.0	5.9	0.010		
run 411	0.0	209	14.0	0.96	20	1.00	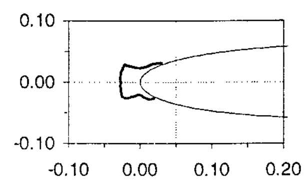	0.011	0.034	18	1.1	0.0	0.024		
run 520	2.9	395	14.0	1.03	20	0.75	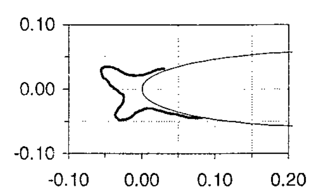	0.005	0.060	22	2.0	2.9	0.095		

TABLE G-2.4(i). STUDIES USING ACCRETED OR SIMULATED ICE
(Ref. 56, Flemming and Lednicer, CR 3910, 1985, NACA 0012 Airfoil, c = 6 in
Ice Shapes From Figure 29, Performance Data From Appendices (Continued))

Ice shape identity	Icing Conditions						Ice shape (coordinates normalized with respect to chord)	Upper horn			Performance Data				
	α,°	V, mph	t_{tot}, °F	LWC, g/m^3	MVD, µm	time, min		h/c	x/c	θ, °	Re, 10^6	α,°	ΔC_d at α	$\Delta\alpha$ at $C_{l,max}$	$\Delta C_{l,max}$
run 238	6.0	427	42.1	0.24	20	1.00	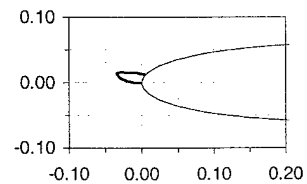	0.005	0.039	5	1.9	6.0	0.001		
run 239	6.0	423	32.7	0.24	20	1.00	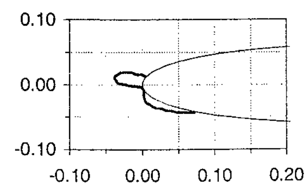	0.005	0.035	12	2.0	6.0	0.006		
run 2079	3.0	408	14.0	0.38	20	0.75	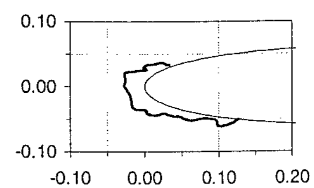	0.029	0.057	-7	2.0	3.0	0.015		
run 2273	3.0	408	14.0	0.66	20	0.75	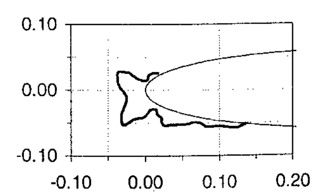	0.006	0.044	22	2.0	3.0	0.046		

TABLE G-2.4(i). STUDIES USING ACCRETED OR SIMULATED ICE
(Ref. 56, Flemming and Lednicer, CR 3910, 1985, NACA 0012 Airfoil, c = 6 in
Ice Shapes From Figure 29, Performance Data From Appendices (Continued))

Ice shape identity	Icing Conditions						Ice shape (coordinates normalized with respect to chord)	Upper horn			Performance Data				
	α, °	V, mph	t_{tot}, °F	LWC, g/m^3	MVD, µm	time, min		h/c	x/c	θ, °	Re, 10^6	α, °	ΔC_d at α	$\Delta\alpha$ at $C_{l,max}$	$\Delta C_{l,max}$
run 585	-0.1	415	14.0	1.03	20	0.75	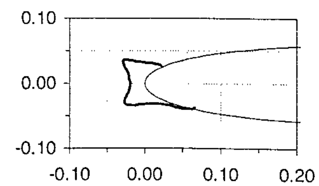	0.025	0.054	12	2.0	-0.1	0.014		
run 565	6.0	408	14.0	1.03	20	0.75	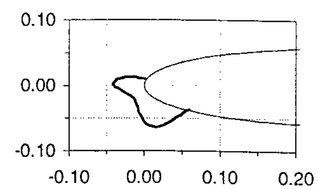	0.002	0.042	-1	2.0	6.0	0.019		
run 2248	0.1	428	14.0	0.66	20	0.75	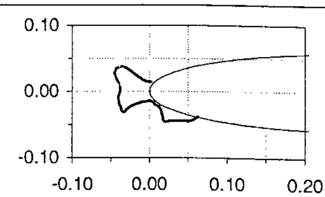	0.006	0.052	32	0.9	0.1	0.025		
run 1883	0.0	415	14.0	0.38	20	0.75	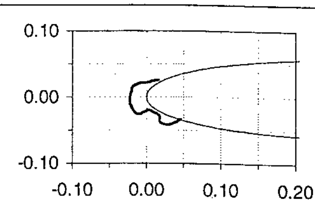	0.025	0.044	-12	2.0	0.0	0.011		

TABLE G-2.4(i). STUDIES USING ACCRETED OR SIMULATED ICE
(Ref. 56, Flemming and Lednicer, CR 3910, 1985, NACA 0012 Airfoil, c = 6 in
Ice Shapes From Figure 29, Performance Data From Appendices (Continued))

Ice shape identity	Icing Conditions						Ice shape (coordinates normalized with respect to chord)	Upper horn			Performance Data				
	α,°	V, mph	t_{tot}, °F	LWC, g/m^3	MVD, µm	time, min		h/c	x/c	θ, °	Re, 10^6	α,°	ΔC_d at α	$\Delta\alpha$ at $C_{l,max}$	$\Delta C_{l,max}$
run 2261	5.9	408	14.0	0.66	20	1.00	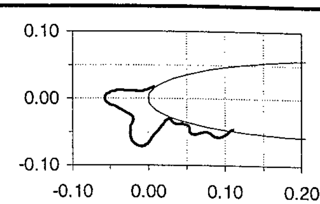	0.011	0.063	-7	2.0	5.9	0.018		
run 2269	6.0	408	14.0	0.66	20	0.33	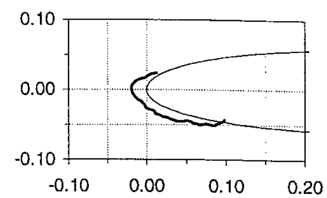	0.019	0.036	-19	2.0	6.0	0.006		
run 2267	6.0	408	14.0	0.94	20	1.00	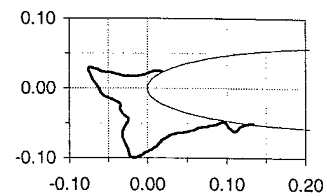	0.022	0.096	3	2.0	6.0	0.131		
run 2265	5.9	408	14.0	0.94	20	0.75	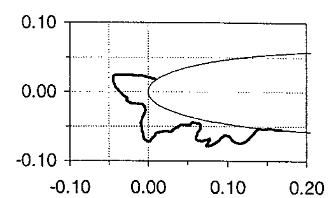	0.011	0.054	7	2.0	5.9	0.068		

TABLE G-2.4(i). STUDIES USING ACCRETED OR SIMULATED ICE
(Ref. 56, Flemming and Lednicer, CR 3910, 1985, NACA 0012 Airfoil, c = 6 in
Ice Shapes From Figure 29, Performance Data From Appendices (Continued))

Ice shape identity	Icing Conditions						Ice shape (coordinates normalized with respect to chord)	Upper horn			Performance Data				
	α,°	V, mph	t_{tot}, °F	LWC, g/m^3	MVD, µm	time, min		h/c	x/c	θ, °	Re, 10^6	α,°	ΔC_d at α	$\Delta\alpha$ at $C_{l,max}$	$\Delta C_{l,max}$
run 2061	6.0	408	14.0	0.38	20	0.75	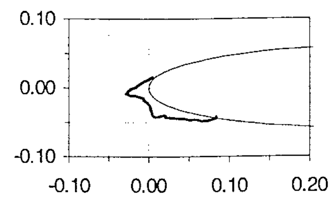	0.008	0.043	-35	2.0	6.0	0.004		

TABLE G-2.4(ii). STUDIES USING ACCRETED OR SIMULATED ICE
(Ref. 56, Flemming and Lednicer, CR 3910, 1985, SC1095 Airfoil, c = 6 in
Ice Shapes From Figure 30, Performance Data From Appendices)

Ice shape identity	Icing Conditions						Ice shape (coordinates normalized with respect to chord)	Upper horn			Performance Data				
	α,°	V, mph	t_{tot}, °F	LWC, g/m^3	MVD, µm	time, min		h/c	x/c	θ, °	Re, 10^6	α,°	ΔC_d at α	$\Delta\alpha$ at $C_{l,max}$	$\Delta C_{l,max}$
run 2319	6.0	209	14.0	1.40	20	1.00	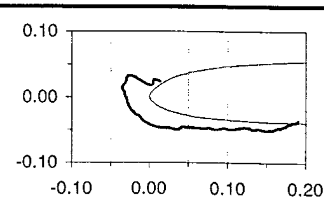	0.006	0.039	35	1.1	6.0	0.089		
run 2317	6.0	209	14.0	1.00	20	1.00	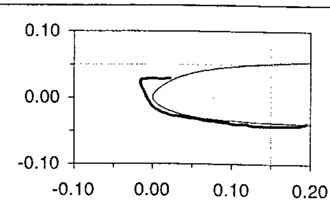	0.031	0.047	-2	1.1	6.0	0.037		
run 2328	6.0	213	32.0	0.66	20	1.00	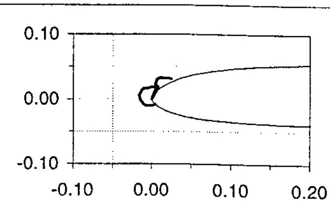	0.014	0.027	-7	1.0	6.0	0.022		
run 709	6.0	211	23.0	1.75	20	0.75	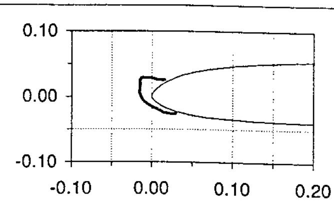	0.021	0.034	7	1.1	6.0	0.064		

TABLE G-2.4 (ii). STUDIES USING ACCRETED OR SIMULATED ICE
(Ref. 56, Flemming and Lednicer, CR 3910, 1985, SC1095 Airfoil, c = 6 in
Ice Shapes From Figure 30, Performance Data From Appendices (Continued))

Ice shape identity	Icing Conditions						Ice shape (coordinates normalized with respect to chord)	Upper horn			Performance Data					
	α,°	V, mph	t_{tot}, °F	LWC, g/m^3	MVD, µm	time, min		h/c	x/c	θ, °	Re, 10^6	α,°	ΔC_d at α	$\Delta\alpha$ at $C_{l,max}$	$\Delta C_{l,max}$
run 730	5.9	218	23.0	1.06	20	0.75	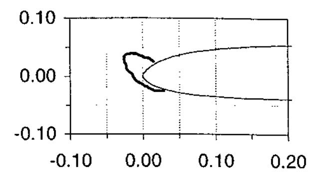	0.018	0.039	32	1.1	5.9	0.046		
run 697	6.0	286	14.0	0.62	20	1.00	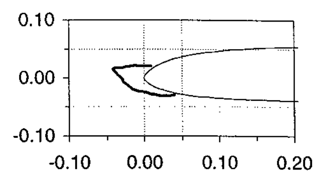	0.015	0.056	-3	1.5	6.0	0.038		
run 711	3.0	415	14.0	1.40	20	0.75	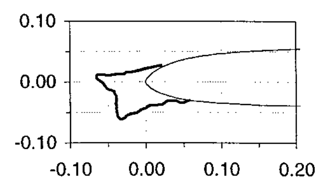	0.027	0.095	-11	2.1	3.0	0.035		
run 742	3.1	279	14.0	0.62	20	1.00	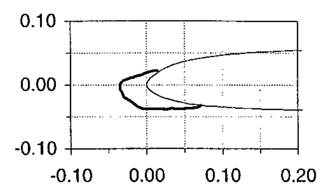	0.020	0.057	-20	1.5	3.1	0.024		

TABLE G-2.4 (ii). STUDIES USING ACCRETED OR SIMULATED ICE
(Ref. 56, Flemming and Lednicer, CR 3910, 1985, SC1095 Airfoil, c = 6 in
Ice Shapes From Figure 30, Performance Data From Appendices (Continued))

Ice shape identity	Icing Conditions						Ice shape (coordinates normalized with respect to chord)	Upper horn			Performance Data				
	α,°	V, mph	t_{tot}, °F	LWC, g/m^3	MVD, µm	time, min		h/c	x/c	θ, °	Re, 10^6	α,°	ΔC_d at α	$\Delta\alpha$ at $C_{l,max}$	$\Delta C_{l,max}$
run 261	6.0	345	23.0	0.30	20	1.00	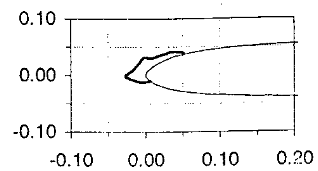	0.054	0.058	-7	1.7	6.0	0.012		
run 754	3.1	415	14.0	0.50	20	0.75	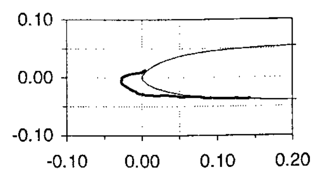	0.007	0.036	-19	2.1	3.1	0.013		
run 594	0.0	408	14.0	1.03	20	0.75	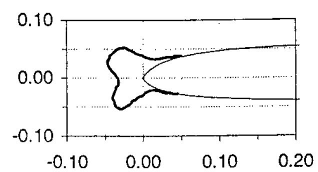	0.022	0.057	30	2.1	0.0	0.084		
run 713	3.0	381	11.5	1.40	20	0.75	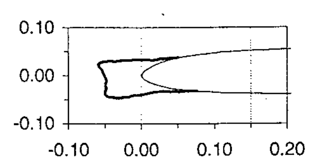	0.051	0.110	-5	2.0	3.0			

TABLE G-2.4 (ii). STUDIES USING ACCRETED OR SIMULATED ICE
(Ref. 56, Flemming and Lednicer, CR 3910, 1985, SC1095 Airfoil, c = 6 in
Ice Shapes From Figure 30, Performance Data From Appendices (Continued))

Ice shape identity	Icing Conditions						Ice shape (coordinates normalized with respect to chord)	Upper horn			Performance Data					
	α,°	V, mph	t_{tot}, °F	LWC, g/m^3	MVD, µm	time, min		h/c	x/c	θ, °	Re, 10^6	α,°	ΔC_d at α	$\Delta\alpha$ at $C_{l,max}$	$\Delta C_{l,max}$
run 600	6.0	408	14.0	1.03	20	0.75	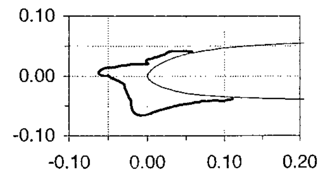	0.016	0.075	-6	2.1	6.0	0.025		
run 629	6.1	404	5.0	1.03	20	1.00	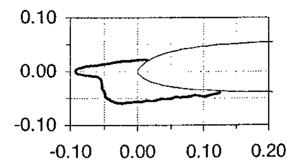	0.019	0.114	-10	2.1	6.1	0.009		
run 2315	0.0	408	14.0	0.66	20	0.75	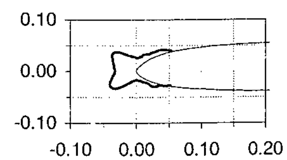	0.015	0.052	23	2.0	0.0	0.036		
run 2311	3.0	418	36.0	1.40	20	0.75	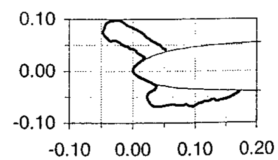	0.056	0.102	37	2.0	3.0	0.081		

TABLE G-2.4 (ii). STUDIES USING ACCRETED OR SIMULATED ICE (Ref. 56, Flemming and Lednicer, CR 3910, 1985, SC1095 Airfoil, c = 6 in Ice Shapes From Figure 30, Performance Data From Appendices (Continued))

Ice shape identity	Icing Conditions						Ice shape (coordinates normalized with respect to chord)	Upper horn			Performance Data				
	α,°	V, mph	t_{tot}, °F	LWC, g/m^3	MVD, µm	time, min		h/c	x/c	θ, °	Re, 10^6	α,°	ΔC_d at α	$\Delta\alpha$ at $C_{l,max}$	$\Delta C_{l,max}$
run 2313	3.0	408	14.0	0.66	20	0.75	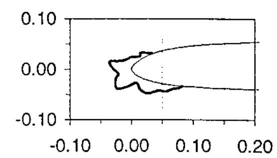	0.027	0.064	-10	2.0	3.0	0.020		
run 2326	6.0	416	32.0	0.66	20	0.75	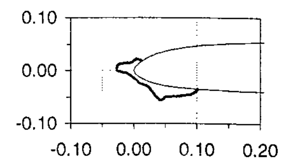	0.010	0.035	-4	1.9	6.0	0.004		
run 2324	6.0	412	23.0	0.66	20	0.75	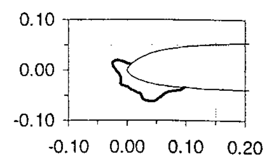	0.006	0.031	22	2.0	6.0	0.009		
run 2321	6.0	404	5.0	0.66	20	0.75	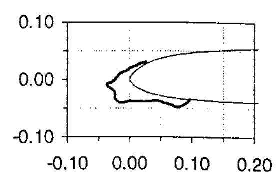	0.034	0.083	-30	2.1	6.0	0.009		

TABLE G-2.4 (ii). STUDIES USING ACCRETED OR SIMULATED ICE
(Ref. 56, Flemming and Lednicer, CR 3910, 1985, SC1095 Airfoil, c = 6 in
Ice Shapes From Figure 30, Performance Data From Appendices (Continued))

Ice shape identity	Icing Conditions						Ice shape (coordinates normalized with respect to chord)	Upper horn			Performance Data				
	α,°	V, mph	t_{tot}, °F	LWC, g/m^3	MVD, μm	time, min		h/c	x/c	θ, °	Re, 10^6	α,°	ΔC_d at α	$\Delta\alpha$ at $C_{l,max}$	$\Delta C_{l,max}$
run 726	6.1	408	14.0	0.24	20	2.00	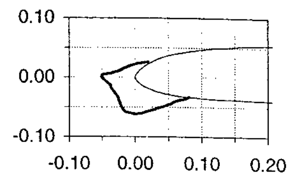	0.025	0.080	-17	2.1	6.1	0.011		
run 637	5.9	421	14.0	0.85	20	0.75	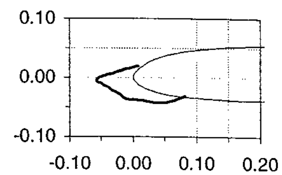	0.015	0.076	-18	2.0	5.9	-0.001		
run 718	6.0	415	14.0	1.40	20	0.75	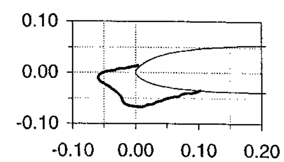	0.009	0.070	-13	2.1	6.0			

TABLE G-2.4(iii). STUDIES USING ACCRETED OR SIMULATED ICE
(Ref. 56, Flemming and Lednicer, CR 3910, 1985, SSC-A09 Airfoil, c = 6 in
Ice Shapes From Figure 31, Performance Data From Appendices)

Ice shape identity	Icing Conditions						Ice shape (coordinates normalized with respect to chord)	Upper horn			Performance Data				
	α,°	V, mph	t_{tot}, °F	LWC, g/m^3	MVD, μm	time, min		h/c	x/c	θ, °	Re, 10^6	α,°	ΔC_d at α	$\Delta\alpha$ at $C_{l,max}$	$\Delta C_{l,max}$
run 1102	0.0	209	14.0	1.75	20	1.00	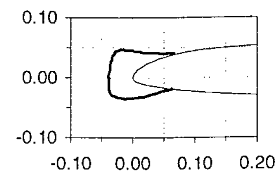	0.094	0.067	5	1.1	0.0	0.0547		
run 923	6.0	195	14.0	1.75	20	1.00	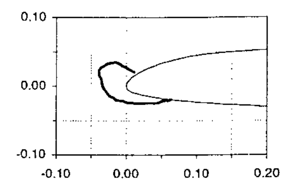	0.038	0.016	29	1.1	6.0	0.1085		
run 2144	6.0	211	23.0	1.00	20	1.00	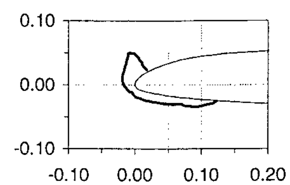	0.039	0.019	54	1.1	6.0	0.0669		
run 2146	6.0	211	23.0	0.66	20	1.00	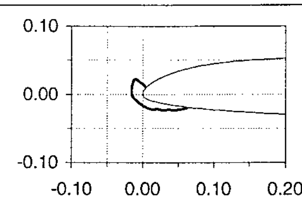	0.021	0.005	43	1.1	6.0	0.0472		

TABLE G-2.4(iii). STUDIES USING ACCRETED OR SIMULATED ICE
(Ref. 56, Flemming and Lednicer, CR 3910, 1985, SSC-A09 Airfoil, c = 6 in
Ice Shapes From Figure 31, Performance Data From Appendices (Continued))

Ice shape identity	Icing Conditions						Ice shape (coordinates normalized with respect to chord)	Upper horn			Performance Data				
	α,°	V, mph	t_{tot}, °F	LWC, g/m^3	MVD, µm	time, min		h/c	x/c	θ, °	Re, 10^6	α,°	ΔC_d at α	$\Delta\alpha$ at $C_{l,max}$	$\Delta C_{l,max}$
run 2148	6.0	211	23.0	0.35	20	1.00	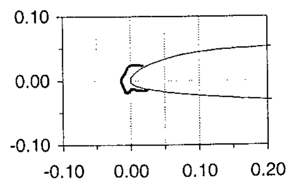	0.021	0.022	9	1.1	6.0	0.0193		
run 2142	6.0	205	-4.0	1.00	20	1.00	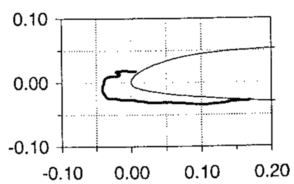	0.041	0.006	-2	1.2	6.0	0.0244		
run 2140	6.0	205	-4.0	0.66	20	1.00	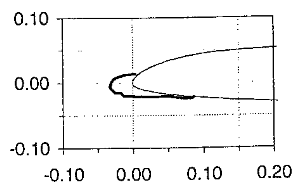	0.037	0.008	-12	1.2	6.0	0.0192		
run 2117	6.0	272	14.0	0.48	20	1.00	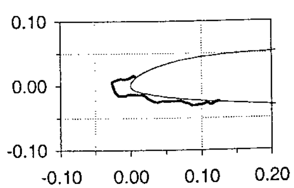	0.039	0.012	-15	1.4	6.0	0.0293		

TABLE G-2.4(iii). STUDIES USING ACCRETED OR SIMULATED ICE
(Ref. 56, Flemming and Lednicer, CR 3910, 1985, SSC-A09 Airfoil, c = 6 in
Ice Shapes From Figure 31, Performance Data From Appendices (Continued))

Ice shape identity	Icing Conditions						Ice shape (coordinates normalized with respect to chord)	Upper horn			Performance Data				
	α,°	V, mph	t_{tot}, °F	LWC, g/m^3	MVD, µm	time, min		h/c	x/c	θ, °	Re, 10^6	α,°	ΔC_d at α	$\Delta\alpha$ at $C_{l,max}$	$\Delta C_{l,max}$
run 2162	6.0	279	14.0	0.48	20	1.00	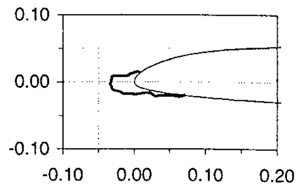	0.035	0.004	-2	1.4	6.0	-		
run 1114	3.0	408	14.0	0.58	20	0.75	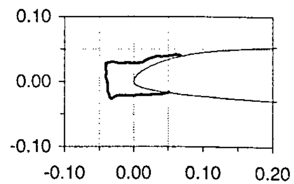	0.077	0.037	0	2.0	3.0	0.0254		
run 1116	3.0	415	14.0	0.58	20	0.75	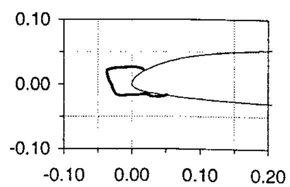	0.057	0.021	0	2.1	3.0	0.0221		
run 884	5.9	272	14.0	0.62	20	1.00	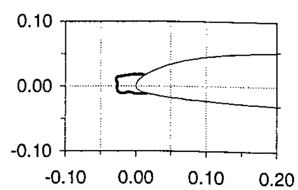	0.043	0.014	-7	1.5	5.9	0.0248		

TABLE G-2.4(iii). STUDIES USING ACCRETED OR SIMULATED ICE
(Ref. 56, Flemming and Lednicer, CR 3910, 1985, SSC-A09 Airfoil, c = 6 in
Ice Shapes From Figure 31, Performance Data From Appendices (Continued))

Ice shape identity	Icing Conditions						Ice shape (coordinates normalized with respect to chord)	Upper horn			Performance Data				
	α,°	V, mph	t_{tot}, °F	LWC, g/m^3	MVD, µm	time, min		h/c	x/c	θ, °	Re, 10^6	α,°	ΔC_d at α	$\Delta\alpha$ at $C_{l,max}$	$\Delta C_{l,max}$
run 2228	0.0	402	14.0	0.58	20	0.75	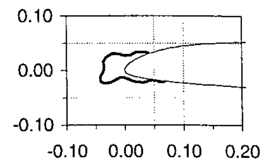	0.070	0.046	-1	2.0	0.0	0.0354		
run 2152	0.0	408	14.0	0.33	20	0.75	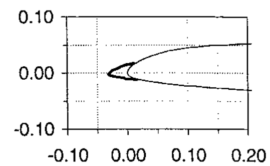	0.047	0.012	-25	2.0	0.0	0.0128		
run 2150	0.0	408	14.0	0.35	20	0.75	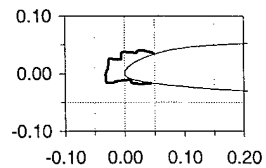	0.044	0.017	10	2.0	0.0	0.0219		
run 931	6.0	415	14.0	0.85	20	0.75	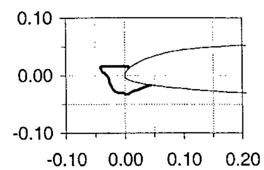	0.051	0.010	1	2.1	6.0	0.0267		

TABLE G-2.4(iii). STUDIES USING ACCRETED OR SIMULATED ICE
(Ref. 56, Flemming and Lednicer, CR 3910, 1985, SSC-A09 Airfoil, c = 6 in
Ice Shapes From Figure 31, Performance Data From Appendices (Continued))

Ice shape identity	Icing Conditions						Ice shape (coordinates normalized with respect to chord)	Upper horn			Performance Data				
	α,°	V, mph	t_{tot}, °F	LWC, g/m^3	MVD, µm	time, min		h/c	x/c	θ, °	Re, 10^6	α,°	ΔC_d at α	$\Delta\alpha$ at $C_{l,max}$	$\Delta C_{l,max}$
run 1088	0.0	402	14.0	0.58	20	0.75	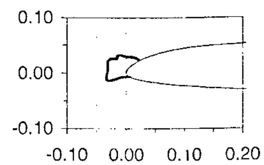	0.054	0.025	2	2.0	0.0	0.0335		
run 859	6.2	415	14.0	0.50	20	0.75	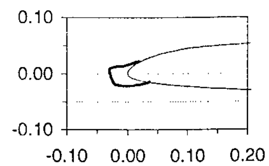	0.053	0.022	-13	2.1	6.2	0.0051		
run 861	0.0	415	14.0	0.50	20	0.75	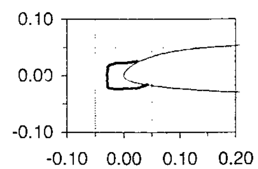	0.058	0.029	-10	2.1	0.0	0.0245		
run 868	0.0	408	14.0	0.50	20	1.00	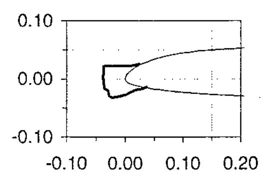	0.066	0.028	-3	2.0	0.0	-		

TABLE G-2.4(iii). STUDIES USING ACCRETED OR SIMULATED ICE
(Ref. 56, Flemming and Lednicer, CR 3910, 1985, SSC-A09 Airfoil, c = 6 in
Ice Shapes From Figure 31, Performance Data From Appendices (Continued))

Ice shape identity	Icing Conditions						Ice shape (coordinates normalized with respect to chord)	Upper horn			Performance Data				
	α,°	V, mph	t_{tot}, °F	LWC, g/m^3	MVD, µm	time, min		h/c	x/c	θ, °	Re, 10^6	α,°	ΔC_d at α	$\Delta\alpha$ at $C_{l,max}$	$\Delta C_{l,max}$
run 927	6.0	415	14.0	0.85	20	0.50	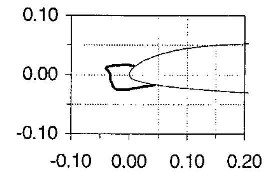	0.051	0.011	-4	2.1	6.0	0.0130		
run 1110	6.0	415	14.0	0.35	20	0.50	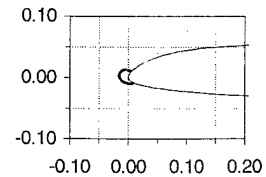	0.016	0.005	10	2.1	6.0	0.0051		
run 1112	6.0	415	14.0	1.31	20	0.50	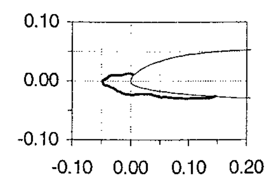	0.041	0.005	-2	2.1	6.0	0.0396		
run 2218	5.9	408	14.0	0.85	20	1.00	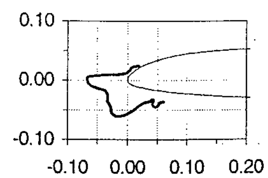	0.072	0.005	-4	2.0	5.9	0.0503		

TABLE G-2.4(iii). STUDIES USING ACCRETED OR SIMULATED ICE
(Ref. 56, Flemming and Lednicer, CR 3910, 1985, SSC-A09 Airfoil, c = 6 in
Ice Shapes From Figure 31, Performance Data From Appendices (Continued))

Ice shape identity	Icing Conditions						Ice shape (coordinates normalized with respect to chord)	Upper horn			Performance Data				
	α,°	V, mph	t_{tot}, °F	LWC, g/m^3	MVD, µm	time, min		h/c	x/c	θ, °	Re, 10^6	α,°	ΔC_d at α	$\Delta\alpha$ at $C_{l,max}$	$\Delta C_{l,max}$
run 2132	6.0	408	14.0	0.49	20	1.00	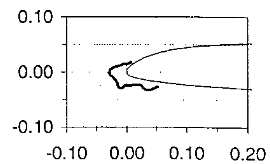	0.051	0.019	-18	2.0	6.0	0.0107		
run 2134	6.0	400	-4.0	0.53	20	0.75	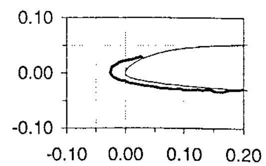	0.047	0.030	-12	2.1	6.0	0.0063		
run 2113	6.0	412	23.0	0.35	20	0.75	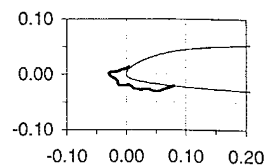	0.040	0.009	-17	2.0	6.0	0.0095		
run 2108	5.9	416	32.0	0.38	20	0.75	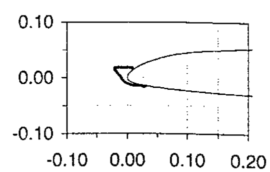	0.034	0.013	3	1.9	5.9	0.0127		

TABLE G-2.4(iii). STUDIES USING ACCRETED OR SIMULATED ICE
(Ref. 56, Flemming and Lednicer, CR 3910, 1985, SSC-A09 Airfoil, c = 6 in
Ice Shapes From Figure 31, Performance Data From Appendices (Continued))

Ice shape identity	Icing Conditions						Ice shape (coordinates normalized with respect to chord)	Upper horn			Performance Data				
	α,°	V, mph	t_{tot}, °F	LWC, g/m^3	MVD, µm	time, min		h/c	x/c	θ, °	Re, 10^6	α,°	ΔC_d at α	$\Delta\alpha$ at $C_{l,max}$	$\Delta C_{l,max}$
run 2115	6.0	412	23.0	0.38	20	0.75	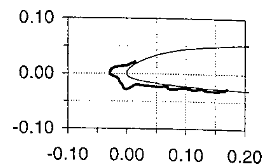	0.054	0.023	-17	2.0	6.0	0.0099		
run 2220	5.9	401	-2.0	0.66	20	0.75	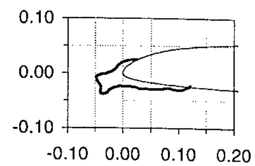	0.055	0.004	-16	2.1	5.9	0.0115		
run 2226	5.9	412	23.0	0.66	20	0.75	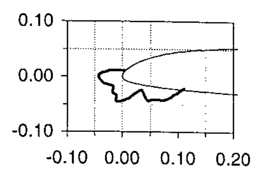	0.048	0.006	-9	2.0	5.9	0.0241		
run 2225	5.9	416	32.0	0.66	20	0.75	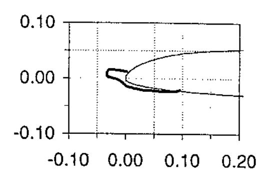	0.037	0.006	9	1.9	5.9	0.0167		

TABLE G-2.4(iii). STUDIES USING ACCRETED OR SIMULATED ICE
(Ref. 56, Flemming and Lednicer, CR 3910, 1985, SSC-A09 Airfoil, c = 6 in
Ice Shapes From Figure 31, Performance Data From Appendices (Continued))

Ice shape identity	Icing Conditions						Ice shape (coordinates normalized with respect to chord)	Upper horn			Performance Data				
	α,°	V, mph	t_{tot}, °F	LWC, g/m^3	MVD, µm	time, min		h/c	x/c	θ, °	Re, 10^6	α,°	ΔC_d at α	$\Delta\alpha$ at $C_{l,max}$	$\Delta C_{l,max}$
run 2222	5.9	401	-2.0	1.00	20	0.75	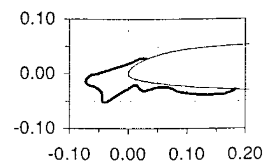	0.110	0.032	-18	2.1	5.9	0.0168		
run 2138	6.0	400	-4.0	0.62	20	0.75	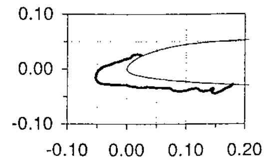	0.080	0.026	-21	2.1	6.0	0.0073		
run 2136	6.0	400	-4.0	0.35	20	0.75	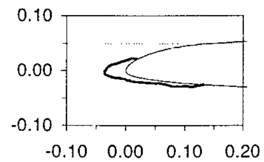	0.056	0.020	-17	2.1	6.0	0.0064		
run 1129	0.0	395	14.0	1.36	20	0.75	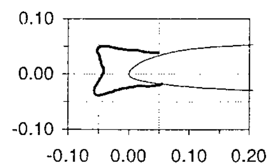	0.106	0.056	8	2.0	0.0	0.1017		

TABLE G-2.4(iii). STUDIES USING ACCRETED OR SIMULATED ICE (Ref. 56, Flemming and Lednicer, CR 3910, 1985, SSC-A09 Airfoil, c = 6 in Ice Shapes From Figure 31, Performance Data From Appendices (Continued))

Ice shape identity	Icing Conditions						Ice shape (coordinates normalized with respect to chord)	Upper horn			Performance Data				
	α,°	V, mph	t_{tot}, °F	LWC, g/m^3	MVD, µm	time, min		h/c	x/c	θ, °	Re, 10^6	α,°	ΔC_d at α	$\Delta\alpha$ at $C_{l,max}$	$\Delta C_{l,max}$
run 1122	0.0	467	14.0	0.64	20	0.75	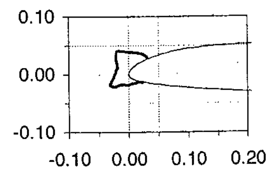	0.054	0.033	14	2.2	0.0	0.0304		

TABLE G-2.4(iv). STUDIES USING ACCRETED OR SIMULATED ICE (Ref. 56, Flemming and Lednicer, CR 3910, 1985, VR-7 Airfoil, c = 6.38 in Ice Shapes From Figure 32, Performance Data From Appendices)

Ice shape identity	Icing Conditions						Ice shape (coordinates normalized with respect to chord)	Upper horn			Performance Data				
	α,°	V, mph	t_{tot}, °F	LWC, g/m^3	MVD, µm	time, min		h/c	x/c	θ, °	Re, 10^6	α,°	ΔC_d at α	$\Delta\alpha$ at $C_{l,max}$	$\Delta C_{l,max}$
run 2166	5.8	209	14.0	1.20	20	1.00	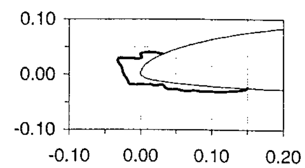	0.049	0.018	2	1.2	5.8	0.0276		
run 2164	5.8	209	14.0	0.30	20	1.00	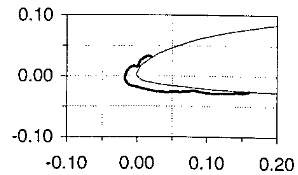	0.011	0.004	20	1.2	5.8	0.0203		
run 2170	5.8	272	14.0	1.40	20	1.00	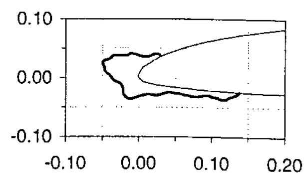	0.080	0.031	-5	1.5	5.8	0.0553		
run 2172	5.8	279	14.0	1.00	20	1.00	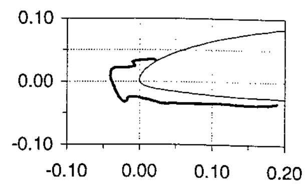	0.051	0.014	-3	1.5	5.8	0.0315		

TABLE G-2.4(iv). STUDIES USING ACCRETED OR SIMULATED ICE
(Ref. 56, Flemming and Lednicer, CR 3910, 1985, VR-7 Airfoil, c = 6.38 in
Ice Shapes From Figure 32, Performance Data From Appendices (Continued))

Ice shape identity	Icing Conditions						Ice shape (coordinates normalized with respect to chord)	Upper horn			Performance Data				
	α,°	V, mph	t_{tot}, °F	LWC, g/m^3	MVD, µm	time, min		h/c	x/c	θ, °	Re, 10^6	α,°	ΔC_d at α	$\Delta\alpha$ at $C_{l,max}$	$\Delta C_{l,max}$
run 2168	5.8	272	14.0	0.76	20	1.00	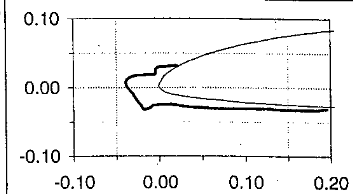	0.039	0.007	-2	1.5	5.8	0.0244		
run 2192	6.0	341	14.0	1.00	20	1.50	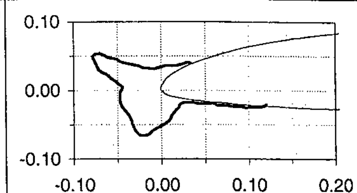	0.093	0.012	19	1.9	6.0	0.1609		
run 2178	5.8	341	14.0	1.00	20	1.50	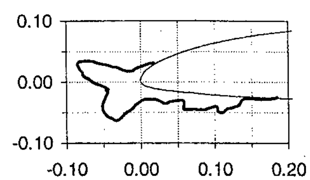	0.086	0.081	19	1.9	5.8			
run 2176	5.9	348	14.0	1.00	20	1.00	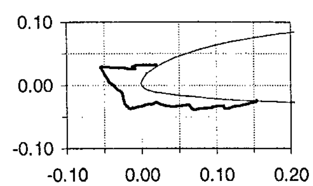	0.069	0.014	4	1.9	5.9	0.0590		

TABLE G-2.4(iv). STUDIES USING ACCRETED OR SIMULATED ICE
(Ref. 56, Flemming and Lednicer, CR 3910, 1985, VR-7 Airfoil, c = 6.38 in
Ice Shapes From Figure 32, Performance Data From Appendices (Continued))

Ice shape identity	Icing Conditions						Ice shape (coordinates normalized with respect to chord)	Upper horn			Performance Data				
	α,°	V, mph	t_{tot}, °F	LWC, g/m^3	MVD, μm	time, min		h/c	x/c	θ, °	Re, 10^6	α,°	ΔC_d at α	$\Delta\alpha$ at $C_{l,max}$	$\Delta C_{l,max}$
run 2174	5.9	341	14.0	1.00	20	0.50	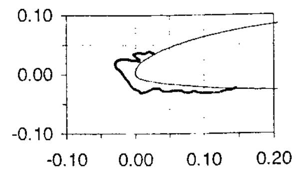	0.037	0.011	7	1.9	5.9	0.0272		
run 2180	5.8	415	14.0	0.30	20	0.75	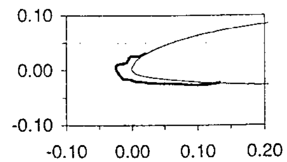	0.031	0.006	-14	2.2	5.8			
run 762	0.0	408	14.0	0.50	20	1.00	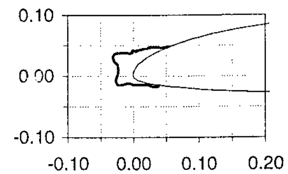	0.065	0.037	-1	2.2	0.0	0.0302		
run 764	0.0	408	14.0	0.50	20	0.75	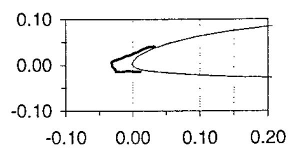	0.074	0.034	-28	2.2	0.0	0.0224		

TABLE G-2.4(iv). STUDIES USING ACCRETED OR SIMULATED ICE
(Ref. 56, Flemming and Lednicer, CR 3910, 1985, VR-7 Airfoil, c = 6.38 in
Ice Shapes From Figure 32, Performance Data From Appendices (Continued))

Ice shape identity	Icing Conditions						Ice shape (coordinates normalized with respect to chord)	Upper horn			Performance Data				
	α,°	V, mph	t_{tot}, °F	LWC, g/m^3	MVD, µm	time, min		h/c	x/c	θ, °	Re, 10^6	α,°	ΔC_d at α	$\Delta\alpha$ at $C_{l,max}$	$\Delta C_{l,max}$
run 770	6.0	286	14.0	0.62	20	1.00	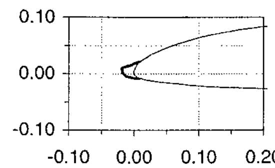	0.030	0.009	-22	1.6	6.0	0.0207		
run 784	3.0	408	14.0	0.50	20	1.00	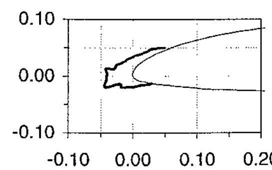	0.046	0.004	1	2.2	3.0	0.0241		
run 936	3.0	415	14.0	0.50	20	1.00	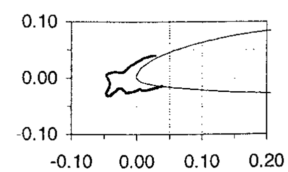	0.050	0.004	-6	2.2	3.0	0.0273		
run 2184	5.8	408	14.0	1.00	20	0.75	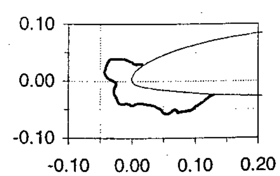	0.055	0.020	10	2.2	5.8			

TABLE G-2.4(iv). STUDIES USING ACCRETED OR SIMULATED ICE (Ref. 56, Flemming and Lednicer, CR 3910, 1985, VR-7 Airfoil, c = 6.38 in Ice Shapes From Figure 32, Performance Data From Appendices (Continued))

Ice shape identity	Icing Conditions						Ice shape (coordinates normalized with respect to chord)	Upper horn			Performance Data				
	α,°	V, mph	t_{tot}, °F	LWC, g/m^3	MVD, µm	time, min		h/c	x/c	θ, °	Re, 10^6	α,°	ΔC_d at α	$\Delta\alpha$ at $C_{l,max}$	$\Delta C_{l,max}$
run 2182	5.8	415	14.0	0.66	20	0.75	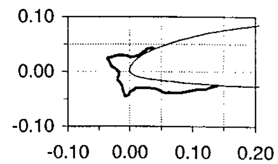	0.053	0.017	-3	2.2	5.8			
run 2188	6.0	209	14.0	0.66	20	1.00	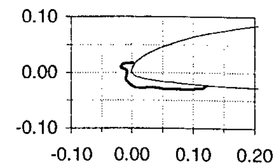	0.020	0.006	-3	1.2	6.0	0.0195		

TABLE G-2.4(v). STUDIES USING ACCRETED OR SIMULATED ICE
(Ref. 56, Flemming and Lednicer, CR 3910, 1985, SC1094 Airfoil, c = 6 in
Ice Shapes From Figure 33, Performance Data From Appendices)

Ice shape identity	Icing Conditions						Ice shape (coordinates normalized with respect to chord)	Upper horn			Performance Data				
	α,°	V, mph	t_{tot}, °F	LWC, g/m^3	MVD, µm	time, min		h/c	x/c	θ, °	Re, 10^6	α,°	ΔC_d at α	$\Delta\alpha$ at $C_{l,max}$	$\Delta C_{l,max}$
run 1335	9.0	279	14.0	0.62	20	1.00	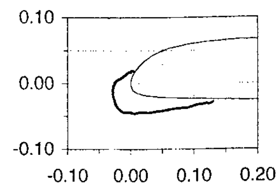	0.040	0.008	-28	1.4	9.0	0.0523		
run 1281	6.0	216	14.0	0.66	20	1.00	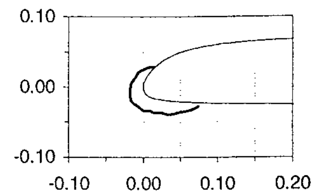	0.025	0.018	-20	1.1	6.0	0.0234		
run 1309	6.0	272	14.0	0.62	20	1.00	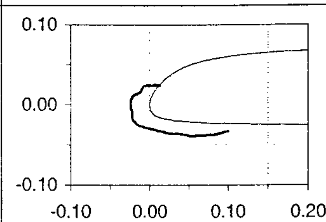	0.021	0.012	-2	1.4	6.0	0.0258		
run 1363	6.0	335	14.0	1.06	20	1.00	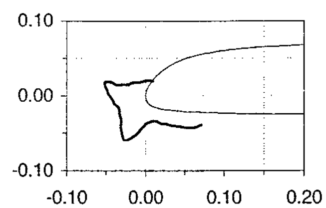	0.059	0.008	0	1.8	6.0	0.1852		

TABLE G-2.4(v). STUDIES USING ACCRETED OR SIMULATED ICE
(Ref. 56, Flemming and Lednicer, CR 3910, 1985, SC1094 Airfoil, c = 6 in
Ice Shapes From Figure 33, Performance Data From Appendices (Continued))

Ice shape identity	Icing Conditions						Ice shape (coordinates normalized with respect to chord)	Upper horn			Performance Data				
	α,°	V, mph	t_{tot}, °F	LWC, g/m^3	MVD, μm	time, min		h/c	x/c	θ, °	Re, 10^6	α,°	ΔC_d at α	$\Delta\alpha$ at $C_{l,max}$	$\Delta C_{l,max}$
run 1348	6.0	341	14.0	0.31	20	1.00	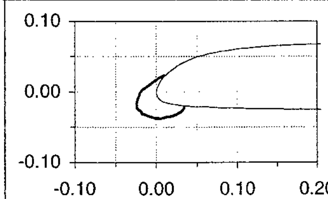	0.038	0.009	-39	1.8	6.0	0.0120		
run 1346	6.0	341	14.0	0.72	20	1.00	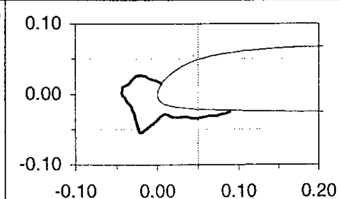	0.032	0.005	24	1.7	6.0	0.0342		
run 1379	6.0	415	14.0	1.12	20	0.75	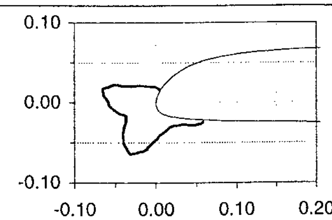	0.071	0.006	1	2.1	6.0	0.0567		
run 1419	6.0	328	14.0	1.06	20	1.00	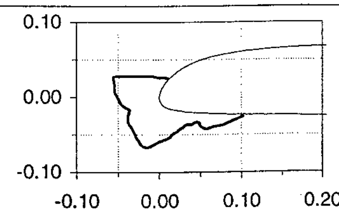	0.068	0.013	2	1.7	6.0	0.1123		

TABLE G-2.4(v). STUDIES USING ACCRETED OR SIMULATED ICE
(Ref. 56, Flemming and Lednicer, CR 3910, 1985, SC1094 Airfoil, c = 6 in
Ice Shapes From Figure 33, Performance Data From Appendices (Continued))

Ice shape identity	Icing Conditions						Ice shape (coordinates normalized with respect to chord)	Upper horn			Performance Data				
	α,°	V, mph	t_{tot}, °F	LWC, g/m^3	MVD, μm	time, min		h/c	x/c	θ, °	Re, 10^6	α,°	ΔC_d at α	$\Delta\alpha$ at $C_{l,max}$	$\Delta C_{l,max}$
run 1385	6.0	408	14.0	1.31	20	0.75	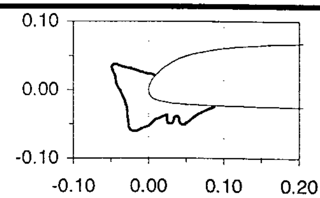	0.059	0.009	17	2.1	6.0	0.1046		
run 1401	0.0	402	14.0	0.58	20	0.75	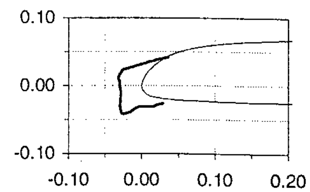	0.065	0.033	-18	2.1	0.0	0.0469		
run 1413	0.0	395	14.0	0.58	20	1.00	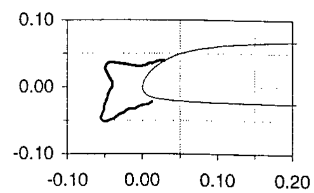	0.063	0.015	10	2.0	0.0	0.0859		
run 1425	0.0	441	14.0	0.64	20	0.75	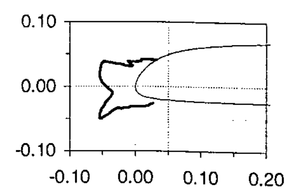	0.065	0.014	11	2.2	0.0	0.0925		

TABLE G-2.4(v). STUDIES USING ACCRETED OR SIMULATED ICE
(Ref. 56, Flemming and Lednicer, CR 3910, 1985, SC1094 Airfoil, c = 6 in
Ice Shapes From Figure 33, Performance Data From Appendices (Continued))

Ice shape identity	Icing Conditions						Ice shape (coordinates normalized with respect to chord)	Upper horn			Performance Data				
	α,°	V, mph	t_{tot}, °F	LWC, g/m^3	MVD, µm	time, min		h/c	x/c	θ, °	Re, 10^6	α,°	ΔC_d at α	$\Delta\alpha$ at $C_{l,max}$	$\Delta C_{l,max}$
run 1417	6.0	415	14.0	1.50	20	0.75	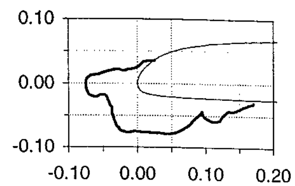	0.102	0.024	-15	2.1	6.0	0.0344		
run 1383	6.0	408	14.0	1.50	20	0.75	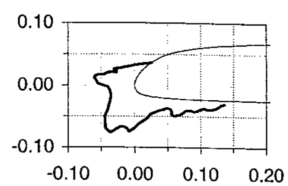	0.088	0.024	-14	2.1	6.0	0.0430		
run 1359	6.0	415	14.0	0.58	20	1.00	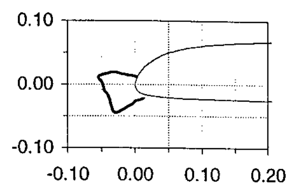	0.047	0.002	15	2.1	6.0	0.0163		
run 1357	6.0	408	14.0	0.58	20	0.75	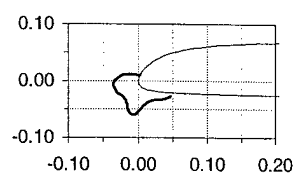	0.025	0.003	4	2.1	6.0	0.0072		

TABLE G-2.4(vi). STUDIES USING ACCRETED OR SIMULATED ICE
(Ref. 56, Flemming and Lednicer, CR 3910, 1985, SC1012 Airfoil, c = 6 in
Ice Shapes From Figure 34, Performance Data From Appendices)

Ice shape identity	Icing Conditions						Ice shape (coordinates normalized with respect to chord)	Upper horn			Performance Data				
	α,°	V, mph	t_{tot}, °F	LWC, g/m^3	MVD, µm	time, min		h/c	x/c	θ, °	Re, 10^6	α,°	ΔC_d at α	$\Delta\alpha$ at $C_{l,max}$	$\Delta C_{l,max}$
run 1039	3.0	216	14.0	0.66	20	1.00	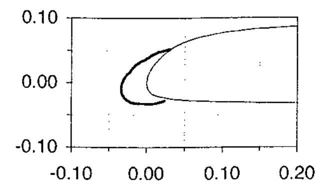	0.053	0.031	-28	1.1	3.0	0.0167		
run 1078	3.0	408	14.0	0.58	20	0.75	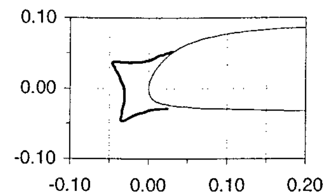	0.080	0.032	-10	2.1	3.0	0.0523		
run 1086	3.0	211	23.0	0.66	20	1.00	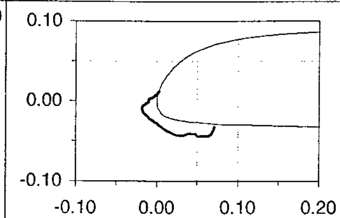	0.028	0.002	-42	1.1	3.0	0.0212		
run 1314	6.0	272	14.0	1.14	20	1.00	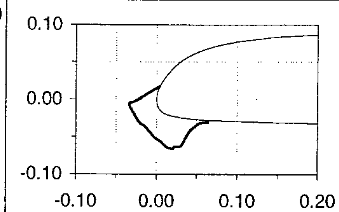	0.044	0.004	-31	1.4	6.0	0.0594		

TABLE G-2.4(vi). STUDIES USING ACCRETED OR SIMULATED ICE
(Ref. 56, Flemming and Lednicer, CR 3910, 1985, SC1012 Airfoil, c = 6 in
Ice Shapes From Figure 34, Performance Data From Appendices (Continued))

Ice shape identity	Icing Conditions						Ice shape (coordinates normalized with respect to chord)	Upper horn			Performance Data				
	α,°	V, mph	t_{tot}, °F	LWC, g/m^3	MVD, µm	time, min		h/c	x/c	θ, °	Re, 10^6	α,°	ΔC_d at α	$\Delta\alpha$ at $C_{l,max}$	$\Delta C_{l,max}$
run 2344	6.0	207	5.0	1.00	20	1.00	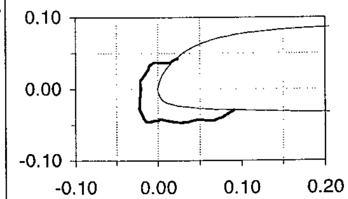	0.024	0.017	1	1.1	6.0	0.0328		
run 2346	6.0	204	23.0	1.00	20	1.00	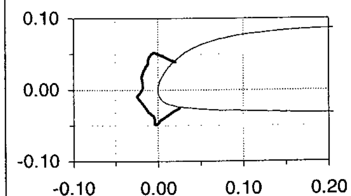	0.028	0.019	30	1.1	6.0	0.0463		
run 2348	6.0	213	32.0	1.00	20	1.00	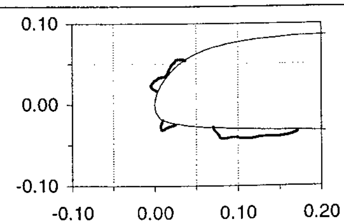	0.011	0.037	3	1.1	6.0	0.0326		
run 2342	6.0	209	14.0	1.40	20	1.00	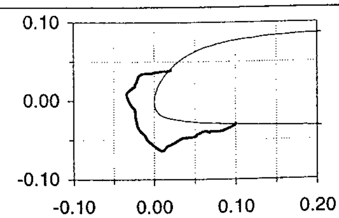	0.035	0.018	-6	1.1	6.0	0.0999		

TABLE G-2.4(vi). STUDIES USING ACCRETED OR SIMULATED ICE
(Ref. 56, Flemming and Lednicer, CR 3910, 1985, SC1012 Airfoil, c = 6 in
Ice Shapes From Figure 34, Performance Data From Appendices (Continued))

Ice shape identity	Icing Conditions						Ice shape (coordinates normalized with respect to chord)	Upper horn			Performance Data				
	α,°	V, mph	t_{tot}, °F	LWC, g/m^3	MVD, µm	time, min		h/c	x/c	θ, °	Re, 10^6	α,°	ΔC_d at α	$\Delta\alpha$ at $C_{l,max}$	$\Delta C_{l,max}$
run 2340	5.9	209	14.0	1.00	20	1.00	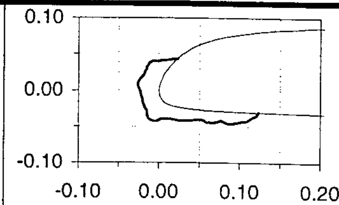	0.033	0.023	-7	1.1	5.9	0.0311		
run 1023	6.0	279	14.0	0.30	20	1.00	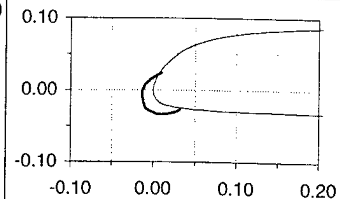	0.029	0.007	-46	1.5	6.0	0.0174		
run 1013	6.0	279	14.0	0.62	20	1.00	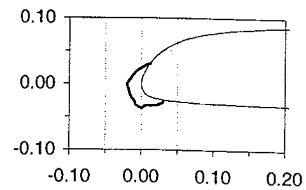	0.043	0.012	-42	1.5	6.0	0.0271		
run 1009	6.0	279	14.0	1.14	20	1.00	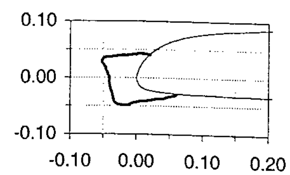	0.071	0.021	-5	1.5	6.0	0.0588		

TABLE G-2.4(vi). STUDIES USING ACCRETED OR SIMULATED ICE
(Ref. 56, Flemming and Lednicer, CR 3910, 1985, SC1012 Airfoil, c = 6 in
Ice Shapes From Figure 34, Performance Data From Appendices (Continued))

Ice shape identity	Icing Conditions						Ice shape (coordinates normalized with respect to chord)	Upper horn			Performance Data				
	α,°	V, mph	t_{tot}, °F	LWC, g/m^3	MVD, μm	time, min		h/c	x/c	θ, °	Re, 10^6	α,°	ΔC_d at α	$\Delta\alpha$ at $C_{l,max}$	$\Delta C_{l,max}$
run 1239	6.0	300	14.0	1.53	20	1.00	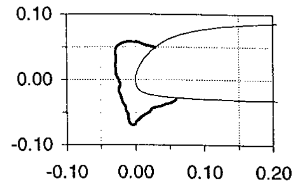	0.049	0.029	18	1.6	6.0	0.1185		
run 1220	6.0	272	14.0	1.75	20	1.00	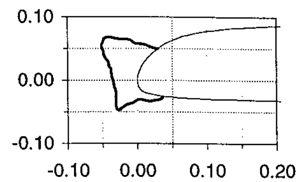	0.077	0.029	14	1.5	6.0	0.1241		
run 2330	5.9	272	14.0	0.30	20	5.00	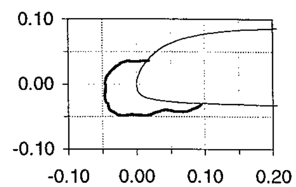	0.033	0.016	0	1.5	5.9	0.0176		
run 1045	6.0	362	15.6	0.72	20	0.75	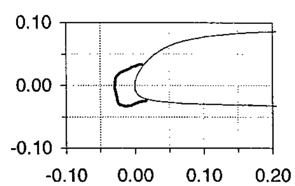	0.044	0.014	-25	1.8	6.0	0.0239		

TABLE G-2.4(vi). STUDIES USING ACCRETED OR SIMULATED ICE
(Ref. 56, Flemming and Lednicer, CR 3910, 1985, SC1012 Airfoil, c = 6 in
Ice Shapes From Figure 34, Performance Data From Appendices (Continued))

Ice shape identity	Icing Conditions						Ice shape (coordinates normalized with respect to chord)	Upper horn			Performance Data				
	α,°	V, mph	t_{tot}, °F	LWC, g/m^3	MVD, µm	time, min		h/c	x/c	θ, °	Re, 10^6	α,°	ΔC_d at α	$\Delta\alpha$ at $C_{l,max}$	$\Delta C_{l,max}$
run 1048	6.0	341	14.0	0.72	20	1.00	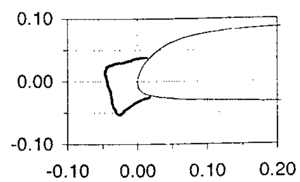	0.067	0.019	-16	1.8	6.0	0.0324		
run 2338	-0.2	408	14.0	0.66	20	0.75	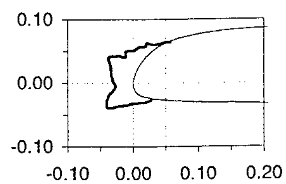	0.058	0.020	1	2.1	-0.2	0.0865		
run 1061	6.0	421	14.0	0.35	20	0.75	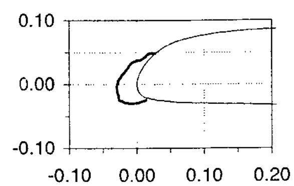	0.032	0.023	-16	2.1	6.0	0.0028		
run 1033	9.0	272	14.0	0.62	20	1.00	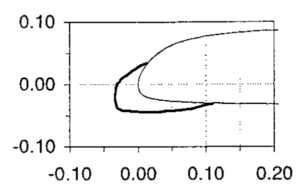	0.057	0.014	-36	1.5	9.0	0.0736		

TABLE G-2.4(vi). STUDIES USING ACCRETED OR SIMULATED ICE
(Ref. 56, Flemming and Lednicer, CR 3910, 1985, SC1012 Airfoil, c = 6 in
Ice Shapes From Figure 34, Performance Data From Appendices (Continued))

Ice shape identity	Icing Conditions						Ice shape (coordinates normalized with respect to chord)	Upper horn			Performance Data				
	α,°	V, mph	t_{tot}, °F	LWC, g/m^3	MVD, µm	time, min		h/c	x/c	θ, °	Re, 10^6	α,°	ΔC_d at α	$\Delta\alpha$ at $C_{l,max}$	$\Delta C_{l,max}$
run 1068	6.0	421	14.0	0.58	20	1.00	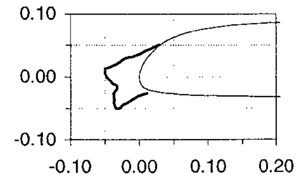	0.091	0.032	-26	2.1	6.0	0.0122		
run 1051	6.0	415	14.0	0.58	20	0.75	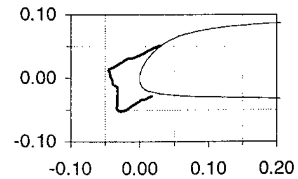	0.089	0.034	-27	2.1	6.0			
run 1070	6.0	421	14.0	1.12	20	0.75	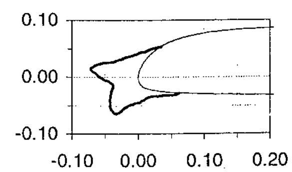	0.113	0.034	-20	2.1	6.0	0.0298		
run 2334	6.0	408	14.0	0.90	20	1.00	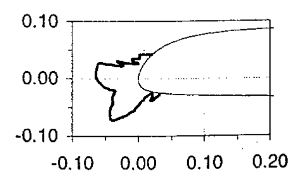	0.066	0.005	8	2.1	6.0	0.0321		

TABLE G-2.4(vi). STUDIES USING ACCRETED OR SIMULATED ICE
(Ref. 56, Flemming and Lednicer, CR 3910, 1985, SC1012 Airfoil, c = 6 in
Ice Shapes From Figure 34, Performance Data From Appendices (Continued)

Ice shape identity	Icing Conditions						Ice shape (coordinates normalized with respect to chord)	Upper horn			Performance Data				
	α,°	V, mph	t_{tot}, °F	LWC, g/m^3	MVD, µm	time, min		h/c	x/c	θ, °	Re, 10^6	α,°	ΔC_d at α	$\Delta\alpha$ at $C_{l,max}$	$\Delta C_{l,max}$
run 2332	6.0	408	14.0	0.90	20	0.75	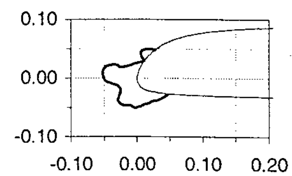	0.064	0.011	-14	2.1	6.0	0.0134		
run 2336	6.0	408	14.0	0.90	20	0.33	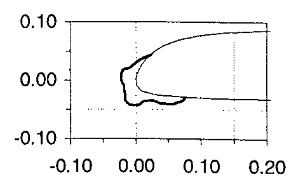	0.049	0.023	-31	2.1	6.0	0.0052		
run 1231	6.0	428	14.0	0.58	20	0.75	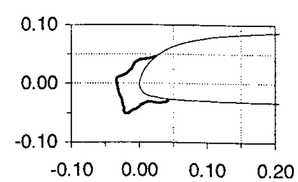	0.052	0.013	-26	2.1	6.0	0.0091		
run 1233	6.0	415	14.0	0.58	11	0.75	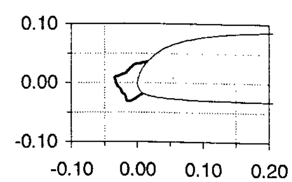	0.050	0.011	-25	2.1	6.0	0.0064		

TABLE G-2.4(vi). STUDIES USING ACCRETED OR SIMULATED ICE
(Ref. 56, Flemming and Lednicer, CR 3910, 1985, SC1012 Airfoil, c = 6 in
Ice Shapes From Figure 34, Performance Data From Appendices (Continued)

Ice shape identity	Icing Conditions						Ice shape (coordinates normalized with respect to chord)	Upper horn			Performance Data				
	α,°	V, mph	t_{tot}, °F	LWC, g/m^3	MVD, µm	time, min		h/c	x/c	θ, °	Re, 10^6	α,°	ΔC_d at α	$\Delta\alpha$ at $C_{l,max}$	$\Delta C_{l,max}$
run 1237	6.0	421	14.0	0.58	50	0.75	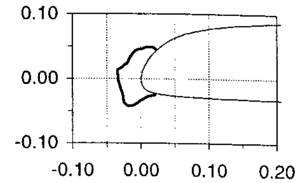	0.066	0.023	-28	2.1	6.0	0.0143		
run 1229	0.0	480	14.0	0.64	20	0.75	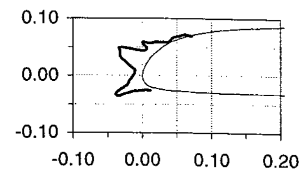	0.053	0.018	13	2.3	0.0	0.0347		

TABLE G-2.4(vii). STUDIES USING ACCRETED OR SIMULATED ICE (Ref. 56, Flemming and Lednicer, CR 3910, 1985, OH-58 Airfoil, c = 5.25 in Ice Shapes From Figure 35, Performance Data From Appendices)

Ice shape identity	Icing Conditions						Ice shape (coordinates normalized with respect to chord)	Upper horn			Performance Data				
	α,°	V, mph	t_{tot}, °F	LWC, g/m^3	MVD, µm	time, min		h/c	x/c	θ, °	Re, 10^6	α,°	ΔC_d at α	$\Delta\alpha$ at $C_{l,max}$	$\Delta C_{l,max}$
run 1165	0.0	408	14.0	0.58	20	0.63	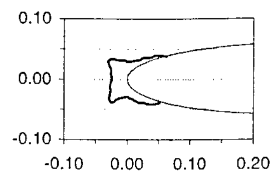	0.090	0.060	-3	1.8	0.0	0.0197		
run 1163	6.0	348	14.0	0.72	20	0.85	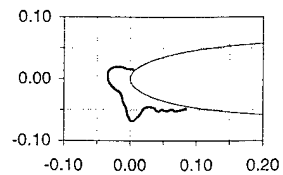	0.036	0.006	20	1.6	6.0	0.0301		
run 1149	6.0	279	14.0	0.62	20	0.85	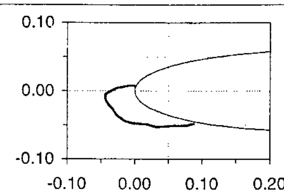	0.048	0.003	-17	1.3	6.0	0.0273		
run 2238	6.1	408	14.0	1.00	20	0.75	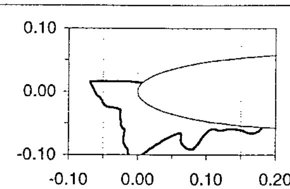	0.077	0.007	1	1.7	6.1	0.0865		

TABLE G-2.4(vii). STUDIES USING ACCRETED OR SIMULATED ICE
(Ref. 56, Flemming and Lednicer, CR 3910, 1985, OH-58 Airfoil, c = 5.25 in
Ice Shapes From Figure 35, Performance Data From Appendices (Continued))

Ice shape identity	Icing Conditions						Ice shape (coordinates normalized with respect to chord)	Upper horn			Performance Data				
	α,°	V, mph	t_{tot}, °F	LWC, g/m^3	MVD, µm	time, min		h/c	x/c	θ, °	Re, 10^6	α,°	ΔC_d at α	$\Delta\alpha$ at $C_{l,max}$	$\Delta C_{l,max}$
run 1874	6.1	395	14.0	0.35	20	0.75	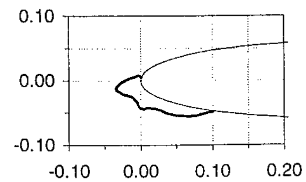	0.041	0.002	-27	1.7				
run 1879	5.5	415	14.0	0.59	20	0.75	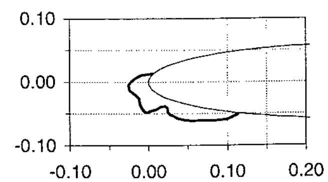	0.037	0.006	-29	1.8	5.5	0.0018		
run 1188	0.0	480	14.0	0.64	20	0.63	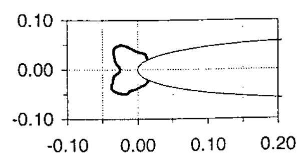	0.049	0.016	39	2.0	0.0	0.0183		

TABLE G-2.4(viii). STUDIES USING ACCRETED OR SIMULATED ICE
(Ref. 56, Flemming and Lednicer, CR 3910, 1985, S-58 Airfoil, c = 2.69 in
Ice Shapes From Figures 36, Performance Data From Appendices)

Ice shape identity	Icing Conditions						Ice shape (coordinates normalized with respect to chord)	Upper horn			Performance Data				
	α,°	V, mph	t_{tot}, °F	LWC, g/m^3	MVD, µm	time, min		h/c	x/c	θ, °	Re, 10^6	α,°	ΔC_d at α	$\Delta\alpha$ at $C_{l,max}$	$\Delta C_{l,max}$
run 2005	11.0	209	14.0	0.66	20	1.00	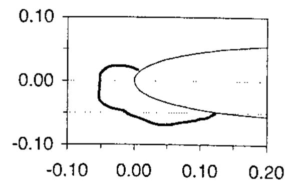	0.048	0.010	17	0.5	11.0	0.0239		
run 2003	9.0	209	14.0	0.66	20	1.00	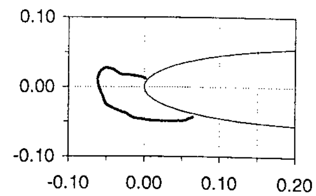	0.062	0.006	16	0.5	9.0	0.1452		
run 1998	6.0	202	14.0	0.66	20	1.00	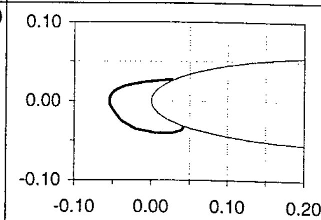	0.084	0.030	-10	0.5	6.0	0.0573		
run 2009	0.0	209	14.0	0.66	20	1.00	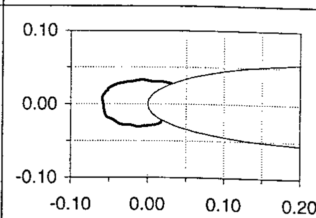	0.082	0.029	-3	0.5	0.0	0.0347		

TABLE G-2.4(viii). STUDIES USING ACCRETED OR SIMULATED ICE
(Ref. 56, Flemming and Lednicer, CR 3910, 1985, S-58 Airfoil, c = 2.69 in
Ice Shapes From Figures 36, Performance Data From Appendices (Continued))

Ice shape identity	Icing Conditions						Ice shape (coordinates normalized with respect to chord)	Upper horn			Performance Data				
	α,°	V, mph	t_{tot}, °F	LWC, g/m^3	MVD, µm	time, min		h/c	x/c	θ, °	Re, 10^6	α,°	ΔC_d at α	$\Delta\alpha$ at $C_{l,max}$	$\Delta C_{l,max}$
run 2000	6.0	209	14.0	1.00	20	1.00	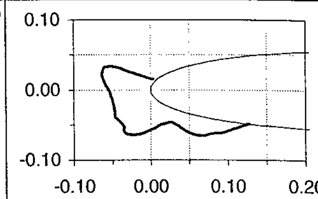	0.069	0.007	19	0.5	6.0	0.1286		
run 2007	6.0	209	14.0	0.40	20	1.00	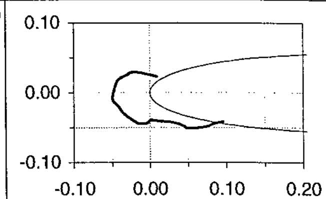	0.044	0.019	13	0.5	6.0	0.0559		
run 1988	6.0	341	14.0	0.66	20	1.00	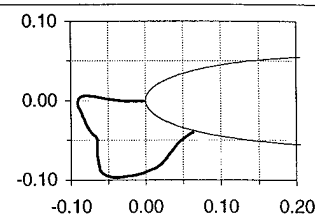	0.091	0.000	5	0.8	6.0	0.1519		
run 1990	6.0	341	14.0	0.66	20	0.75	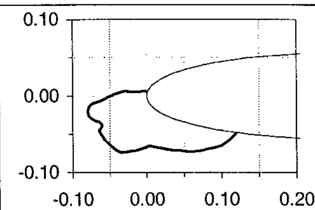	0.084	0.001	-13	0.8	6.0	0.0579		

TABLE G-2.4(viii). STUDIES USING ACCRETED OR SIMULATED ICE
(Ref. 56, Flemming and Lednicer, CR 3910, 1985, S-58 Airfoil, c = 2.69 in
Ice Shapes From Figures 36, Performance Data From Appendices (Continued))

Ice shape identity	Icing Conditions						Ice shape (coordinates normalized with respect to chord)	Upper horn			Performance Data				
	α,°	V, mph	t_{tot}, °F	LWC, g/m^3	MVD, µm	time, min		h/c	x/c	θ, °	Re, 10^6	α,°	ΔC_d at α	$\Delta\alpha$ at $C_{l,max}$	$\Delta C_{l,max}$
run 1992	6.1	408	14.0	0.38	20	0.75	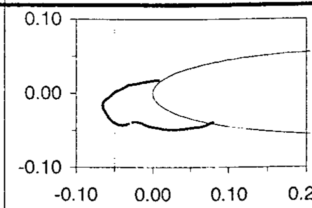	0.086	0.014	-21	0.9	6.1	0.0148		
run 1996	3.0	408	14.0	0.38	20	0.75	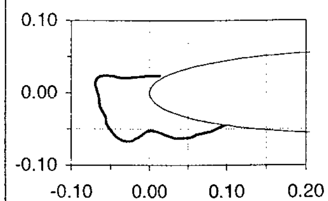	0.088	0.022	1	0.9	3.0	0.0536		
run 2011	0.0	408	14.0	0.38	20	0.75	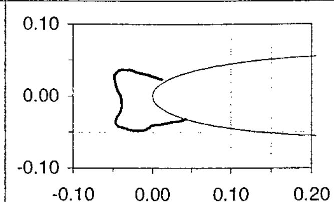	0.065	0.019	13	0.9	0.0	0.0725		
run 2240	6.0	408	14.0	0.66	20	0.75	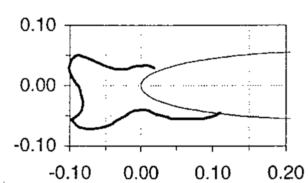	0.103	0.004	26	0.9	6.0	0.2212		

TABLE G-2.4(viii). STUDIES USING ACCRETED OR SIMULATED ICE
(Ref. 56, Flemming and Lednicer, CR 3910, 1985, S-58 Airfoil, c = 2.69 in
Ice Shapes From Figures 36, Performance Data From Appendices (Continued))

Ice shape identity	Icing Conditions						Ice shape (coordinates normalized with respect to chord)	Upper horn			Performance Data					
	α,°	V, mph	t_{tot}, °F	LWC, g/m^3	MVD, µm	time, min		h/c	x/c	θ, °	Re, 10^6	α,°	ΔC_d at α	$\Delta\alpha$ at $C_{l,max}$	$\Delta C_{l,max}$
run 2246	3.0	415	14.0	0.66	20	0.75	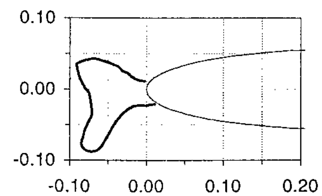	0.097	0.004	28	0.9	3.0	0.2493		
run 2244	6.0	402	14.0	1.00	20	0.50	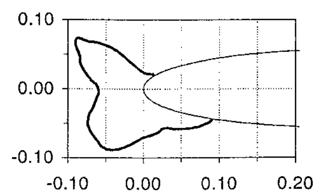	0.116	0.015	27	0.9	6.0	0.1860		
run 1994	6.1	402	14.0	0.62	20	0.75	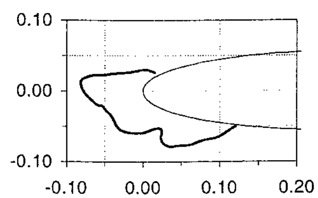	0.106	0.022	-5	0.9	6.1	0.0371		
run 2015	0.0	480	14.0	0.38	20	0.75	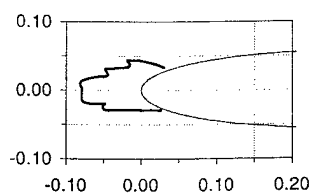	0.116	0.035	-6	1.0	0.0	0.0226		

TABLE G-2.4(viii). STUDIES USING ACCRETED OR SIMULATED ICE (Ref. 56, Flemming and Lednicer, CR 3910, 1985, S-58 Airfoil, c = 2.69 in Ice Shapes From Figures 36, Performance Data From Appendices (Continued))

Ice shape identity	Icing Conditions						Ice shape (coordinates normalized with respect to chord)	Upper horn			Performance Data				
	α,°	V, mph	t_{tot}, °F	LWC, g/m^3	MVD, µm	time, min		h/c	x/c	θ, °	Re, 10^6	α,°	ΔC_d at α	$\Delta\alpha$ at $C_{l,max}$	$\Delta C_{l,max}$
run 2013	0.0	464	21.0	0.38	20	0.75	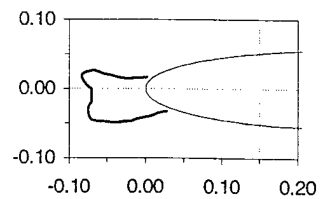	0.094	0.011	4	1.0	0.0	0.0716		

TABLE G-2.4(ix). STUDIES USING ACCRETED OR SIMULATED ICE
(Ref. 56, Flemming and Lednicer, CR 3910, 1985, CCA Airfoil, c = 6 in
Ice Shapes From Figure 37, Performance Data From Appendices)

Ice shape identity	Icing Conditions						Ice shape (coordinates normalized with respect to chord)	Upper horn			Performance Data				
	α,°	V, mph	t_{tot}, °F	LWC, g/m^3	MVD, µm	time, min		h/c	x/c	θ, °	Re, 10^6	α,°	ΔC_d at α	$\Delta\alpha$ at $C_{l,max}$	$\Delta C_{l,max}$
run 2302	6.0	209	14.0	0.66	20	1.00	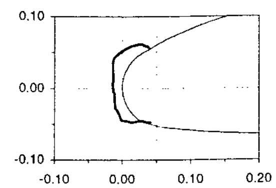	0.054	0.040	-13	1.1	6.0	-0.0005		
run 2299	0.0	209	14.0	0.66	20	1.00	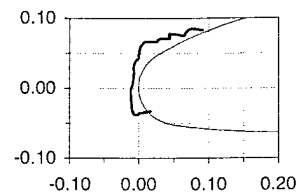	0.052	0.061	1	1.1	0.0	0.0187		
run 2296	0.0	209	14.0	0.66	20	1.00	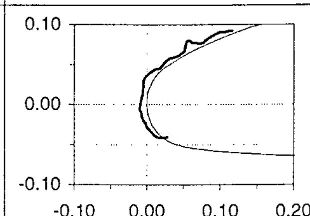	0.019	0.026	-10	1.1	0.0	-0.0068		
run 2289	0.0	408	14.0	0.66	20	0.75	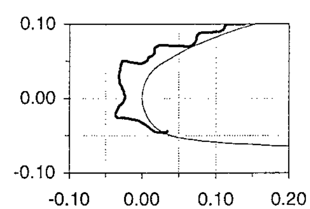	0.048	0.020	11	2.0	0.0	0.0048		

TABLE G-2.4(ix). STUDIES USING ACCRETED OR SIMULATED ICE
(Ref. 56, Flemming and Lednicer, CR 3910, 1985, CCA Airfoil, c = 6 in
Ice Shapes From Figure 37, Performance Data From Appendices (Continued))

Ice shape identity	Icing Conditions						Ice shape (coordinates normalized with respect to chord)	Upper horn			Performance Data				
	α,°	V, mph	t_{tot}, °F	LWC, g/m^3	MVD, µm	time, min		h/c	x/c	θ, °	Re, 10^6	α,°	ΔC_d at α	$\Delta\alpha$ at $C_{l,max}$	$\Delta C_{l,max}$
run 2286	0.0	341	14.0	0.66	20	1.00	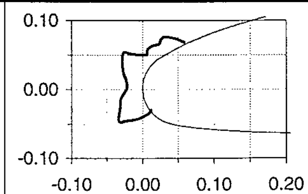	0.057	0.031	6	1.8	0.0	0.0192		
run 2283	0.0	209	14.0	0.66	20	1.00	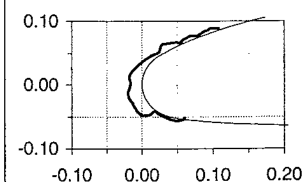	0.037	0.063	-4	1.1	0.0	0.0121		
run 2292	0.0	415	14.0	0.66	20	0.75	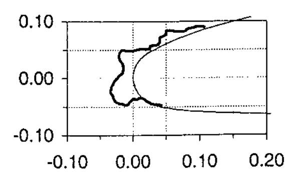	0.053	0.034	-2	2.0	0.0	-0.0038		
run 2294	0.0	348	14.0	0.66	20	1.00	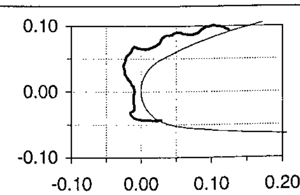	0.047	0.033	23	1.8	0.0	0.0164		

TABLE G-2.5(i). STUDIES USING ACCRETED OR SIMULATED ICE
(Ref. 60, Gray, TN 4151, 1958, NACA 65A004 Airfoil, c = 72 in
Ice Shapes and Performance Data From Table II, pp 18-19)

Ice shape identity	Icing Conditions						Ice shape (coordinates normalized with respect to chord)	Upper horn			Performance Data				
	α,°	V, mph	t_{tot}, °F	LWC, g/m^3	MVD, µm	time, min		h/c	x/c	θ, °	Re, 10^6	α,°	ΔC_d at α	$\Delta\alpha$ at $C_{l,max}$	$\Delta C_{l,max}$
p 19 row 1	0	175	10	1.86	19.0	3	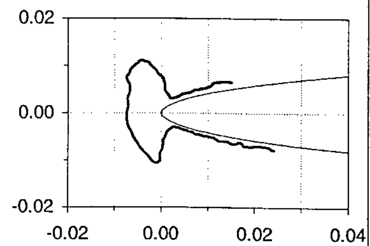	0.009	0.0020	53	11.2	0.0	0.009		
p 19 row 2	0	175	10	1.86	19.0	6	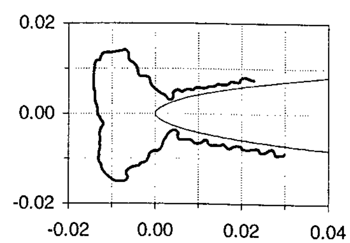	0.017	0.0029	48	11.2	0.0	0.020		
p 19 row 3	0	175	10	1.86	19.0	10	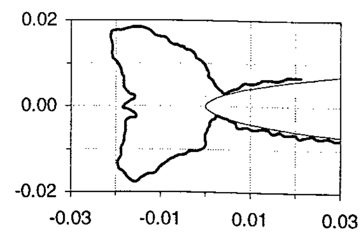	0.028	0.0032	51	11.2	0.0	0.031		

TABLE G-2.5(i). STUDIES USING ACCRETED OR SIMULATED ICE
(Ref. 60, Gray, TN 4151, 1958, NACA 65A004 Airfoil, c = 72 in
Ice Shapes and Performance Data From Table II, pp 18-19 (Continued))

Ice shape identity	Icing Conditions						Ice shape (coordinates normalized with respect to chord)	Upper horn			Performance Data				
	α,°	V, mph	t_{tot}, °F	LWC, g/m^3	MVD, µm	time, min		h/c	x/c	θ, °	Re, 10^6	α,°	ΔC_d at α	$\Delta\alpha$ at $C_{l,max}$	$\Delta C_{l,max}$
p 19 row 4	0	175	25	1.45	16.5	3	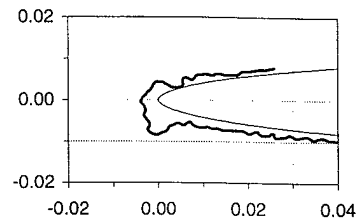	0.006	0.0036	36	10.6	0.0	-		
p 19 row 5	0	175	25	1.45	16.5	7	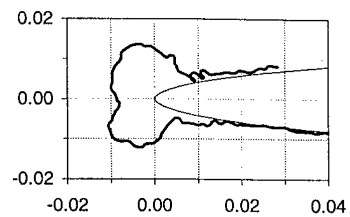	0.014	0.0093	42	10.6	0.0	-		
p 19 row 6	0	175	25	1.45	16.5	12	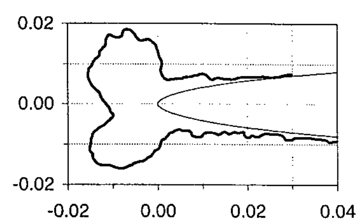	0.021	0.0039	58	10.6	0.0	-		

TABLE G-2.5(i). STUDIES USING ACCRETED OR SIMULATED ICE
(Ref. 60, Gray, TN 4151, 1958, NACA 65A004 Airfoil, c = 72 in
Ice Shapes and Performance Data From Table II, pp 18-19 (Continued))

Ice shape identity	Icing Conditions						Ice shape (coordinates normalized with respect to chord)	Upper horn			Performance Data				
	α,°	V, mph	t_{tot}, °F	LWC, g/m^3	MVD, µm	time, min		h/c	x/c	θ, °	Re, 10^6	α,°	ΔC_d at α	$\Delta\alpha$ at $C_{l,max}$	$\Delta C_{l,max}$
p 19 row 7	0	175	10	0.95	13.7	10	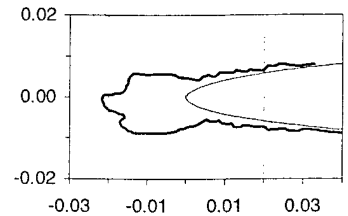	0.019	0.0150	5	11.2	0.0	0.007		
p 19 row 8	0	175	10	1.45	16.5	9	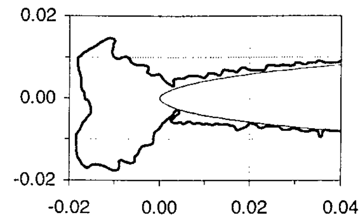	0.019	0.0039	40	11.2	0.0	0.020		
p 19 row 9	0	275	10	0.90	15.0	7	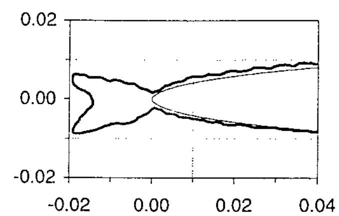	0.021	0.0012	21	16.6	0.0	0.010		

TABLE G-2.5(i). STUDIES USING ACCRETED OR SIMULATED ICE
(Ref. 60, Gray, TN 4151, 1958, NACA 65A004 Airfoil, c = 72 in
Ice Shapes and Performance Data From Table II, pp 18-19 (Continued))

Ice shape identity	Icing Conditions						Ice shape (coordinates normalized with respect to chord)	Upper horn			Performance Data				
	α,°	V, mph	t_{tot}, °F	LWC, g/m^3	MVD, µm	time, min		h/c	x/c	θ, °	Re, 10^6	α,°	ΔC_d at α	$\Delta\alpha$ at $C_{l,max}$	$\Delta C_{l,max}$
p 19 row 10	0	275	25	1.20	17.5	12	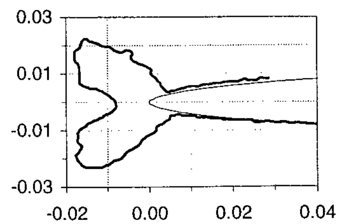	0.028	0.0050	50	15.7	0.0	0.038		
p 19 row 11	0	275	25	0.63	12.5	14.4	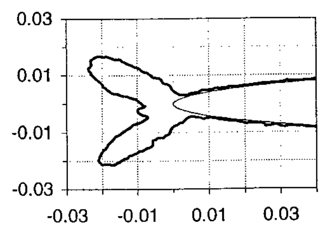	0.028	0.0023	38	15.7	0.0	0.031		
p 19 row 12	0	275	25	0.90	15.0	9	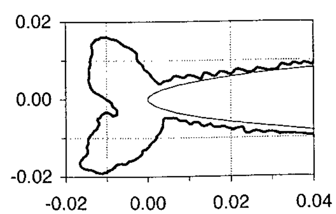	0.019	0.0032	50	15.7	0.0	0.026		

TABLE G-2.5(ii). STUDIES USING ACCRETED OR SIMULATED ICE
(Ref. 60, Gray, TN 4151, 1958, NACA 65A004 Airfoil, c = 72 in
Ice Shapes and Performance Data From Table II, pp 20-21)

Ice shape identity	Icing Conditions						Ice shape (coordinates normalized with respect to chord)	Upper horn			Performance Data				
	α,°	V, mph	t_{tot}, °F	LWC, g/m^3	MVD, µm	time, min		h/c	x/c	θ, °	Re, 10^6	α,°	ΔC_d at α	$\Delta\alpha$ at $C_{l,max}$	$\Delta C_{l,max}$
p 21 row 1	0	275	0	0.90	15	7	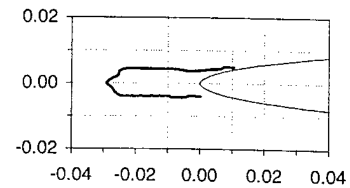	0.028	0.0078	2	17.2	0.0	-		
p 21 row 2	2	175	0	1.45	16.5	5	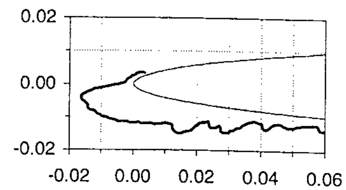	0.018	0.0004	-14	11.6	2.0	0.007		
p 21 row 3	2	175	0	1.45	16.5	10	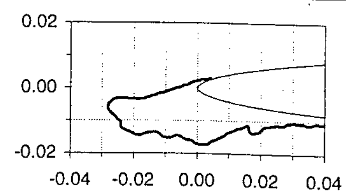	0.033	0.0048	-13	11.6	2.0	0.011		
p 21 row 4	2	175	0	0.95	13.7	12	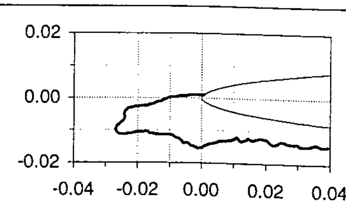	0.026	0.0064	-11	11.6	2.0	0.009		

TABLE G-2.5(ii). STUDIES USING ACCRETED OR SIMULATED ICE
(Ref. 60, Gray, TN 4151, 1958, NACA 65A004 Airfoil, c = 72 in
Ice Shapes and Performance Data From Table II, pp 20-21 (Continued))

Ice shape identity	Icing Conditions						Ice shape (coordinates normalized with respect to chord)	Upper horn			Performance Data				
	α, °	V, mph	t_{tot}, °F	LWC, g/m^3	MVD, μm	time, min		h/c	x/c	θ, °	Re, 10^6	α, °	ΔC_d at α	$\Delta\alpha$ at $C_{l,max}$	$\Delta C_{l,max}$
p 21 row 5	2	175	10	0.95	13.7	12.25	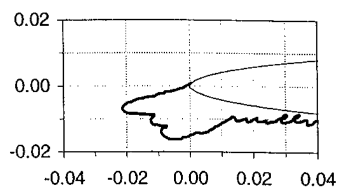	0.024	0.0003	-13	11.2	2.0	0.008		
p 21 row 6	2	175	10	1.86	19	5.75	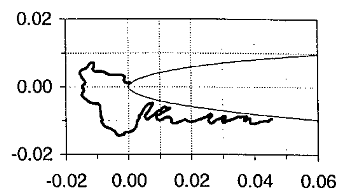	0.016	0.0002	18	11.2	2.0	0.018		
p 21 row 7	2	175	10	1.45	16.5	9.17	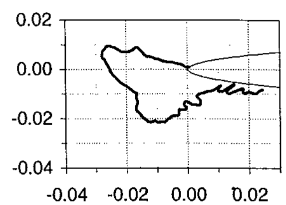	0.028	0.0004	20	11.2	2.0	0.023		
p 21 row 8	2	175	25	1.45	16.5	3	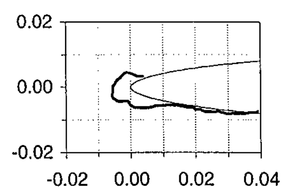	0.005	0.0038	21	10.6	2.0	0.009		

TABLE G-2.5(ii). STUDIES USING ACCRETED OR SIMULATED ICE
(Ref. 60, Gray, TN 4151, 1958, NACA 65A004 Airfoil, c = 72 in
Ice Shapes and Performance Data From Table II, pp 20-21 (Continued))

Ice shape identity	Icing Conditions						Ice shape (coordinates normalized with respect to chord)	Upper horn			Performance Data				
	α,°	V, mph	t_{tot}, °F	LWC, g/m^3	MVD, µm	time, min		h/c	x/c	θ, °	Re, 10^6	α,°	ΔC_d at α	$\Delta\alpha$ at $C_{l,max}$	$\Delta C_{l,max}$
p 21 row 9	2	175	25	1.45	16.5	7	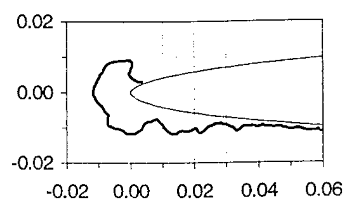	0.010	0.0038	63	10.6	2.0	0.016		
p 21 row 10	2	175	25	1.45	16.5	14	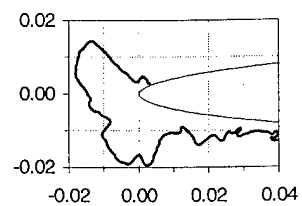	0.021	0.0010	43	10.6	2.0	0.030		
p 21 row 11	2	175	25	1.45	16.5	13	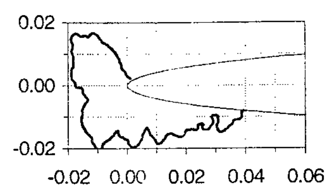	0.023	0.0011	52	10.6	2.0	0.027		

TABLE G-2.5(iii). STUDIES USING ACCRETED OR SIMULATED ICE
(Ref. 60, Gray, TN 4151, 1958, NACA 65A004 Airfoil, c = 72 in
Ice Shapes and Performance Data From Table II, pp 22-23)

Ice shape identity	Icing Conditions						Ice shape (coordinates normalized with respect to chord)	Upper horn			Performance Data				
	α,°	V, mph	t_{tot}, °F	LWC, g/m^3	MVD, μm	time, min		h/c	x/c	θ, °	Re, 10^6	α,°	ΔC_d at α	$\Delta\alpha$ at $C_{l,max}$	$\Delta C_{l,max}$
p 23 row 1	2	275	0	0.90	15	7	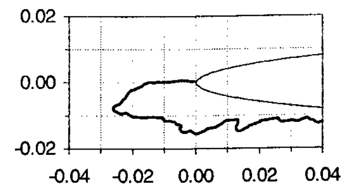	0.024	0.000	-5	17.2	2.0	0.006		
p 23 row 2	2	275	25	0.90	15	3	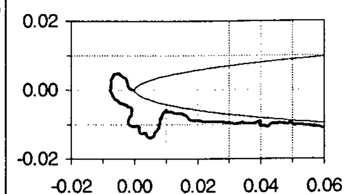	0.008	0.000	41	15.7	2.0	0.011		
p 23 row 3	2	275	25	0.90	15	8	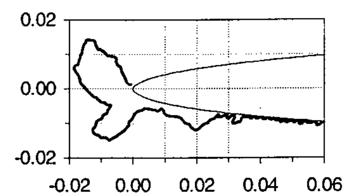	0.019	0.000	46	15.7	2.0	0.024		
p 23 row 4	2	275	25	0.90	15	12	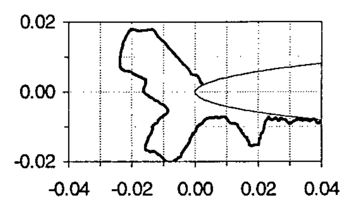	0.024	0.002	45	15.7	2.0	0.037		

TABLE G-2.5(iii). STUDIES USING ACCRETED OR SIMULATED ICE
(Ref. 60, Gray, TN 4151, 1958, NACA 65A004 Airfoil, c = 72 in
Ice Shapes and Performance Data From Table II, pp 22-23 (Continued))

Ice shape identity	Icing Conditions						Ice shape (coordinates normalized with respect to chord)	Upper horn			Performance Data				
	α,°	V, mph	t_{tot}, °F	LWC, g/m³	MVD, µm	time, min		h/c	x/c	θ, °	Re, 10^6	α,°	ΔC_d at α	$\Delta\alpha$ at $C_{l,max}$	$\Delta C_{l,max}$
p 23 row 5	2	275	25	0.90	15	9	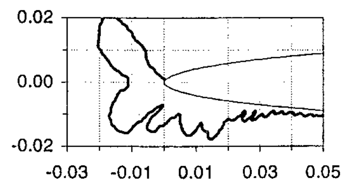	0.028	0.000	51	15.7	2.0	0.025		
p 23 row 6	2	275	0	0.90	15	-	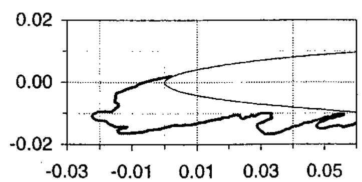	0.019	0.002	-18	17.2	2.0	0.006		
p 23 row 7	2	275	10	0.90	15	-	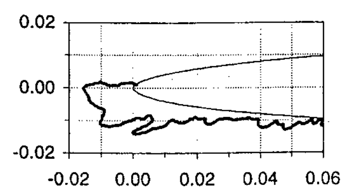	0.017	0.001	4	16.6	2.0	0.012		
p 23 row 8	4	175	10	0.95	13.7	13	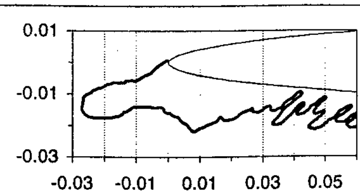	0.030	0.000	-22	11.2	4.0	-0.003		

TABLE G-2.5(iii). STUDIES USING ACCRETED OR SIMULATED ICE
(Ref. 60, Gray, TN 4151, 1958, NACA 65A004 Airfoil, c = 72 in
Ice Shapes and Performance Data From Table II, pp 22-23 (Continued))

Ice shape identity	Icing Conditions						Ice shape (coordinates normalized with respect to chord)	Upper horn			Performance Data					
	α,°	V, mph	t_{tot}, °F	LWC, g/m^3	MVD, μm	time, min		h/c	x/c	θ, °	Re, 10^6	α,°	ΔC_d at α	$\Delta\alpha$ at $C_{l,max}$	$\Delta C_{l,max}$
p 23 row 9	4	175	10	1.45	16.5	10	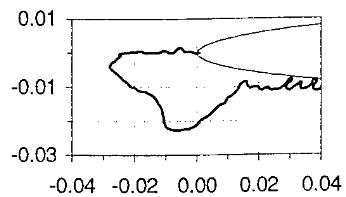	0.030	0.000	0	11.2	4.0	0.021		
p 23 row 10	4	175	10	1.86	19	8	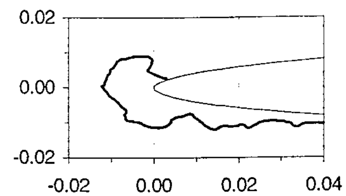	0.021	0.003	21	11.2	4.0	0.028		

TABLE G-2.5(iv). STUDIES USING ACCRETED OR SIMULATED ICE
(Ref. 60, Gray, TN 4151, 1958, NACA 65A004 Airfoil, c = 72 in
Ice Shapes and Performance Data From Table II, pp 24-25)

Ice shape identity	Icing Conditions						Ice shape (coordinates normalized with respect to chord)	Upper horn			Performance Data				
	α, °	V, mph	t_{tot}, °F	LWC, g/m^3	MVD, µm	time, min		h/c	x/c	θ, °	Re, 10^6	α, °	ΔC_d at α	$\Delta\alpha$ at $C_{l,max}$	$\Delta C_{l,max}$
p 25 row 1	4	175	25	0.95	13.7	10.33	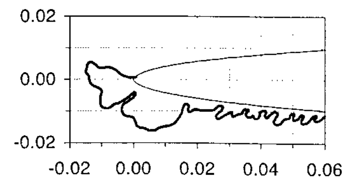	0.016	0.000	20	10.6	4.0	0.020		
p 25 row 2	4	175	25	1.45	16.5	3	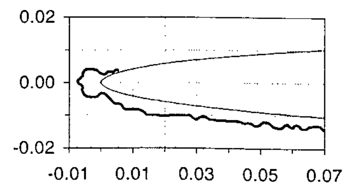	0.007	0.002	34.2	10.6	4.0	-		
p 25 row 3	4	175	25	1.45	16.5	12	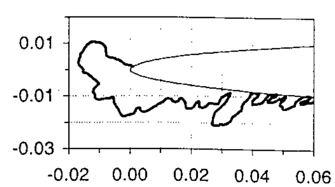	0.019	0.001	39.2	10.6	4.0	-		
p 25 row 4	4	275	0	0.45	11.3	17.67	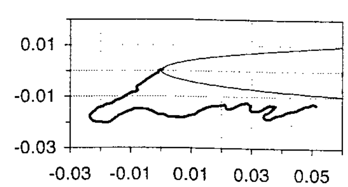	0.031	0.000	-35	17.2	4.0	-0.006		

TABLE G-2.5(iv). STUDIES USING ACCRETED OR SIMULATED ICE
(Ref. 60, Gray, TN 4151, 1958, NACA 65A004 Airfoil, c = 72 in
Ice Shapes and Performance Data From Table II, pp 24-25 (Continued))

Ice shape identity	Icing Conditions						Ice shape (coordinates normalized with respect to chord)	Upper horn			Performance Data				
	α,°	V, mph	t_{tot}, °F	LWC, g/m^3	MVD, µm	time, min		h/c	x/c	θ, °	Re, 10^6	α,°	ΔC_d at α	$\Delta\alpha$ at $C_{l,max}$	$\Delta C_{l,max}$
p 25 row 5	4	275	0	0.90	15	8.33	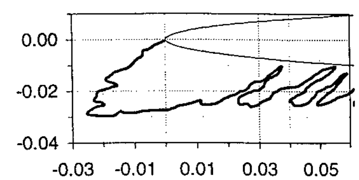	0.037	0.000	-34	17.2	4.0	-0.004		
p 25 row 6	4	275	10	0.63	12.5	13.67	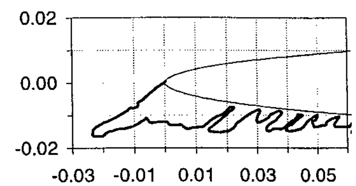	0.028	0.000	-34	16.6	4.0	-0.006		
p 25 row 7	4	275	10	0.90	15	10.75	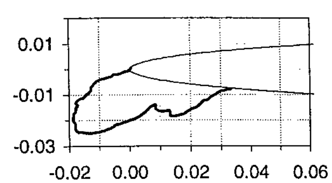	0.028	0.000	-28	16.6	4.0	0.008		
p 25 row 8	4	275	25	0.90	15	11.25	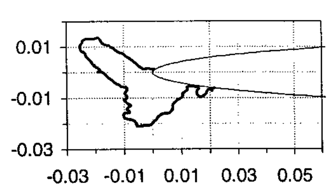	0.028	0.000	35	15.7	4.0	0.042		

TABLE G-2.5(iv). STUDIES USING ACCRETED OR SIMULATED ICE
(Ref. 60, Gray, TN 4151, 1958, NACA 65A004 Airfoil, c = 72 in
Ice Shapes and Performance Data From Table II, pp 24-25 (Continued))

Ice shape identity	Icing Conditions						Ice shape (coordinates normalized with respect to chord)	Upper horn			Performance Data				
	α,°	V, mph	t_{tot}, °F	LWC, g/m^3	MVD, µm	time, min		h/c	x/c	θ, °	Re, 10^6	α,°	ΔC_d at α	$\Delta\alpha$ at $C_{l,max}$	$\Delta C_{l,max}$
p 25 row 9	4	275	25	1.20	17.5	7	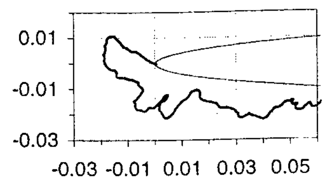	0.021	0.000	33	15.7	4.0	0.033		
p 25 row 10	4	275	10	1.20	17.5	7.5	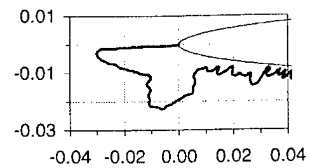	0.030	0.000	-1	16.6	4.0	0.018		
p 25 row 11	4	175	25	1.45	16.5	6	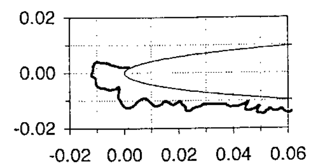	0.012	0.002	13	10.6	4.0	0.016		

TABLE G-2.5(v). STUDIES USING ACCRETED OR SIMULATED ICE
(Ref. 60, Gray, TN 4151, 1958, NACA 65A004 Airfoil, c = 72 in
Ice Shapes and Performance Data From Table II, pp 26-27)

Ice shape identity	Icing Conditions						Ice shape (coordinates normalized with respect to chord)	Upper horn			Performance Data					
	α,°	V, mph	t_{tot}, °F	LWC, g/m^3	MVD, µm	time, min		h/c	x/c	θ, °	Re, 10^6	α,°	ΔC_d at α	$\Delta\alpha$ at $C_{l,max}$	$\Delta C_{l,max}$
p 27 row 1	6	175	10	1.45	16.5	10	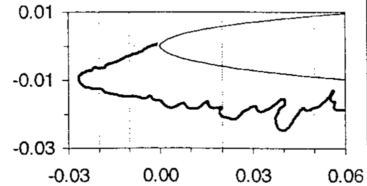	0.028	0	-19	11.2	6.0	-0.003		
p 27 row 2	6	175	10	1.86	19	10.5	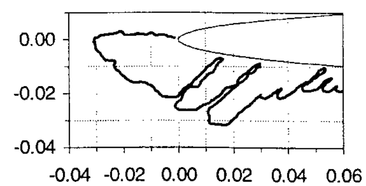	0.030	0	3	11.2	6.0	0.028		
p 27 row 3	6	175	10	0.95	13.7	13	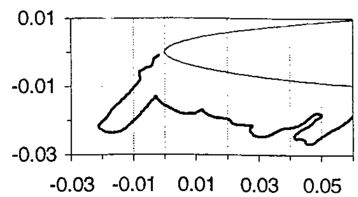	0.028	0	-46	11.2	6.0	-0.029		
p 27 row 4	6	175	25	1.45	16.5	10	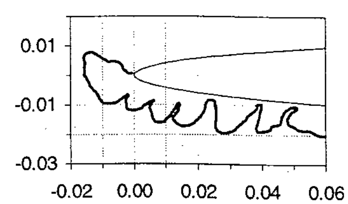	0.017	0	27	10.6	6.0	-		

TABLE G-2.5(v). STUDIES USING ACCRETED OR SIMULATED ICE
(Ref. 60, Gray, TN 4151, 1958, NACA 65A004 Airfoil, c = 72 in
Ice Shapes and Performance Data From Table II, pp 26-27 (Continued))

Ice shape identity	Icing Conditions						Ice shape (coordinates normalized with respect to chord)	Upper horn			Performance Data				
	α,°	V, mph	t_{tot}, °F	LWC, g/m^3	MVD, µm	time, min		h/c	x/c	θ, °	Re, 10^6	α,°	ΔC_d at α	$\Delta\alpha$ at $C_{l,max}$	$\Delta C_{l,max}$
p 27 row 5	8	175	10	1.86	19	8	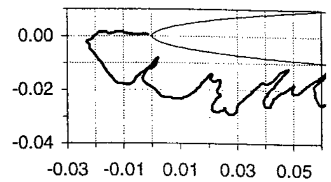	0.021	0	1	11.2	8.0	0.016		
p 27 row 6	8	175	10	0.95	13.7	12	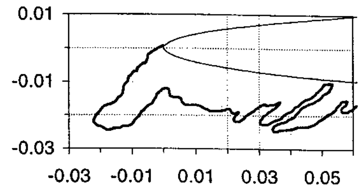	0.031	0	-47	11.2	8.0	-0.045		
p 27 row 7	8	175	10	1.45	16.5	11	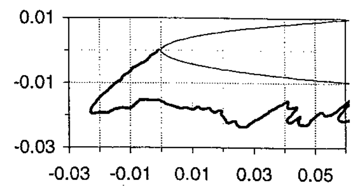	0.028	0	-40	11.2	8.0	-0.030		
p 27 row 8	8	175	0	1.45	16.5	7	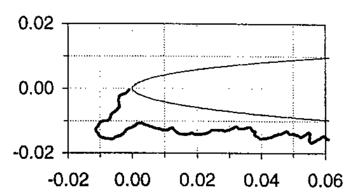	0.017	0	-52	11.6	8.0	-		

TABLE G-2.5(v). STUDIES USING ACCRETED OR SIMULATED ICE
(Ref. 60, Gray, TN 4151, 1958, NACA 65A004 Airfoil, c = 72 in
Ice Shapes and Performance Data From Table II, pp 26-27 (Continued))

Ice shape identity	Icing Conditions						Ice shape (coordinates normalized with respect to chord)	Upper horn			Performance Data				
	α,°	V, mph	t_{tot}, °F	LWC, g/m^3	MVD, µm	time, min		h/c	x/c	θ, °	Re, 10^6	α,°	ΔC_d at α	$\Delta\alpha$ at $C_{l,max}$	$\Delta C_{l,max}$
p 27 row 9	8	175	0	1.45	16.5	-	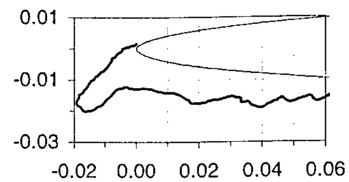	0.024	0.0016	-52	11.6	8.0	-0.043		
p 27 row 10	8	175	25	1.45	16.5	-	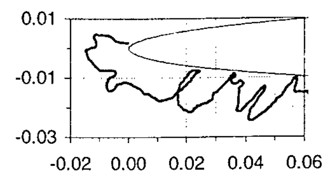	0.012	0	15	10.6	8.0	0.021		

TABLE G-2.5(vi). STUDIES USING ACCRETED OR SIMULATED ICE
(Ref. 60, Gray, TN 4151, 1958, NACA 65A004 Airfoil, c = 72 in
Ice Shapes and Performance Data From Table II, pp 28-29)

Ice shape identity	Icing Conditions						Ice shape (coordinates normalized with respect to chord)	Upper horn			Performance Data				
	α,°	V, mph	t_{tot}, °F	LWC, g/m^3	MVD, μm	time, min		h/c	x/c	θ, °	Re, 10^6	α,°	ΔC_d at α	$\Delta\alpha$ at $C_{l,max}$	$\Delta C_{l,max}$
p 29 row 1	10	125	10	2.00	18	10	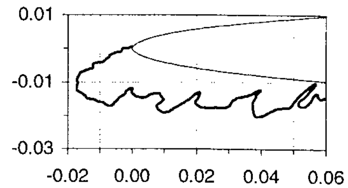	0.020	0.000	-30	8.12	10.0	-0.002		
p 29 row 2	11	125	10	2.00	18	11.5	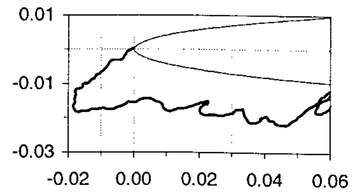	0.024	0.000	-34	8.12	11.0	-0.011		
p 29 row 3	11	125	10	1.40	15	10	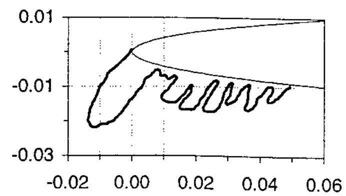	0.023	0.000	-49	8.12	11.0	-0.028		
p 29 row 4	2	175	10	0.95	13.7	12.25	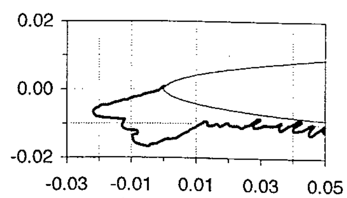	0.024	0.000	-13	11.15	4.0	0.001		
												6.0	-0.005		
												8.0	-0.016		
												10.0	-0.008		
												11.0	0.006		

TABLE G-2.5(vi). STUDIES USING ACCRETED OR SIMULATED ICE
(Ref. 60, Gray, TN 4151, 1958, NACA 65A004 Airfoil, c = 72 in
Ice Shapes and Performance Data From Table II, pp 28-29 (Continued))

Ice shape identity	Icing Conditions						Ice shape (coordinates normalized with respect to chord)	Upper horn			Performance Data				
	α,°	V, mph	t_{tot}, °F	LWC, g/m^3	MVD, µm	time, min		h/c	x/c	θ, °	Re, 10^6	α,°	ΔC_d at α	$\Delta\alpha$ at $C_{l,max}$	$\Delta C_{l,max}$
p 29 row 5	2	175	10	1.86	19	5.75	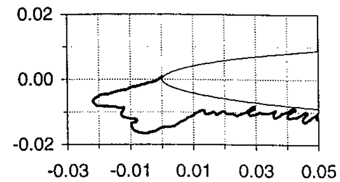	0.016	0.000	18	11.15	4.0	0.021		
												6.0	0.025		
												8.0	0.027		
												10.0	0.021		
												11.0	0.016		
p 29 row 6	4	175	25	0.95	13.7	10.33	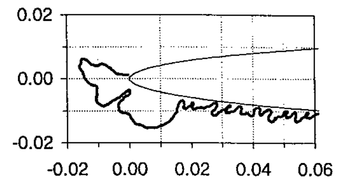	0.016	0.000	20	10.56	6.0	0.019		
												8.0	0.017		
												10.0	0.016		
												0.0	0.010		
												2.0	0.014		
p 29 row 7	4	175	10	1.86	19	8	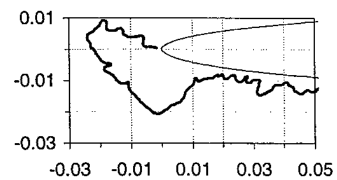	0.021	0.000	21	11.15	6.0	0.032		
												8.0	0.033		
												10.0	0.029		
												2.0	0.024		

TABLE G-2.6. STUDIES USING ACCRETED OR SIMULATED ICE
(Ref. 122, Olsen, Shaw, and Newton, NASA TM 835556, 1984, NACA 0012 Airfoil, c = 21 in
Performance Data From Figure 31)

Ice shape identity	Icing Conditions						Ice shape (coordinates normalized with respect to chord)	Upper horn			Performance Data				
	α,°	V, mph	t_{tot}, °F	LWC, g/m^3	MVD, µm	time, min		h/c	x/c	θ, °	Re, 10^6	α,°	ΔC_d at α	$\Delta\alpha$ at $C_{l,max}$	$\Delta C_{l,max}$
Fig. 6(a)	4	130	-15	1.00	12	5	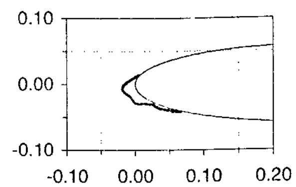	0.030	0.0064	-35	2.73	4.0	0.004		
												8.0	0.006		
												11.0	0.018		
												-3.0	0.006		
												0.0	0.006		
Fig. 6(b)	4	130	18	2.10	20	5	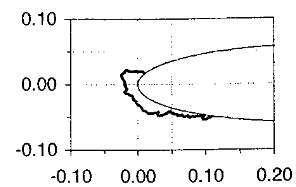	0.029	0.010	8	2.41	4.0	0.021		
												8.0	0.067		
												2.0	0.018		
												0.0	0.016		
												-3.0	0.020		
												5.5	0.028		
Fig. 7(a) AOA = 0	0	130	-15	1.00	12	5	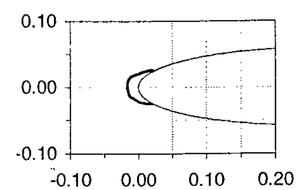	0.034	0.022	-16	2.73	0.0	0.002		
												0.0	0.003		
Fig. 7(a) AOA = 4	4	130	-15	1.00	12	5	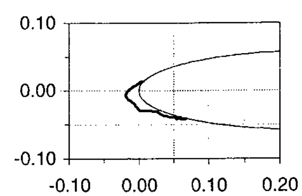	0.030	0.0064	-35	2.73	4.0	0.004		

TABLE G-2.6. STUDIES USING ACCRETED OR SIMULATED ICE
(Ref. 122, Olsen, Shaw, and Newton, NASA TM 83556, 1984, NACA 0012 Airfoil, c = 21 in
Performance Data From Figure 31 (Continued))

Ice shape identity	Icing Conditions						Ice shape (coordinates normalized with respect to chord)	Upper horn			Performance Data				
	α,°	V, mph	t_{tot}, °F	LWC, g/m^3	MVD, µm	time, min		h/c	x/c	θ, °	Re, 10^6	α,°	ΔC_d at α	$\Delta\alpha$ at $C_{l,max}$	$\Delta C_{l,max}$
Fig. 7(a) AOA = 8	8	130	-15	1.00	12	5	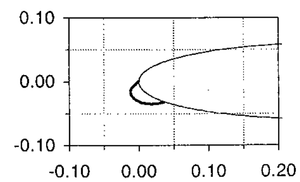	0.015	-0.0001	-45	2.73	8.0	0.007		
Fig. 7(b) AOA = 0	0	130	18	2.10	20	5	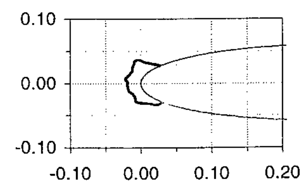	0.033	0.027	15	2.41	0.0	0.017		
Fig. 7(b) AOA = 4	4	130	18	2.10	20	5	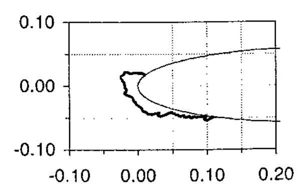	0.029	0.0102	8	2.41	4.0	0.027		
Fig. 7(b) AOA = 8	8	130	18	2.10	20	5	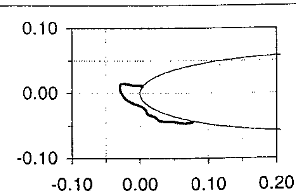	0.029	0.0038	8	2.41	8.0	0.043		

TABLE G-2.6. STUDIES USING ACCRETED OR SIMULATED ICE
(Ref. 122, Olsen, Shaw, and Newton, NASA TM 83556, 1984, NACA 0012 Airfoil, c = 21 in
Performance Data From Figure 31 (Continued))

Ice shape identity	Icing Conditions						Ice shape (coordinates normalized with respect to chord)	Upper horn			Performance Data				
	α,°	V, mph	t_{tot}, °F	LWC, g/m^3	MVD, µm	time, min		h/c	x/c	θ, °	Re, 10^6	α,°	ΔC_d at α	$\Delta\alpha$ at $C_{l,max}$	$\Delta C_{l,max}$
Fig 10 209 kph -26°C	4	130	-15	1.30	20	8	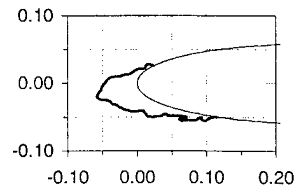	0.066	-0.0401	16	2.73	4.0	0.012		
Fig 10 209 kph -20°C	4	130	-4	1.30	20	8	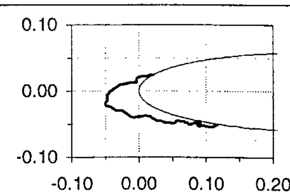	0.033	-0.0282	6	2.62	4.0	0.011		
Fig 10 209 kph -18°C	4	130	0	1.30	20	8	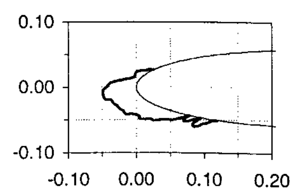	0.050	-0.0365	14	2.58	4.0	0.015		
												4.0	0.014		
Fig 10 209 kph -15°C	4	130	5	1.30	20	8	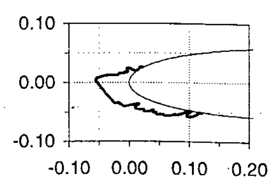	0.069	-0.0540	11	2.53	4.0	0.014		

TABLE G-2.6. STUDIES USING ACCRETED OR SIMULATED ICE
(Ref. 122, Olsen, Shaw, and Newton, NASA TM 83556, 1984, NACA 0012 Airfoil, c = 21 in
Performance Data From Figure 31 (Continued))

Ice shape identity	Icing Conditions						Ice shape (coordinates normalized with respect to chord)	Upper horn			Performance Data				
	α,°	V, mph	t_{tot}, °F	LWC, g/m^3	MVD, µm	time, min		h/c	x/c	θ, °	Re, 10^6	α,°	ΔC_d at α	$\Delta\alpha$ at $C_{l,max}$	$\Delta C_{l,max}$
Fig 10 209 kph -12°C	4	130	10	1.30	20	8	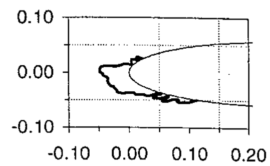	0.053	0.0069	6	2.49	4.0	0.014		
Fig 10 209 kph -8°C	4	130	18	1.30	20	8	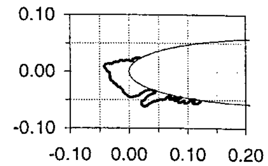	0.048	-0.0380	7	2.41	4.0	0.022		
												4.0	0.014		
Fig 10 209 kph -5°C	4	130	23	1.30	20	8	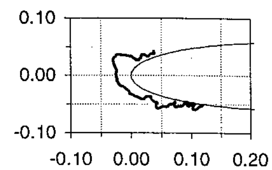	0.044	-0.0229	-17	2.37	4.0	0.053		
Fig 10 209 kph -2°C	4	130	28	1.30	20	8	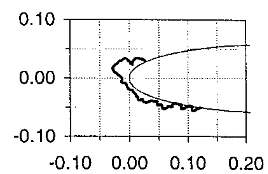	0.019	0.0099	-17	2.33	4.0	0.021		

TABLE G-2.6. STUDIES USING ACCRETED OR SIMULATED ICE
(Ref. 122, Olsen, Shaw, and Newton, NASA TM 83556, 1984, NACA 0012 Airfoil, c = 21 in
Performance Data From Figure 31 (Continued))

Ice shape identity	Icing Conditions						Ice shape (coordinates normalized with respect to chord)	Upper horn			Performance Data					
	α,°	V, mph	t_{tot}, °F	LWC, g/m^3	MVD, μm	time, min		h/c	x/c	θ, °	Re, 10^6	α,°	ΔC_d at α	$\Delta\alpha$ at $C_{l,max}$	$\Delta C_{l,max}$
Fig 10 209 kph -1°C	4	130	30	1.30	20	8	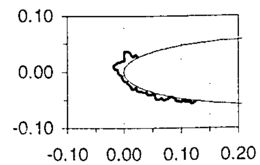	0.024	0.0015	-22	2.31	4.0	0.019		
Fig 10 338 kph -26°C	4	210	-15	1.05	20	6.2	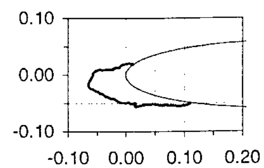	0.067	-0.0535	-11	4.34	4.0	0.017		
Fig 10 338 kph -17°C	4	210	1	1.05	20	6.2	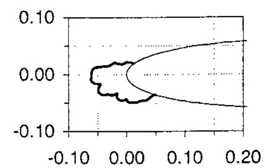	0.067	-0.0540	-6	4.08	4.0	0.021		
Fig 10 338 kph -12°C	4	210	11	1.05	20	6.2	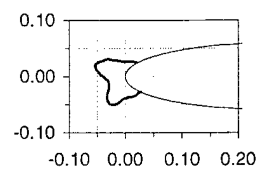	0.054	-0.0328	6	3.93	4.0	0.030		

TABLE G-2.6. STUDIES USING ACCRETED OR SIMULATED ICE
(Ref. 122, Olsen, Shaw, and Newton, NASA TM 83556, 1984, NACA 0012 Airfoil, c = 21 in
Performance Data From Figure 31 (Continued))

Ice shape identity	Icing Conditions						Ice shape (coordinates normalized with respect to chord)	Upper horn			Performance Data				
	α,°	V, mph	t_{tot}, °F	LWC, g/m^3	MVD, µm	time, min		h/c	x/c	θ, °	Re, 10^6	α,°	ΔC_d at α	$\Delta\alpha$ at $C_{l,max}$	$\Delta C_{l,max}$
Fig 10 338 kph -8°C	4	210	18	1.05	20	6.2	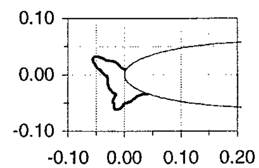	0.058	-0.0504	22	3.83	4.0	0.054		
Fig 10 338 kph -2°C	4	210	28	1.05	20	6.2	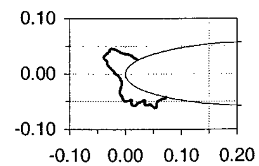	0.051	-0.0252	23	3.70	4.0	0.069		
Fig 13 145 kph	4	90	18	1.30	20	8	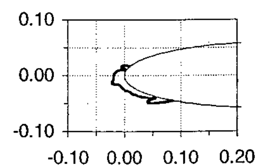	0.0088	0.0039	-8	1.68	4.0	0.009		
Fig 13 209 kph	4	130	18	1.30	20	8	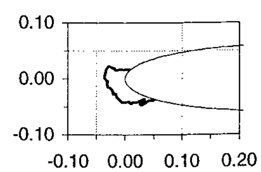	0.038	0.0091	8	2.41	4.0	0.023		

TABLE G-2.6. STUDIES USING ACCRETED OR SIMULATED ICE
(Ref. 122, Olsen, Shaw, and Newton, NASA TM 83556, 1984, NACA 0012 Airfoil, c = 21 in
Performance Data From Figure 31 (Continued))

Ice shape identity	Icing Conditions						Ice shape (coordinates normalized with respect to chord)	Upper horn			Performance Data				
	α,°	V, mph	t_{tot}, °F	LWC, g/m^3	MVD, µm	time, min		h/c	x/c	θ, °	Re, 10^6	α,°	ΔC_d at α	$\Delta\alpha$ at $C_{l,max}$	$\Delta C_{l,max}$
Fig 13 338 kph	4	210	18	1.30	20	8	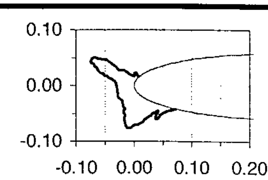	0.085	0.0079	24	3.83	4.0	0.111		
Fig 14 A 14 µm	4	130	18	1.30	14	8	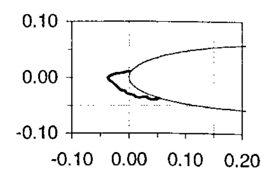	0.038	0.0028	-12	2.41	4.0	0.008		
Fig 14 A 20 µm	4	130	18	1.30	20	8	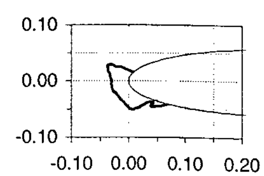	0.044	0.0079	18	2.41	4.0	0.032		
Fig 14 A 26 µm	4	130	18	1.30	26	8	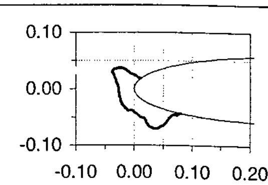	0.037	0.0115	30	2.41	4.0	0.068		

TABLE G-2.6. STUDIES USING ACCRETED OR SIMULATED ICE
(Ref. 122, Olsen, Shaw, and Newton, NASA TM 83556, 1984, NACA 0012 Airfoil, c = 21 in
Performance Data From Figure 31 (Continued))

Ice shape identity	Icing Conditions						Ice shape (coordinates normalized with respect to chord)	Upper horn			Performance Data				
	α,°	V, mph	t_{tot}, °F	LWC, g/m^3	MVD, µm	time, min		h/c	x/c	θ, °	Re, 10^6	α,°	ΔC_d at α	$\Delta\alpha$ at $C_{l,max}$	$\Delta C_{l,max}$
Fig 14 A 36 µm	4	130	18	1.30	36	8	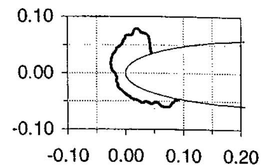	0.034	0.0452	76	2.41	4.0	0.098		
Fig 14 B 14 µm	4	130	28	1.30	14	8	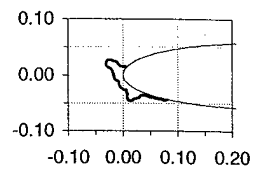	0.055	0.0039	-7	2.33	4.0	0.02447		
Fig 14 B 20 µm	4	130	28	1.30	20	8	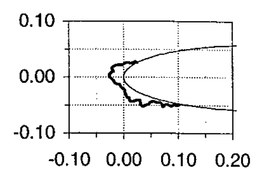	0.048	0.0061	28	2.33	4.0	0.02205		
Fig 14 B 26 µm	4	130	28	1.30	26	8	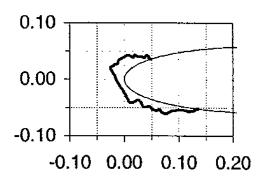	0.053	0.0129	35	2.33	4.0	0.0274		

TABLE G-2.6. STUDIES USING ACCRETED OR SIMULATED ICE
(Ref. 122, Olsen, Shaw, and Newton, NASA TM 83556, 1984, NACA 0012 Airfoil, c = 21 in
Performance Data From Figure 31 (Continued))

Ice shape identity	Icing Conditions						Ice shape (coordinates normalized with respect to chord)	Upper horn			Performance Data				
	α, °	V, mph	t_{tot}, °F	LWC, g/m^3	MVD, μm	time, min		h/c	x/c	θ, °	Re, 10^6	α, °	ΔC_d at α	$\Delta\alpha$ at $C_{l,max}$	$\Delta C_{l,max}$
Fig 14 C 14 μm	4	130	-15	1.30	14	8	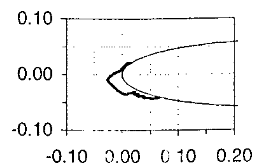	0.051	0.0154	-35	2.73	4.0	0.005		
Fig 14 C 20 μm	4	130	-15	1.30	20	8	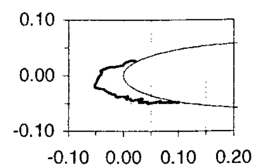	0.065	0.0223	-15	2.73	4.0	0.012		
Fig 14 C 26 μm	4	130	-15	1.30	26	8	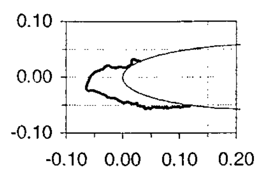	0.082	0.0306	-14	2.73	4.0	0.013		
Fig 14 D 14 μm	4	130	18	1.30	14	3	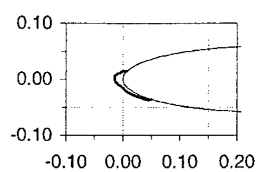	0.024	0.0074	-23	2.41	4.0	0.005		

TABLE G-2.6. STUDIES USING ACCRETED OR SIMULATED ICE
(Ref. 122, Olsen, Shaw, and Newton, NASA TM 83556, 1984, NACA 0012 Airfoil, c = 21 in
Performance Data From Figure 31 (Continued))

Ice shape identity	Icing Conditions						Ice shape (coordinates normalized with respect to chord)	Upper horn			Performance Data				
	α,°	V, mph	t_{tot}, °F	LWC, g/m^3	MVD, μm	time, min		h/c	x/c	θ, °	Re, 10^6	α,°	ΔC_d at α	$\Delta\alpha$ at $C_{l,max}$	$\Delta C_{l,max}$
Fig 14 D 20 μm	4	130	18	1.30	20	3	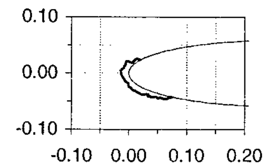	0.023	0.0191	-7	2.41	4.0	0.012		
Fig 14 D 26 μm	4	130	18	1.30	26	3	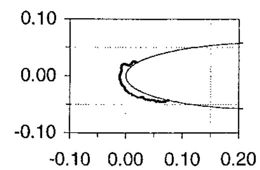	0.026	0.0204	-1	2.41	4.0	0.021		
Fig 14 E 14 μm	4	210	18	1.05	14	6.2	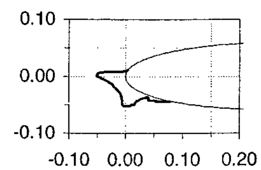	0.0552	0.0039	-7	3.83	4.0	0.0239		
Fig 14 E 20 μm	4	210	18	1.05	20	6.2	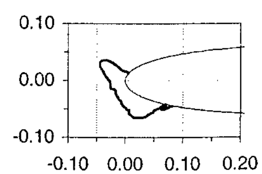	0.0484	0.0061	28	3.83	4.0	0.0881		

TABLE G-2.6. STUDIES USING ACCRETED OR SIMULATED ICE
(Ref. 122, Olsen, Shaw, and Newton, NASA TM 83556, 1984, NACA 0012 Airfoil, c = 21 in
Performance Data From Figure 31 (Continued))

Ice shape identity	Icing Conditions						Ice shape (coordinates normalized with respect to chord)	Upper horn			Performance Data				
	α,°	V, mph	t_{tot}, °F	LWC, g/m^3	MVD, µm	time, min		h/c	x/c	θ, °	Re, 10^6	α,°	ΔC_d at α	$\Delta\alpha$ at $C_{l,max}$	$\Delta C_{l,max}$
Fig 14 E 26 µm	4	210	18	1.05	26	6.2	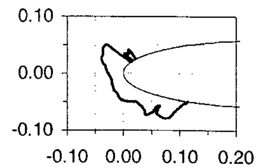	0.0527	0.0129	35	3.83	4.0	0.1196		
Fig 14 F 14 µm	4	130	0	1.3	14	8	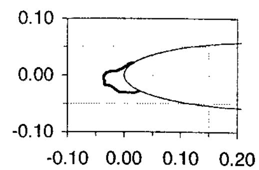	0.053	0.0160	-21	2.58	4.0	0.00765		
Fig 14 F 20 µm	4	130	0	1.3	20	8	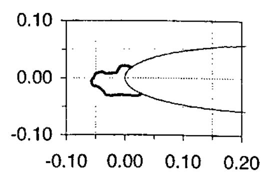	0.060	0.0116	-10	2.58	4.0	0.0123		
Fig 14 F 26 µm	4	130	0	1.3	26	8	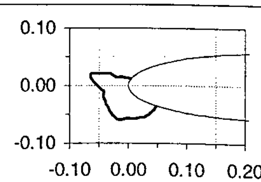	0.067	0.0041	8	2.58	4.0	0.0274		

TABLE G-2.6. STUDIES USING ACCRETED OR SIMULATED ICE
(Ref. 122, Olsen, Shaw, and Newton, NASA TM 83556, 1984, NACA 0012 Airfoil, c = 21 in
Performance Data From Figure 31 (Continued))

Ice shape identity	Icing Conditions						Ice shape (coordinates normalized with respect to chord)	Upper horn			Performance Data				
	α,°	V, mph	t_{tot}, °F	LWC, g/m³	MVD, µm	time, min		h/c	x/c	θ, °	Re, 10^6	α,°	ΔC_d at α	$\Delta\alpha$ at $C_{l,max}$	$\Delta C_{l,max}$
Fig 15 A 1 g/m³	4	130	18	1.00	20	8	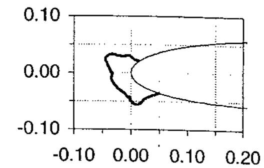	0.051	0.0143	13	2.41	4.0	0.019		
Fig 15 A 1.3 g/m³	4	130	18	1.30	20	8	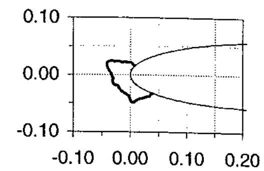	0.042	0.0075	12	2.41	4.0	0.024		
Fig 15 A 1.6 g/m³	4	130	18	1.60	20	8	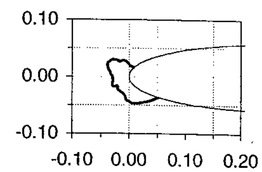	0.038	0.0080	23	2.41	4.0	0.039		
Fig 15 B 1 g/m³	4	130	0	1.00	20	8	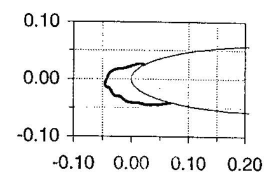	0.063	0.0230	-13	2.58	4.0	0.014		

TABLE G-2.6. STUDIES USING ACCRETED OR SIMULATED ICE
(Ref. 122, Olsen, Shaw, and Newton, NASA TM 83556, 1984, NACA 0012 Airfoil, c = 21 in
Performance Data From Figure 31 (Continued))

Ice shape identity	Icing Conditions						Ice shape (coordinates normalized with respect to chord)	Upper horn			Performance Data				
	α,°	V, mph	t_{tot}, °F	LWC, g/m^3	MVD, µm	time, min		h/c	x/c	θ, °	Re, 10^6	α,°	ΔC_d at α	$\Delta\alpha$ at $C_{l,max}$	$\Delta C_{l,max}$
Fig 15 B 1.3 g/m^3	4	130	0	1.30	20	8	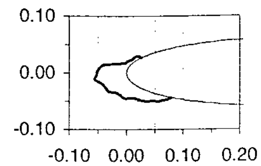	0.068	0.0264	-12	2.58	4.0	0.018		
Fig 15 B 2 g/m^3	4	130	0	2.00	20	8	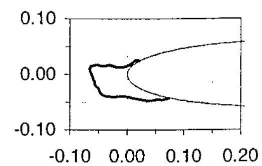	0.084	0.0214	-7	2.58	4.0	0.024		

TABLE G-2.7. STUDIES USING ACCRETED OR SIMULATED ICE
(Refs. 150 and 151, Shin and Bond, NASA TM 105374 and TM 105743, 1984, NACA 0012 Airfoil, c = 21 in
Drag Data: Figures 6 and 7 (TM 105374) and Table 2 (TM 105743))

Ice shape identity	Icing Conditions						Ice shape (coordinates normalized with respect to chord)	Upper horn			Performance Data				
	α,°	V, mph	t_{tot}, °F	LWC, g/m^3	MVD, µm	time, min		h/c	x/c	θ, °	Re, 10^6	α,°	ΔC_d at α	$\Delta\alpha$ at $C_{l,max}$	$\Delta C_{l,max}$
6-25-91 run 9	4	150	-15	1.00	20	6	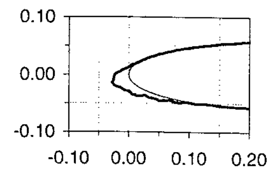	0.042	0.0146	-27	3.1	4.0	0.0125		
7-25-91 run 5	4	150	-15	1.00	20	6	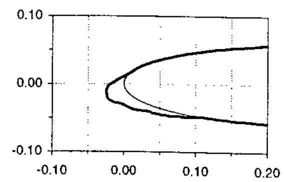	0.037	0.010	-32	3.1	4.0	0.0109		
7-30-91 run 2	4	150	-15	1.00	20	6	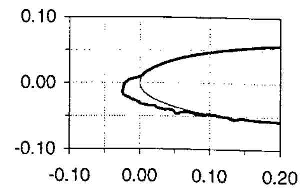	0.023	0.004	-18	3.1	4.0	0.0127		
7-30-91 run 3	4	150	-15	1.00	20	6	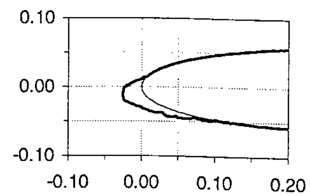	0.035	0.0084	-26	3.1	4.0	0.0127		

TABLE G-2.7. STUDIES USING ACCRETED OR SIMULATED ICE
(Refs. 150 and 151, Shin and Bond, NASA TM 105374 and TM 105743, 1984, NACA 0012 Airfoil, c = 21 in
Drag Data: Figures 6 and 7 (TM 105374) and Table 2 (TM 105743) (Continued))

Ice shape identity	Icing Conditions						Ice shape (coordinates normalized with respect to chord)	Upper horn			Performance Data				
	α,°	V, mph	t_{tot}, °F	LWC, g/m^3	MVD, µm	time, min		h/c	x/c	θ, °	Re, 10^6	α,°	ΔC_d at α	$\Delta\alpha$ at $C_{l,max}$	$\Delta C_{l,max}$
6-25-91 run 8	4	150	1	1.00	20	6	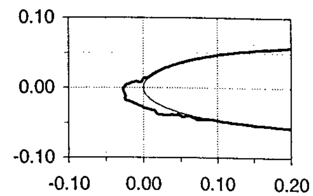	0.034	0.0081	-20	2.9	4.0	0.0123		
6-25-91 run 6	4	150	12	1.00	20	6	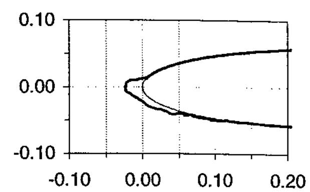	0.030	0.0074	-12	2.8	4.0	0.0125		
7-23-91 run 4	4	150	12	1.00	20	6	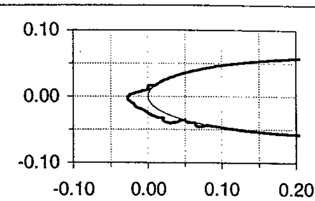	0.030	0.0042	-16	2.8	4.0	0.0123		
6-24-91 run 4	4	150	18	1.00	20	6	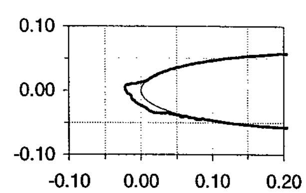	0.029	0.0068	-12	2.7	4.0	0.0165		

TABLE G-2.7. STUDIES USING ACCRETED OR SIMULATED ICE
(Refs. 150 and 151, Shin and Bond, NASA TM 105374 and TM 105743, 1984, NACA 0012 Airfoil, c = 21 in
Drag Data: Figures 6 and 7 (TM 105374) and Table 2 (TM 105743) (Continued))

Ice shape identity	Icing Conditions						Ice shape (coordinates normalized with respect to chord)	Upper horn			Performance Data				
	α,°	V, mph	t_{tot}, °F	LWC, g/m^3	MVD, µm	time, min		h/c	x/c	θ, °	Re, 10^6	α,°	ΔC_d at α	$\Delta\alpha$ at $C_{l,max}$	$\Delta C_{l,max}$
6-28-91 run 1	4	150	22	1.00	20	6	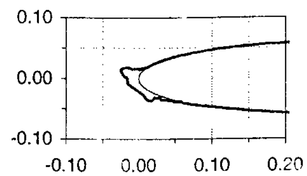	0.034	0.0097	-2	2.7	4.0	0.0230		
7-22-91 run 1	4	150	22	1.00	20	6	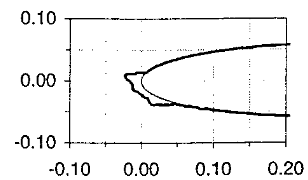	0.029	0.0059	-5	2.7	4.0	0.0209		
7-22-91 run 2	4	150	22	1.00	20	6	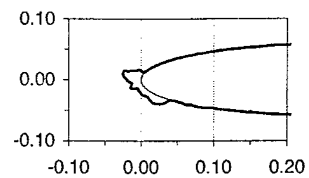	0.030	0.0059	4	2.7	4.0	0.0224		
7-29-91 run 2	4	150	22	1.00	20	6	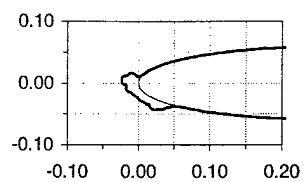	0.026	0.0042	0	2.7	4.0	0.0243		

TABLE G-2.7. STUDIES USING ACCRETED OR SIMULATED ICE
(Refs. 150 and 151, Shin and Bond, NASA TM 105374 and TM 105743, 1984, NACA 0012 Airfoil, c = 21 in
Drag Data: Figures 6 and 7 (TM 105374) and Table 2 (TM 105743) (Continued))

Ice shape identity	Icing Conditions						Ice shape (coordinates normalized with respect to chord)	Upper horn			Performance Data				
	α,°	V, mph	t_{tot}, °F	LWC, g/m^3	MVD, µm	time, min		h/c	x/c	θ, °	Re, 10^6	α,°	ΔC_d at α	$\Delta\alpha$ at $C_{l,max}$	$\Delta C_{l,max}$
6-25-91 run 3	4	150	25	1.00	20	6	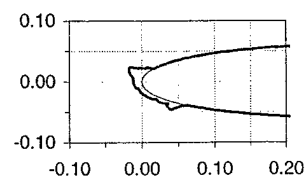	0.033	0.0161	5	2.7	4.0	0.0433		
6-28-91 run 8	4	150	25	1.00	20	6	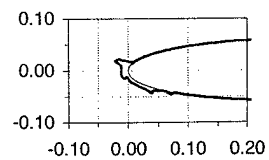	0.026	0.0083	15	2.7	4.0	0.0457		
7-29-91 run 1	4	150	25	1.00	20	6	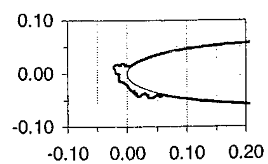	0.028	0.0073	4	2.7	4.0	0.0370		
6-25-91 run 1	4	150	28	1.00	20	6	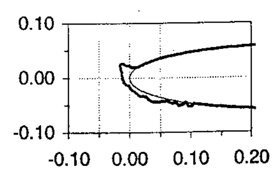	0.026	0.0114	20	2.6	4.0	0.0471		

TABLE G-2.7. STUDIES USING ACCRETED OR SIMULATED ICE
(Refs. 150 and 151, Shin and Bond, NASA TM 105374 and TM 105743, 1984, NACA 0012 Airfoil, c = 21 in
Drag Data: Figures 6 and 7 (TM 105374) and Table 2 (TM 105743) (Continued))

Ice shape identity	Icing Conditions						Ice shape (coordinates normalized with respect to chord)	Upper horn			Performance Data				
	α,°	V, mph	t_{tot}, °F	LWC, g/m^3	MVD, µm	time, min		h/c	x/c	θ, °	Re, 10^6	α,°	ΔC_d at α	$\Delta\alpha$ at $C_{l,max}$	$\Delta C_{l,max}$
6-28-91 run 5	4	150	28	1.00	20	6	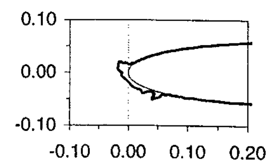	0.0254	0.0102	7	2.6	4.0	0.0404		
7-31-91 run 4	4	150	28	1.00	20	6	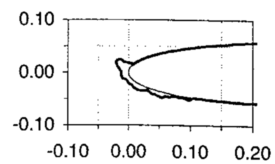	0.028	0.0083	18	2.6	4.0	0.0526		
8-2-91 run 9	4	230	-15	0.55	20	7	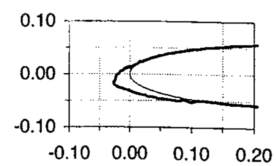	0.034	0.0126	-26	4.6	4.0	0.0112		
8-3-91 run 8	4	230	-15	0.55	20	7	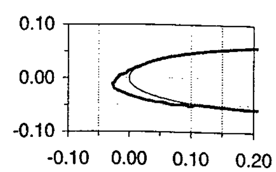	0.051	0.0152	-31	4.6	4.0	0.0109		

TABLE G-2.7. STUDIES USING ACCRETED OR SIMULATED ICE
(Refs. 150 and 151, Shin and Bond, NASA TM 105374 and TM 105743, 1984, NACA 0012 Airfoil, c = 21 in
Drag Data: Figures 6 and 7 (TM 105374) and Table 2 (TM 105743) (Continued))

Ice shape identity	Icing Conditions						Ice shape (coordinates normalized with respect to chord)	Upper horn			Performance Data				
	α,°	V, mph	t_{tot}, °F	LWC, g/m^3	MVD, µm	time, min		h/c	x/c	θ, °	Re, 10^6	α,°	ΔC_d at α	$\Delta\alpha$ at $C_{l,max}$	$\Delta C_{l,max}$
8-3-91 run 9	4	230	-15	0.55	20	7	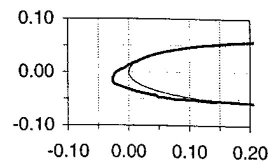	0.048	0.0130	-31	4.6	4.0	0.0110		
8-2-91 run 8	4	230	1	0.55	20	7	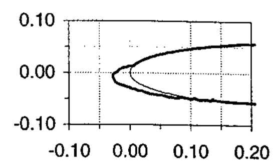	0.039	0.0054	-29	4.3	4.0	0.0128		
8-1-91 run 4	4	230	12	0.55	20	7	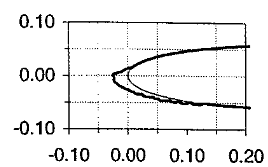	0.034	0.0071	-23	4.1	4.0	0.0185		
8-2-91 run 6	4	230	12	0.55	20	7	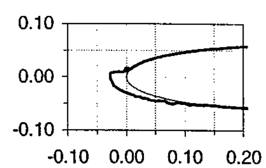	0.031	0.0035	-8	4.1	4.0	0.0148		

TABLE G-2.7. STUDIES USING ACCRETED OR SIMULATED ICE
(Refs. 150 and 151, Shin and Bond, NASA TM 105374 and TM 105743, 1984, NACA 0012 Airfoil, c = 21 in
Drag Data: Figures 6 and 7 (TM 105374) and Table 2 (TM 105743) (Continued))

Ice shape identity	Icing Conditions						Ice shape (coordinates normalized with respect to chord)	Upper horn			Performance Data				
	α,°	V, mph	t_{tot}, °F	LWC, g/m^3	MVD, µm	time, min		h/c	x/c	θ, °	Re, 10^6	α,°	ΔC_d at α	$\Delta\alpha$ at $C_{l,max}$	$\Delta C_{l,max}$
8-3-91 run 7	4	230	12	0.55	20	7	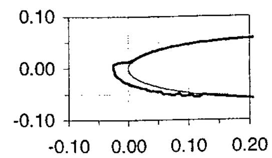	0.031	0.0056	-6	4.1	4.0	0.0186		
8-2-91 run 4	4	230	18	0.55	20	7	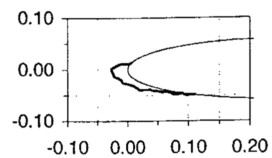	0.034	0.0054	-18	4.0	4.0	0.0162		
8-1-91 run 5	4	230	22	0.55	20	7	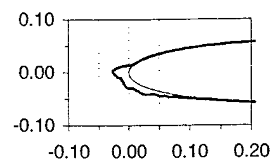	0.036	0.0076	-17	4.0	4.0	0.0204		
8-3-91 run 3	4	230	22	0.55	20	7	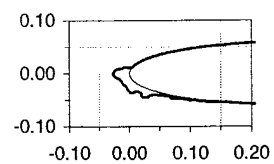	0.033	0.0037	-16	4.0	4.0	0.0223		

TABLE G-2.7. STUDIES USING ACCRETED OR SIMULATED ICE
(Refs. 150 and 151, Shin and Bond, NASA TM 105374 and TM 105743, 1984, NACA 0012 Airfoil, c = 21 in
Drag Data: Figures 6 and 7 (TM 105374) and Table 2 (TM 105743) (Continued))

Ice shape identity	Icing Conditions						Ice shape (coordinates normalized with respect to chord)	Upper horn			Performance Data				
	α,°	V, mph	t_{tot}, °F	LWC, g/m^3	MVD, µm	time, min		h/c	x/c	θ, °	Re, 10^6	α,°	ΔC_d at α	$\Delta\alpha$ at $C_{l,max}$	$\Delta C_{l,max}$
8-3-91 run 4	4	230	22	0.55	20	7	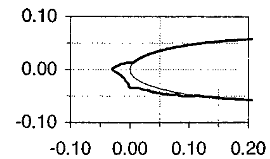	0.037	0.0061	-19	4.0	4.0	0.0202		
8-3-91 run 5	4	230	22	0.55	20	7	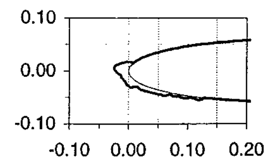	0.028	0.0068	-6	4.0	4.0	0.0241		
8-2-91 run 2	4	230	25	0.55	20	7	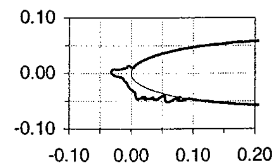	0.0355	0.0037	-6	3.9	4.0	0.0264		
8-3-91 run 2	4	230	25	0.55	20	7	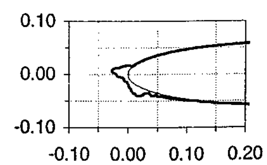	0.0357	0.0080	-11	3.9	4.0	0.0270		

TABLE G-2.7. STUDIES USING ACCRETED OR SIMULATED ICE
(Refs. 150 and 151, Shin and Bond, NASA TM 105374 and TM 105743, 1984, NACA 0012 Airfoil, c = 21 in
Drag Data: Figures 6 and 7 (TM 105374) and Table 2 (TM 105743) (Continued))

Ice shape identity	Icing Conditions						Ice shape (coordinates normalized with respect to chord)	Upper horn			Performance Data				
	α,°	V, mph	t_{tot}, °F	LWC, g/m^3	MVD, µm	time, min		h/c	x/c	θ, °	Re, 10^6	α,°	ΔC_d at α	$\Delta\alpha$ at $C_{l,max}$	$\Delta C_{l,max}$
8-2-91 run 1	4	230	28	0.55	20	7	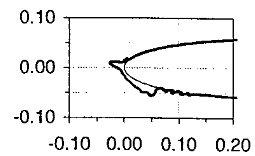	0.0315	0.0052	-1	3.9	4.0	0.0322		
8-3-91 run 1	4	230	28	0.55	20	7	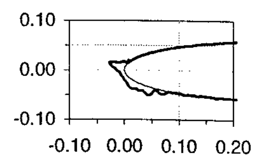	0.034	0.0068	3	3.9	4.0	0.0456		

APPENDIX H—AERODYNAMIC CHARACTERISTICS FOR CONSIDERATION IN DETERMINING CRITICAL ICE SHAPES FOR 14 CFR PART 23, SUBPART B REQUIREMENTS

This table lists 14 Code of Federal Regulations (CFR) Part 23, Subpart B requirements and suggests aerodynamic characteristics(s) for consideration in the determination of critical ice shapes in meeting the requirements. Specifically, the table describes the current performance and handling characteristics requirement of 14 CFR Part 23, Subpart B. The seven columns under the general heading of "Aerodynamic Characteristics" are the primary characteristics related to the specific section of the rule. The table is presented in order to illustrate an approach to determination of critical ice shapes, and suggest aerodynamic characteristics that may be considered. A similar table could be construct for 14 CFR Part 25, Subpart B. There may be cases where it would be advisable to consider additional characteristics, and other cases where it might be determined that it is not necessary to consider all the characteristics listed.

An X in a cell indicates that the characteristic for that column be considered in determining critical ice shapes to be used in meeting the requirement for that row. For example, for 23.145 (longitudinal control) and 23.147 (directional and lateral control), the following columns are checked: C_{lmax}, α_{st}, C_h, *Eff*, *Stab*. This implies that these four characteristics should/must be considered in determining an ice shape to meet these requirements. These characteristics may be evaluated for degradation with respect to airfoil sensitivity due to ice shape or protuberance or roughness representing ice shape.

Section 23/25/27/29.1419a states: "An analysis must be performed to establish, on the basis of the aircraft's operational needs, the adequacy of the ice protection system for the various components of the aircraft. In addition, tests of the ice protection system must be conducted to demonstrate that the aircraft is capable of operating safely in continuous maximum and intermittent maximum icing conditions, as described in Appendix C of Part 25 of this chapter." As used in this section, "capable of operating safely," means that the aircraft performance, controllability, maneuverability, and stability must not be less than that required (in part 23, subpart B, for example).

The aerodynamic characteristics included in the table are:

C_{lmax} = maximum coefficient of lift
C_d = coefficient of drag
L/D = lift to drag ratio
α_{st} = angle of attack at stall
C_h = hinge moment coefficient
C_m = pitching moment coefficient
Eff = control effectiveness
Stab = appropriate longitudinal and lateral directional stability control characteristics

Also:

N/APL = not applicable
N/R = not required

TABLE H-1. AERODYNAMIC CHARACTERISTICS FOR CONSIDERATION IN DETERMINING CRITICAL ICE SHAPES FOR 14 CFR PART 23, SUBPART B REQUIREMENTS

Section	Description	Remarks	Aerodynamic Characteristics							
			C_{lmax}	C_d	L/D	α_{st}	C_h	C_m	*Eff*	*Stab*
	Performance									
23.45	General									
23.49	Stalling speed	Must be met for any airplane that can't meet the OEI requirements. For all other airplanes V_{SO} and V_{S1} must be determined for expected residual ice and the maximum ice on protected surfaces between cycles. There are the Vs values used for all testing that requires ice shapes.				X				
23.51	Takeoff	N/APL								
23.53	Takeoff speeds	N/APL								
23.55	Accelerate-stop distance	Takeoff and takeoff climb performance should be considered of the engine is used to power ice protection systems. This would not include pumps that could draw power from or through the battery, but would be considered of power loads up alternator or generator. Airplanes using bleed air or vacuum should also be considered.	N/R	N/R	N/R	N/R	N/R	N/R	N/R	
23.57	Takeoff path	Should be considered if engine power is used for icing equipment and a power loss is expected because of it.	N/R	N/R	N/R	N/R	N/R	N/R	N/R	

TABLE H-1. AERODYNAMIC CHARACTERISTICS FOR CONSIDERATION IN DETERMINING CRITICAL ICE SHAPES FOR 14 CFR PART 23, SUBPART B REQUIREMENTS (Continued)

Section	Description	Remarks	Aerodynamic Characteristics							
			C_{lmax}	C_d	*L/D*	α_{st}	C_h	C_m	*Eff*	*Stab*
23.59	Takeoff distance and takeoff run	Recommend that takeoff and takeoff climb performance be done with icing systems on for situations where the pilot is taking off into icing conditions.	N/R	N/R	N/R	N/R	N/R	N/R	N/R	
23.61	Takeoff flight path	Should be considered if engine power is used for icing equipment and a power loss is expected because of it.	N/R	N/R	N/R	N/R	N/R	N/R	N/R	
23.65	Climb: All engines operating				X					
23.67	Climb: one engine inoperative	Single engine climb and balked landing climb is covered adequately in AC 23.1419-2 except that multi-engine go around (balked landing) climb must also be considered. These conditions must meet the requirements for a clean airplane. Effects of ice on OEI glide should also be considered and presented in the AFM.			X					
23.75	Landing	Vref is based on Vmc or V_{SO}, so it should be considered. Landing speeds and distances are adequately covered in AC 23.1419-2.				X				
23.77	Balked landing				X	X	X	X	X	

TABLE H-1. AERODYNAMIC CHARACTERISTICS FOR CONSIDERATION IN DETERMINING CRITICAL ICE SHAPES FOR 14 CFR PART 23, SUBPART B REQUIREMENTS (Continued)

Section	Description	Remarks	Aerodynamic Characteristics							
			C_{lmax}	C_d	L/D	α_{st}	C_h	C_m	*Eff*	*Stab*
	Flight Characteristics									
23.141	General	N/APL								
	Controllability and Maneuverability									
23.143	General		X			X	X	X	X	X
23.145	Longitudinal control		X			X	X	X	X	X
23.147	Directional and lateral control		X			X	X	X	X	X
23.149	Minimum control speed		X			X	X	X	X	X
23.151	Acrobatic maneuvers	N/R								
23.153	Control during landings		X			X	X	X	X	X
23.155	Elevator control force in maneuvers								X	X
23.157	Rate of roll		X						X	X
	Trim									
23.161	Trim	N/R								
	Stability						X	X	X	X
23.171	General						X	X	X	X
23.173	Static Longitudinal stability						X	X	X	X

TABLE H-1. AERODYNAMIC CHARACTERISTICS FOR CONSIDERATION IN DETERMINING CRITICAL ICE SHAPES FOR 14 CFR PART 23, SUBPART B REQUIREMENTS (Continued)

			Aerodynamic Characteristics							
Section	Description	Remarks	C_{lmax}	C_d	L/D	α_{st}	C_h	C_m	*Eff*	*Stab*
23.175	Demonstration of static longitudinal stability						X	X	X	X
23.177	Static directional stability						X	X	X	X
23.181	Dynamic stability						X	X	X	X
	Stalls									
23.201	Wings level stall					X				
23.203	Turning flight and accelerated stalls					X				
23.205	Critical engine inoperative stalls					X				
23.207	Stall warning					X				
	Spinning					X				
23.221	Spinning									
	Ground and Water Handling Characteristics									
	Miscellaneous									
23.251	Vibration and buffeting						X	X	X	
23.253	High speed characteristics						X	X	X	

APPENDIX I—WORKING GROUP RECOMMENDATIONS FOR RESEARCH INVESTMENT

This appendix is based on the discussions and voting in the 12A Working Group at the meeting held in Seattle in April 1998.

I.1. PROPOSED AREAS OF RESEARCH.

Several topics for research were proposed by members of the working group. The topics were written on large sheets on a flip chart and then posted around the room to facilitate discussion and voting. The topics from the sheets are given below.

1. Measurement of ice roughness

   - quantification (size, density, shape)
   - reproduction
   - aerotesting
   - correlation with the aero-effects
   - comparison to simulation techniques

     – sandpaper
     – walnut shells
     – other

2.a. Parametric variation of ice accretion

   - geometries and features to study
   - resultant aero-effects

     – horn angle
     – horn length
     – horn location, x/c
     – radius of horn
     – effect of roughness on horn
     – effect of irregularities
     – assessment of Re No. effects
     – scaling

2.b. Variation of airfoil characteristics with the list of 2a. (for example: *t/c*, *r/c*, camber, thickness distribution, etc.)

3. Verify/validate parametric variations of 2a and 2b with ice shapes formed in an icing wind tunnel.

4. Relation of 2D to 3D effects

   - full aircraft
   - aero tunnel
   - flight

5. Effects of secondary ice (ice on nonlifting components; i.e., underneath wings, struts, etc.). Change in drag is concern.

6. Effect of droplet spectra on ice accretion

7. Aero Scaling

   - 2D to 3D
   - roughness
   - one law for lift, another for
   - hinge moment

8. Ice shape scaling methods

   - good to 1/2 or 1/3 scale, 1/6 scale
   - borderline
   - gross ice shapes vs. more detailed
   - representations

9. Screening process for aircraft configuration icing sensitivity.

10. Computational capabilities

    - icing simulation
    - aero simulation with ice accretion
    - 2D
    - 3D

11. Steady and unsteady phenomena

12. Asymmetric ice accretion on aircraft

13. Ice accretion fracturing (shed ice).

I.2. VOTING RESULTS FOR PROPOSED RESEARCH AREAS.

It was decided that these proposed research areas would be prioritized by voting within the working group. Each member was given an opportunity to prioritize the research areas from first to last. The results in the table below were determined as follows: A first place vote counted ten points, a second place vote counted nine points, ..., a tenth place vote counted one point; any lower place vote was allotted zero points.

Some members treated 2a and 2b separately, others as a single item. Some did not prioritize from top to bottom, stopping with their "top ten." Therefore, the results for lower vote getters are lower than they might be.

It was suggested that it would be of interest to see how the industry voting compared to that of the entire group, and this is shown in the fourth column.

		All Members	Industry Members
1	Ice roughness	112	38
2a	Parametric variation	140	50
2b	Variation of airfoil characteristics	107	16
3	Verify/validate parametric variations	106	14
4	2D to 3D	53	10
5	Secondary ice	21	0
6	Droplet spectra effect on ice	18	16
7	Aero scaling	106	36
8	Ice shape scaling	76	38
9	Screening: ice sensitivity	42	0
10	Computational capabilities	43	7
11	Steady and unsteady phenomena	6	0
12	Asymmetric ice accretion	7	0
13	Ice accretion fracturing	9	0

I.1.1 RECOMMENDATIONS BASED ON VOTING RESULTS AND DISCUSSION FOR PROPOSED RESEARCH AREAS.

The voting on proposed areas of research suggest three categories of support.

A. Wide support

1. Measurement of ice roughness

2a. Parametric variation of ice accretion

2b. Variation of airfoil characteristics with the list of 2a (for example: *t/c*, *r/c*, camber, thickness distribution, etc.)

3. Verify/validate parametric variations of 2a and 2b with ice shapes formed in an icing wind tunnel

7. Aero Scaling

B. Reasonable support

8. Ice shape scaling methods

C. Limited support

All remaining items (4, 5, 6, 9, 10, 11, 12, and 13)

The items in category A were extensively discussed, and with the exception of aerodynamic scaling are clearly inter-related. The large vote for each is an indication of a consensus of those present. The item-in category B was also quite fully discussed, and strongly supported by the representative of the helicopter industry and others. However, some of the items in category C were only briefly discussed, and ranking them among themselves based on this vote may be questionable. However, as they did not enjoy the general support of the items in categories A and B, they will not be included in the research recommendations.

The items in category A all require experimental work. Data of a high quality, from wind tunnels capable of high Reynolds numbers, are needed to adequately assess questions as to the influence of ice shape features on the aerodynamic effects of ice shapes. National Aeronautic and Space Administration Glenn Research Center (NASA GRC) and Federal Aviation Administration William J. Hughes Technical Center (FAATC) should carry out cooperative research, utilizing both the Icing Research Tunnel (IRT) and a tunnel such as the Low Turbulence Pressure Tunnel (LTPT), to meet the objectives listed. Note that this is consistent with the need for experimental data as described in the main body of this report for both the "airfoil sensitivity approach" and the "comprehensive aerodynamic approach" to critical ice shapes.

Fundamental work is needed in the measurement and quantification of ice roughness. Progress may be possible through the use of new laser scanning systems. To obtain aerodynamic correlations, icing tests in the IRT should be used to develop castings for use in a tunnel such as the LTPT.

Scaling questions as listed in categories A and B have long bedeviled icing engineering and research. Although progress has been made, and NASA is currently preparing a scaling manual, fundamental questions remain. Industry comments during the discussion underlined the needs of general aviation and commuter aircraft manufacturers for reliable scaling methods. These needs are perhaps most critical in the helicopter industry, where reliance upon scaling methods is unavoidable and some of the issues are quite complex. Transport manufacturers also must utilize scaling methods.

NASA GRC and FAATC should work with industry in formulating an effective strategy for research that will lead to improved practical scaling methods for both fixed wing aircraft and rotorcraft. The approach will probably combine analytical and experimental efforts, and should build on past efforts.

APPENDIX J—ADDITIONAL RECOMMENDATIONS FROM INDUSTRY

The following recommendations were made by members of industry in subgroup reports which are not included in their entirety in the final report. Most of them were discussed at various times during the two meetings of the working group, and they are believed to enjoy quite a wide support in industry. Some are directed primarily at the Federal Aviation Administration (FAA) Certification Service, while others are directed more at the research community, especially National Aeronautic and Space Administration (NASA) Glenn and the FAA William J. Hughes Technical Center.

A simulated ice shape definition process, which is clearly defined and endorsed by the FAA, is needed.

Some improvements are needed in defining the ice shape surface features and roughness.

In order to define other ice shapes with codes, analytical methods need validated improvements that model (1) complex three-dimensional (3D) ice accumulations, (2) residual ice from anti-ice system operation (runback ice), (3) residual ice from deice system operation, and (4) effects of larger droplet sizes.

Continued improvements of the codes are desirable, especially in the heat transfer and roughness models. Improvements to ice accretion predictions are required for three-dimensional geometry with multi-time stepping capability.

Further enhancements and validations are especially required for prediction codes due to inadequate modeling of:

- Droplet breakup and droplet splash, considered as the major change with these new conditions.
- Surface physics (improvement of ice growth governed by the heat and mass balance based on Messinger equations) by taking micro physical ice growth into account with these new conditions.
- Water run back, which includes shedding of excess water and ice from the airfoil surface.
- Ice roughness development, and heat transfer rates and evaporative cooling associated with a rough surface.
- Thermodynamic and mass balance.

There is a need to improve the accuracy of the flow field module used in the icing code. In fact none of the codes model the viscous flow effect (in particular separation and reattachment), and the codes thus predict a flow velocity larger than the actual velocity with an over estimation of the heat transfer coefficient (h). The use of a viscous code could improve the situation, and thus contribute to the extension of the usable domain, which is today roughly limited to M=0.4 associated airfoil angle-of-attack (AOA) = 4 to 5 degrees. This limitation is therefore directly linked to a combination of Mach number and AOA.